DISSERTATION APPROVED BY

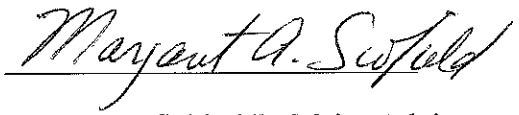

Margaret A. Scofield PhD, Major Advisor

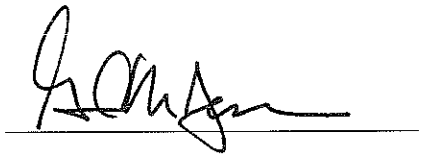

Gail M. Jensen, PhD, Dean

MOLECULAR AND PHARMACOLOGICAL CHARACTERIZATION OF THE RAT RAMP2B SPLICE VARIANT

By

Kelly Monroe Witt

A DISSERTATION

Submitted to the faculty of the Graduate School of Creighton University in partial fulfillment of the requirements for the degree of Doctor of Philosophy in the Department of Pharmacology

---

Omaha, Nebraska, September 2010

ABSTRACT

Receptor activity-modifying protein 2 (RAMP2) forms a hetero-oligomer with the calcitonin receptor-like receptor (CL) homo-oligomer to produce the adrenomedullin receptor 1 (AM_1). RAMP2 has also been shown to associate with other receptors including the calcitonin receptor (CTR), vasoactive intestinal peptide/pituitary adenylate cyclase activating peptide (VPAC) receptor 1, parathyroid hormone (PTH) receptor 1 and glucagon receptor. An adrenomedullin receptor (AM_2) is also formed by the RAMP3 and CL complex.

A partial sequence of a rat RAMP2 splice variant was previously identified in our laboratory. I hypothesized that human tissue expresses RAMP2 splice variants and that a clone of the full-length rat RAMP2 splice variant forms an adrenomedullin receptor with decreased function in the presence of CL. I used RT-PCR to identify a human RAMP2 splice variant containing an additional fifteen nucleotides and five putative amino acid residues in the N-terminus of the accessory protein. The region of the splice variant does not have a specific, known purpose but is located in the variable N-terminus region.

The full-length rat RAMP2b was cloned using RT-PCR and has a twenty-six amino acid deletion in a highly hydrophobic region of the signal peptide. SignalP version 3.0 and Kyte-Doolittle hydropathy plots predict a low probability that the RAMP2b has a signal peptide. Confocal microscopy was used to determine whether the rat RAMP2b trafficked to the plasma membrane. I transiently co-transfected COS-7 cells with an N-terminal HA-tagged CL and either the wild-type RAMP2, containing the intact signal peptide, or the RAMP2b. Non-permeabilized live cells were immunostained with HA

and RAMP2 primary antibodies to determine if epitopes of the proteins were present on the outer surface of the plasma membrane. My studies showed that both the rat RAMP2 and RAMP2b trafficked to the cell membrane in the presence or absence of CL. After determining that the rRAMP2b did traffic to the cell membrane, the adrenomedullin receptor function was studied by stimulating the co-transfected COS-7 cells with adrenomedullin and measuring the cAMP levels. The rRAMP2b and hCL transfected COS-7 cells showed a decrease in adrenomedullin receptor activity.

PREFACE

Adrenomedullin receptors are G protein-coupled receptors (GPCR) that require two or more calcitonin receptor-like receptors (CL, sometimes abbreviated as CRLR and CLR) and either the RAMP2 or RAMP3. GPCRs have an extracellular N-terminus, seven transmembrane domains, and an intracellular C-terminus. Three types of RAMPs (RAMP1-3) have been identified in mammals and the type of RAMP coexpressed with the CL determines the affinity for the peptides.

Adrenomedullin binds to an adrenomedullin receptor and dissociates the G protein complex. Then $G_{\alpha S}$ activates adenylyl cyclase to increase intracellular cAMP levels. A receptor component protein (RCP) may also be required for signal transduction.

Two types of adrenomedullin receptors have been identified based on the type of RAMP in the heterocomplex. AM_1 and AM_2 are comprised of a CL homo-oligomer and either the RAMP2 or RAMP3, respectively. Adrenomedullin stimulation causes internalization of AM_1; whereas, activation of the AM_2 triggers the complex to recycle to the plasma membrane in the presence of *N*–ethylmaleimide-sensitive factor (NSF).

All three of the RAMPs contain a signal peptide that targets the protein for the plasma membrane. The signal peptide usually has a short, positively charged amino-terminal region, a central hydrophobic region and a polar carboxy-terminal region with the cleavage site. Signal peptidase recognizes the signal cleavage site and cleaves off the signal peptide, separating it completely from the protein. RAMP2 splice variants in the signal peptide region have been detected in pufferfish and in rat.

DEDICATION

for my family

ACKNOWLEDGEMENTS

I am deeply indebted to my advisor, Dr. Margaret Scofield, for her words of wisdom and constant support. She not only opens her lab to her students, but also her home. I would like to thank Dr. Peter Abel for his assistance with presentation skills, statistical analysis, stimulating suggestions and regular use of his laboratory. I would like to express gratitude to Dr. Charles Bockman for his assistance with radioligand binding techniques and statistical analysis, use of his laboratory and instructions for formatting abstracts and papers. I am pleased to thank Dr. Joseph Knezetic for letting me sit in on the Molecular and Cell Biology course and participate in the Cellular and Molecular Biology journal club. I am also grateful for his assistance in sequence analysis and overview of grant preparation. I would like to acknowledge Dr. D. David Smith for his ideas and instructions in reporting research data and formatting grant proposals. My committee has shown me patience and enthusiasm while providing me with unending support and encouragement. I will always be grateful for the time they have spent preparing me for my future endeavors.

I would like to thank Dr. Phil Brauer for inspiring me and assisting me with the experimental design and analysis of the confocal microscopy experiments. Dr. Richard Hallworth, Dr. Heather Jensen-Smith, LeAnn Tiede, Dr. Mark Reedy, and Marilou Holmberg also provided invaluable assistance with these experiments. The majority of this research was recorded at the Confocal Microscopy Core Facility funded through the NSF EPSCoR Nebraska Center for Cell Biology (NCCB).

I would like to express gratitude to Dr. Yaping Tu and his laboratory members for help in advancing the transfections and cAMP assay. Their ideas and laboratory

equipment were instrumental in the determination of the function of the rat RAMP2b through luciferase assays. I would also like to thank Dr. James Porter for forwarding me the HA-CL DNA and his useful suggestions and encouragement.

I deeply appreciate Dr. William Jeffries for daily use of his laboratory and for his support during my transition to Creighton University. I am grateful to the two chairs of the Department of Pharmacology during my studies, Dr. Frank Dowd and Dr. Thomas Murray.

I would like to thank all of the summer students and work study students as well as the graduate students, past and present, especially Dr. Herbert Dang and Dr. Boyd Rorabaugh. Lyudmila Batalkina was instrumental in helping with experiments and lab organization and I am grateful for her help. Additionally, I would like to thank Dr. Myron Toews, Dr. Garrett Soukup, Dr. Wanyung Zeng, Dr. Dennis Wolff, and Dr. Philine Wangemann for their assistance during my studies. I appreciate all of the assistance from the staff of the Graduate School, Department of Pharmacology, Department of Biomedical Sciences, Molecular Biology Research Core Facility, UNMC High-Throughput DNA Sequencing and Genotyping Facility, and UNL's DNA Sequencing Facility.

I am pleased to thank The Henry Luce Foundation, Henry Luce III, and the Heritage Foundation for granting me the Clare Boothe Luce Fellowship. I would also like to thank my family and friends.

TABLE OF CONTENTS

LIST OF TABLES

LIST OF FIGURES

ABBREVIATIONS

5-MU: 5-Methyl-6[[3-[4-(2-methoxyphenyl)-1-piperazinyl]propyl]amino]-1,3-dimethyluracil

ANOVA: analysis of variance

AM: adrenomedullin

AM_1: adrenomedullin receptor subtype 1

AM_2: adrenomedullin receptor subtype 2

AMY: amylin

AR: adrenergic receptor

BSA: bovine serum albumin

BIBN4096BS: 1-Piperidinecarboxamide, N-[2-[[5-amino-l-[[4-(4-pyridinyl)-l-piperazinyl]carbonyl]pentyl]amino]-1-[(3,5-dibromo-4-hydroxyphenyl)methyl]-2-oxoethyl]-4-(1,4-dihydro-2-oxo-3(2H)-quinazolinyl)

BMY 7378: 8-(2-[4-(2-methoxyphenyl)-1-piperazinyl]ethyl)-8-azaspiro[4.5]decane-7,9-dione

bp: base pairs

c: chimpanzee

cAMP: cyclic adenosine monophosphate

C-region: carboxy-terminal region

cDNA: complementary deoxyribonucleic acid

CalS: calcium sensing

CGRP: calcitonin gene-related peptide

CL: calcitonin receptor-like receptor

CLR: calcitonin receptor-like receptor

CRE: cyclic adenosine monophosphate response element

CRLR: calcitonin receptor-like receptor

CT: calcitonin

CTR: calcitonin receptor

DAPI: 4',6-diamidino-2-phenylindole

DMEM: Dulbecco's modified Eagle medium

DMSO: dimethyl sulfoxide

DNA: deoxyribonucleic acid

EDTA: ethylenediaminetetraacetic acid

ESE: exonic splicing enhancer

ESS: exonic splicing silencer

ER: endoplasmic reticulum

FBS: fetal bovine serum

g: gerbil

GHRH: growth hormone releasing hormone

GLP: glucagon-like peptide

Gluc: glucagon

GPCR: G protein coupled receptor

h: human

H-region: hydrophobic region

HA: hemagglutinin

HKI: HEPES buffered Krebs solution containing isobutylmethylxanthine

IMD: intermedin

ISE: intronic splicing enhancer

ISS: intronic splicing silencer

$K_{i:}$ equilibrium dissociation constant determined by competition binding

Luc: luciferase

mf: mefugu

N-region: amino-terminal region

NHERF: Na^+/H^+ exchange regulatory factor

ninaA: neither inactivation nor afterpotential A

NSF: *N*–ethylmaleimide-sensitive factor

NSP: no signal peptide

PBS: phosphate buffered saline

PCR: polymerase chain reaction

PI: phosphatidylinositol

PDZ: post synaptic density, disc large protein and ZO=1 proteins

PTH: parathyroid hormone

PTHrP: parathyroid hormone related peptide

r: rat

RACE: rapid amplification cDNA ends

rm: rhesus monkey

RAMP: receptor activity modifying protein

RAMP2-NSP: receptor activity modifying protein subtype 2 mutation with the amino acids in the signal peptide deleted

RanBP2: Ran binding protein 2

RCP: receptor component protein

RLU: relative light units

RNA: ribonucleic acid

RT: reverse transcription

RT-PCR: reverse transcription-polymerase chain reaction

s: salmon

SMA: spiral modiolar artery

SPase I: signal peptidase I

SRP: signal recognition particle

TM: transmembrane

VPAC: vasoactive intestinal peptide/pituitary adenylate cyclase activating peptide

WB-4101: 2-[(2,6-Dimethoxyphenoxyethyl)aminomethyl]-1,4-benzodioxane hydrochloride

CHAPTER 1

BACKGROUND AND OBJECTIVES

Adrenomedullin and Adrenomedullin Receptors

Adrenomedullin, a 52 amino acid peptide, was first isolated from human pheochromocytomas in 1993 (Kitamura et al., 1993). Many cells including the adrenal medulla, blood vessels, and certain regions of the brain synthesize this peptide. Adrenomedullin, a powerful vasodilator, belongs to the calcitonin family of peptides along with calcitonin, amylin, α-CGRP (calcitonin gene-related peptide), β-CGRP, and the most recently discovered intermedin, which is also known as adrenomedullin-2 (Figure 1). Although they have poor sequence homology, each calcitonin family peptide has a six or seven amino acid ring structure near their N-terminus, a predicted α-helix, and an amidated C-terminus.

Because it is a potent vasodilator, adrenomedullin can decrease blood pressure and enhance inflammatory and immune responses. Yoshimoto et al., suggests that adrenomedullin may also act as an endogenous antioxidant in angiotensin II-induced vascular injury (Yoshimoto et al., 2004). Deletion of the adrenomedullin gene is lethal in mice, potentially due to the poor development of the blood vessels and fetal circulation (Brain and Grant, 2004).

Adrenomedullin may play a protective role in various physiological states such as cardiovascular disease, pregnancy, and sepsis where under these conditions adrenomedullin levels are elevated. Adrenomedullin gene therapy of rats with induced hypertension decreases cardiac hypertrophy and renal damage (Zhang et al., 2000).

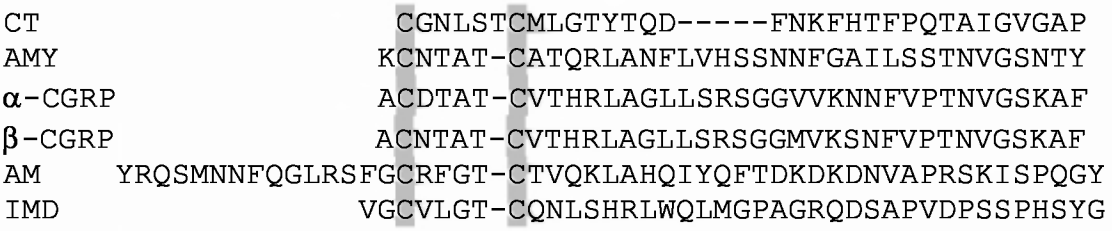

Figure 1. The Calcitonin Family of Peptides. The amino acid sequences of human calcitonin (CT), amylin (AMY), α-calcitonin gene-related peptide (CGRP), β-CGRP, adrenomedullin (AM), and intermedin (IMD) are aligned to show the disulfide bridge, which has been highlighted.

In normal pregnancy, adrenomedullin significantly increases in the reproductive system, but during some pregnancy complications, there is less of an increase in adrenomedullin expression (Hata et al., 1997). Sepsis shows the largest increase in adrenomedullin concentrations, possibly because of the adrenomedullin's antimicrobial, anti-inflammatory, and positive inotropic characteristics (Walsh et al., 1996; Isumi et al., 1998; Allaker et al., 1999; Nishikimi et al., 2003).

The adrenomedullin receptor is a G protein-coupled receptor (GPCR) homo-oligomer that requires an accessory protein for activity. GPCRs have an extracellular N-terminus, seven transmembrane domains, and an intracellular C-terminus. This GPCR has 55% sequence identity to the calcitonin receptor (CTR), and hence is named the calcitonin receptor-like receptor (CL, sometimes abbreviated as CRLR and CLR). The CL receptor may be referred to as the CL protein because it has no known function when expressed without a receptor activity modifying protein (RAMP). CL affinity for its ligand is dependent on a RAMP, which acts as an accessory protein (McLatchie et al., 1998).

Three types of RAMPs (RAMP1-3) have been identified in mammals and the type of RAMP coexpressed with the CL determines the affinity for the peptides. When RAMP1 is coexpressed with CL proteins, it forms a calcitonin gene-related peptide (CGRP) receptor. However, when RAMP2 or RAMP3 coexpresses with CL, adrenomedullin receptors are created, AM_1 and AM_2 respectively (Poyner et al., 2002). RAMPs1-3 can also form amylin receptors (AMY_{1-3}, respectively) when coexpressed with the CTR (Christopoulos et al., 1999). However, the CTR differs from the CL protein in that CTR does not require a RAMP for plasma membrane expression of the receptor

(CTR) and it is the only known member of the calcitonin family that does not require an accessory protein for ligand binding.

The AM_1 receptor is activated by the binding of adrenomedullin, resulting in the dissociation of the G protein complex. Then $G_{\alpha S}$ activates adenylyl cyclase to increase intracellular cAMP levels. A receptor component protein (RCP) may also be required for signal transduction (Luebke et al., 1996; Evans et al., 2000; Prado et al., 2001). Figure 2 shows this proposed mechanism.

Adrenomedullin stimulation also causes internalization of AM_1 predominantly through clathrin-coated vesicles (Kuwasako et al., 2000) (Figure 3). The CL and RAMP2 complex remain together during internalization and are targeted for lysosomal degradation. In contrast, the human RAMP3 has a PDZ (Post synaptic density, Disc large protein and ZO=1 proteins) binding domain in its C-terminal tail (McLatchie et al., 1998). Although the rat RAMP3 does not have a prototypic class I PDZ domain (-DTLL), the receptor complex undergoes resensitization in rat mesangial cells (Parameswaran et al., 2000; Bomberger et al., 2005a). Upon stimulation, AM_2, more specifically the PDZ domain of RAMP3, can interact with *N*–ethylmaleimide-sensitive factor (NSF), which switches the fate of the receptor complex from degradation to trafficking back to the plasma membrane (Figure 3) (Bomberger et al., 2005a). The Na^+/H^+ exchange regulatory factor (NHERF) also interacts with the PDZ domain of RAMP3 causing the receptor complex to remain at the cell surface without desensitizing the receptor (Bomberger et al., 2005b).

Certain disease states may alter the expression of the components of the adrenomedullin receptors (CL, RAMP2, and RAMP3). RAMP2 and CL receptor levels

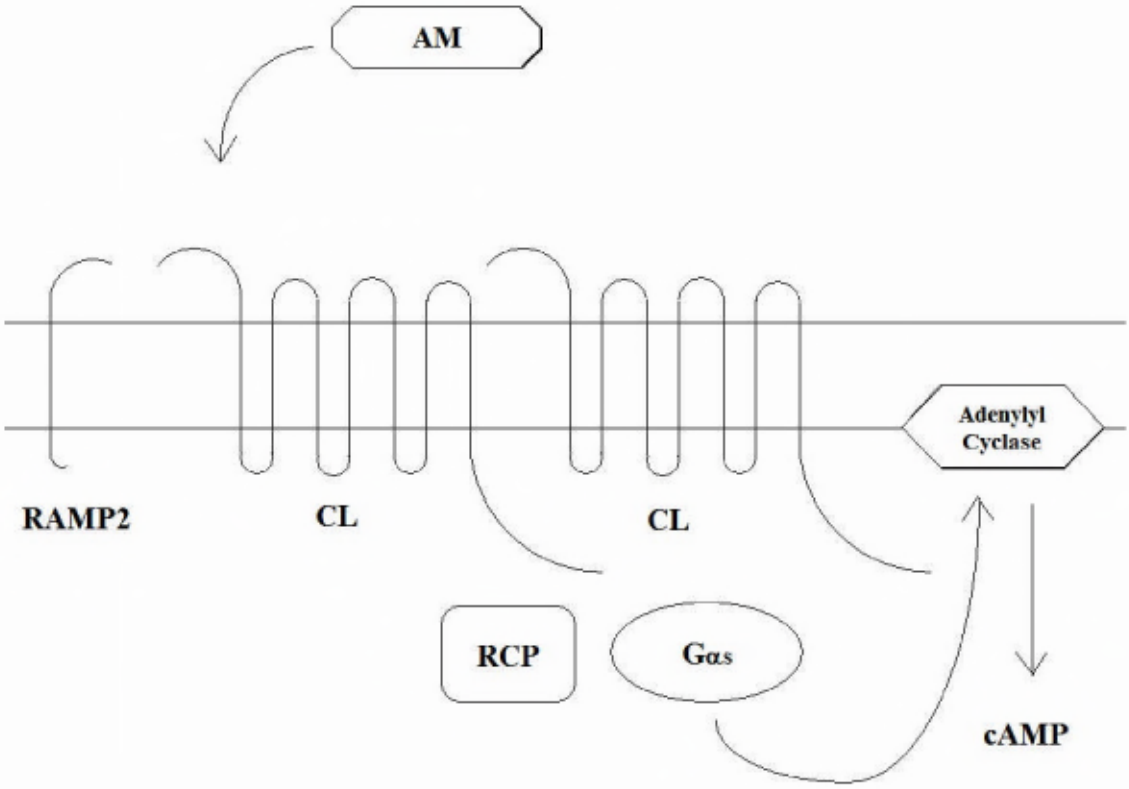

Figure 2. Adrenomedullin stimulation of AM_1. Adrenomedullin (AM) stimulates the adrenomedullin receptor complex, which requires the receptor activity modifying protein (RAMP) 2 and calcitonin receptor like receptor (CL). The exact stoichiometry is unknown. Upon stimulation, the G-protein dissociates activating adenylyl cyclase to increase intracellular cAMP levels. A receptor component protein (RCP) may also be required for signal transduction (Luebke et al., 1996; Evans et al., 2000; Prado et al., 2001).

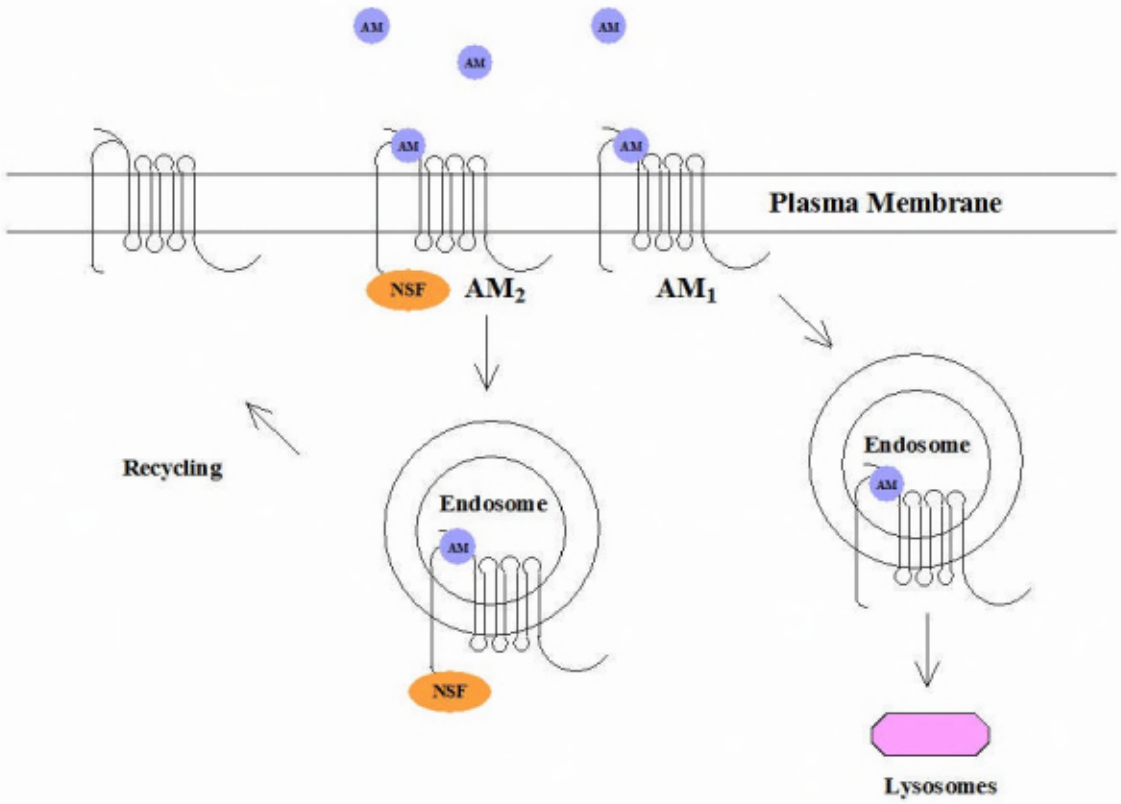

Figure 3. Internalization and recycling of adrenomedullin receptors. After adrenomedullin (AM) stimulation, the adrenomedullin receptors (AM_1 and AM_2) are targeted for either lysosomal degradation or for recycling to the cell surface based on the RAMP (2 or 3, respectively) used in the complex. *N*-ethylmaleimide-sensitive factor (NSF) interacts with RAMP3, allowing the receptor to recycle to the plasma membrane (Bomberger et al., 2005a). This figure was adapted from Hay et al. (Hay et al., 2006).

are increased in the kidney of rats with obstructive nephropathy and the heart of rats with congestive heart failure (Nagae et al., 2000; Totsune et al., 2000). During pregnancy, gene expression of RAMPs1-3 and CL increases, however, patients with preeclampsia have decreased levels of CL, RAMP1, and RAMP2 (Makino et al., 2001; Knerr et al., 2002; Dong et al., 2003; Gangula et al., 2003; Dong et al., 2005; Thota and Yallampalli, 2005).

Sepsis can cause a 40-fold increase in RAMP3 while decreasing the levels of RAMP2 and CL (Ono et al., 2000). During septic shock, adrenomedullin levels increase 20-40 fold while RAMP2 becomes down-regulated and RAMP3 expression up-regulates. Because RAMP3 has a PDZ domain, NHERF can prevent the receptor complex from internalizing without desensitization (Bomberger et al., 2005b). Also, NSF can cause RAMP3 and CL complexes undergoing endocytosis to recycle to the plasma membrane (Bomberger et al., 2005a). Therefore, RAMP3's PDZ domain may play an important role during sepsis and other physiological states.

Receptor Activity Modifying Proteins

RAMPs or RAMP-like proteins have been cloned or predicted for many species including *Homo sapiens*, *Rattus norvegicus*, *Mus musculus*, *Cavia porcellus*, *Sus scrofa*, *Takifugu obscurus, Takifugu rubripes, Tetradon nigroviridis*, *Gallus gallus*, and *Danio rerio* (McLatchie et al., 1998; Husmann et al., 2000; Nagae et al., 2000; Strausberg et al., 2002; Kikumoto et al., 2003; Rival-Gervier et al., 2003; Kato et al., 2005; Nag et al., 2006; Wang et al., 2007). In the Takifugu genus, five RAMPs have been found which may reflect gene duplication in the Tetraodontidae family of fishes (Jaillon et al., 2004; Benitez-Paez, 2006; Nag et al., 2006). The individual RAMPs have a signal peptide, a

large extracellular N-terminus, one transmembrane domain, and a short intracellular C-terminal tail (Muff et al., 2001; Sexton et al., 2001). The N-terminus has very little homology among the RAMPs and most likely contributes to the receptor's function (Fraser et al., 1999). The function of the RAMPs in the absence of a GPCR is also unknown.

RAMPs act as accessory proteins by forming a complex with a GPCR in the endoplasmic reticulum (ER) (Figure 3). For example, RAMP2 forms a complex with CLs in the ER and traffics together to the plasma membrane (Hilairet et al., 2001b). Although some studies show that the CL requires the RAMP for expression at the plasma membrane (Kuwasako et al., 2000), other labs have shown that the CL can traffic to the cell surface independent of RAMP coexpression (Flahaut et al., 2002). The trafficking of RAMP2 and RAMP3 to the cell membrane appears to be dependent on their glycosylation sites (Flahaut et al., 2002). RAMP1 lacks glycosylation sites and requires the presence of CL for trafficking and when expressed alone, RAMP1 remains in the ER. However when glycosylation sites were added, RAMP1 is expressed at the plasma membrane.

Until recently, it was thought that one RAMP interacted with one CL to form a receptor complex. Initially, Hilairet et al. provided evidence that a single RAMP1 associated with one CL (Hilairet et al., 2001a). However, using bimolecular fluorescence complementation with bioluminescence resonance energy transfer, Heroux et al. shows that RAMP1 interacts with two or more CL proteins (Heroux et al., 2007). They further suggest that association with RAMP1 does not disrupt the CL homo-oligomer and that the CL homo-oligomer must compete for a complex with RAMP1 before it forms a RAMP1 homodimer.

Since the individual CL and the RAMP proteins do not bind ligands, work has focused on the pharmacological properties of the different combinations of RAMPs and CL. Although each RAMP and CL protein complex has different affinities for the peptides and antagonists there are few selective antagonists available to unequivocally distinguish between the receptors (Table 1). To complicate the matter further, different cell lines and labs have reported different affinities for these receptors.

RAMPs have been shown to associate with receptors not belonging to the calcitonin family (Table 2) (Christopoulos et al., 2003). RAMP2 can interact with the parathyroid hormone (PTH) 1 and glucagon receptors. RAMP3 associates with the PTH2 receptor (Christopoulos et al., 2003). RAMP1 and RAMP3 also interact with the calcium sensing receptor, a member of the family C of the GPCR superfamily (Bouschet et al., 2005). Recent work shows that the secretin receptor can associate with the RAMP3 (Harikumar et al., 2009). The β-adrenergic receptor may also be affected by RAMP expression (Tilakaratne et al., 2002). In addition, all three human RAMPs interact with vasoactive intestinal peptide/pituitary adenylate cyclase activating peptide (VPAC) 1 receptor, but do not change the receptor's binding pharmacology. However, only RAMP2 exhibits a novel signal transduction role with VPAC1 (Christopoulos et al., 2003). Expressed alone, VPAC1 increases intracellular cAMP via G_s. When RAMP2 is overexpressed, VPAC1 has an increase in phosphatidylinositol (PI) hydrolysis via G_q and the same cAMP response as expressed alone.

Splice Variants

Eukaryotic genes consist of both exons and introns. Introns contain DNA sequences that are spliced from the primary transcript. The remaining DNA sequences

Table 1. Pharmacological Characteristics for calcitonin (CT), amylin (AMY), calcitonin gene-related peptide (CGRP), and adrenomedullin (AM) receptors.

Receptor subtype	**CT**	**AMY**			**CGRP**	**AM**	
	$CT_{(a)}$	**$AMY_{1(a)}$**	**$AMY_{2(a)}$**	**$AMY_{3(a)}$**	**$CGRP_1$**	**AM_1**	**AM_2**
Molecular composition	CTR	CTR + RAMP1	CTR + RAMP2	CTR + RAMP3	CLs + RAMP1	CLs + RAMP2	CLs + RAMP3
Rank order of agonist potency	sCT ≥ hCT ≥ rAMY, αCGRP > AM	sCT ≥ rAMY ≥ αCGRP > hCT > AM	PD	rAMY > αCGRP > AM	αCGRP > AM ≥ AMY ≥ sCT	AM ⋙ αCGRP > AMY > sCT	AM > αCGRP >AMY > sCT
Rank order of antagonist affinity	sCT_{8-32} > AC187 = AC413	sCT_{8-32} = AC187 = AC413 > $CGRP_{8-37}$	ND	sCT_{8-32} = AC187 = AC413 > $CGRP_{8-37}$	BIBN4096BS > $CGRP_{8-37}$ > sCT_{8-32} = AC187	AM_{22-52} ≥ $CGRP_{8-37}$	$CGRP_{8-37}$ ≥ AM_{22-52}

These AMY, CGRP, and AM receptor subtypes are formed by a receptor activity modifying protein (RAMP) and the calcitonin receptor like receptor homo-oligomer (CLs) or the calcitonin receptor subtype a ($CT_{(a)}$). Peptides are from human (h), rat (r), and salmon (s). The rank order of antagonist affinity was not determined (ND) or poorly defined (PD). This figure was adapted from Hay et al. (Hay et al., 2006).

Table 2. G Protein Coupled Receptors (GPCRs) that Associate with Receptor Activity Modifying Proteins (RAMPs).

	RAMP1	RAMP2	RAMP3
VPAC1	■	■	■
VPAC2			
PTH1		■	
PTH2			■
GLP1			
GLP2			
Glucagon		■	
CL	■	■	■
CTR	■	■	■
GHRH			
CalS	■		■
Secretin			■
β-AR	?	?	?

Shaded boxes indicate an interaction of the GPCR with a RAMP. The CL, CTR, and vasoactive intestinal peptide/pituitary adenylate cyclase activating peptide (VPAC) 1 receptor form complexes with all three RAMPs; whereas, the VPAC2 receptor does not. The parathyroid hormone (PTH) receptor 1 and glucagon receptor interact with RAMP2 and the PTH2 receptor complexes with RAMP3. The calcium sensing (CalS) receptor associates with RAMP1 or RAMP3. The secretin receptor associates with RAMP3. The glucagon-like peptide-1 (GLP-1), GLP-2, and growth hormone releasing hormone (GHRH) receptors do not have any significant interactions with the RAMPs. The β-adrenergic receptor may also be affected by RAMP expression. This table was adapted from Christopoulos et al. and Sexton et al. (Christopoulos et al., 2003; Sexton et al., 2006).

are exons. A splice site usually contains an intron with a GT at the 5' end and an AG at the 3' end. The intron also has a branch site in the middle and a polypyrimidine tract at the 3' end. Alternative splice variants are formed when splicing occurs at alternative sites leading to new nucleotide and amino acid sequences. Therefore, a single gene can produce a more diverse population of proteins.

The calcitonin family of peptides consists of several splice variants such as the α-CGRP, which is a product of alternative splicing of the calcitonin gene (Amara et al., 1982). There are also several calcitonin receptor splice variants including the human CTR1 and CTR2; now classified as the hCTRb and hCTRa isoforms, respectively (Gorn et al., 1995; Poyner et al., 2002). The CTRb has an additional 16 amino acids in the first intracellular domain; however, the CTRa is more abundant. Four other human calcitonin receptor splice variants include CTR3 (CTRa where the first 47 amino acids are deleted), CTR4 (a putative variant based on genomic sequencing that has only one transmembrane domain), CTR5 (CTRb that stops in the fourth domain), and CTR6 (CTRa that stops in the fourth domain) (Albrandt et al., 1995; Moore et al., 1995; Beaudreuil et al., 2004). Additional splice variants located near the translation start codon and untranslated regions of the CTR have also been discovered, but not classified (Poyner et al., 2002).

The human RAMP2 gene has four exons and three introns. Two RNA clones derived from expression analysis of chromosome 17 near the BRCA1 locus encode possible human RAMP2 alternative splice variants (Jacob et al., 1995; Derst et al., 2000). These clones are missing exon 3, which contain six of the seven amino acids crucial for adrenomedullin binding (Kuwasako et al., 2001). Our laboratory has discovered a rat RAMP2 splice variant, rRAMP2b, that has 26 amino acids deleted within the N-terminus

in a region containing the signal sequence (Rorabaugh, 2002). In addition RAMP variants have been found in the mefugu *Takifugu obscurus*, but the physiological significance of these variants has not been previously determined (Nag et al., 2006).

Signal Sequences

According to the original signal hypothesis, proteins such as RAMPs required signal sequences to be targeted for transport to the endoplasmic reticulum (ER), plasma membrane, secretory vesicles, or lysosomes (Blobel and Dobberstein, 1975). In contrast cytoplasmic proteins do not contain these sequences. The two types of signal sequences are the cleavable signal peptide at the N-terminal and the internal uncleaved signal anchor that is retained in the mature protein, like a transmembrane domain (Figure 4). A signal peptide usually has a short, positively charged amino-terminal region, a central hydrophobic region and a polar carboxy-terminal region containing the cleavage site (von Heijne, 1985). Translocation to the ER can require the signal recognition particle (SRP) or be SRP-independent. The hydrophobicity of the signal sequence determines which pathway the protein uses. SRP-dependent signal sequences are rich in hydrophobic amino acids; whereas SRP-independent signal sequences contain small or hydroxylated amino acids (Ng et al., 1996).

SRP, a ribonucleoprotein complex, recognizes and binds to the hydrophobic region of amino acids in the signal peptide (Walter and Blobel, 1980). The SRP also interacts with the ribosome to prevent translation of mRNA and binds to the SRP receptor on the ER membrane (Figure 4). The SRP and its receptor dissociate and the ribosomal complex, depending on the signal sequence, forms a new Sec61 complex with trans-acting factors to open a channel, called the translocon. The translocon opens so that the

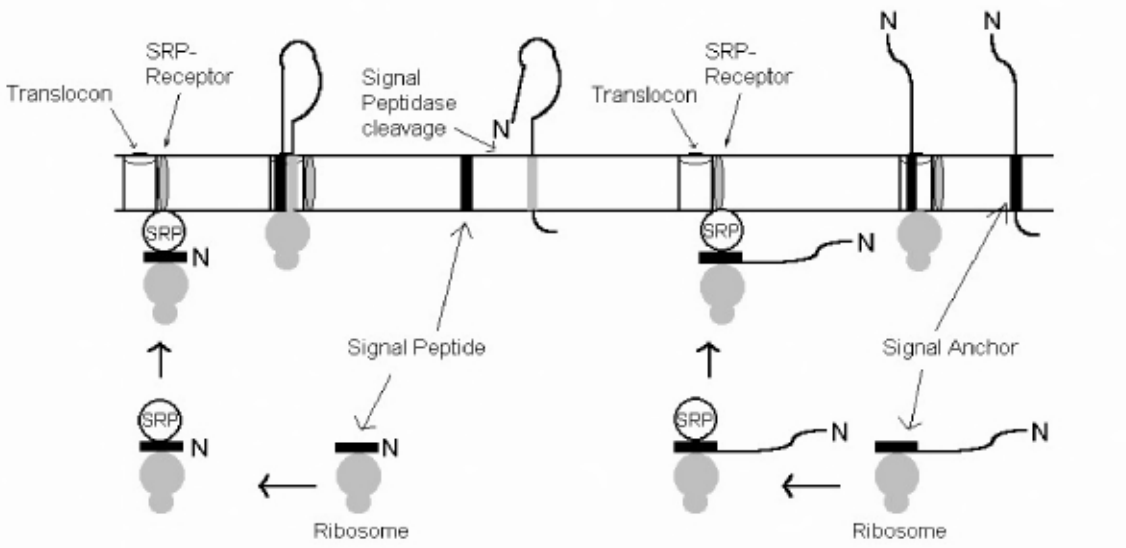

Figure 4. Translocation pathways for signal peptides and signal anchors. A protein with a signal peptide is targeted to the ER when SRP recognizes the hydrophobic core of the signal peptide. Translation stops until SRP binds to the SRP-receptor. The protein enters the translocon on the ER and the signal peptide is embedded in the ER membrane until signal peptidase cleaves off the signal peptide at the cleavage site. A protein with a signal anchor is targeted to the ER when SRP recognizes the hydrophobic signal anchor. SRP binds to the SRP-receptor on the ER and the N-terminus enters the translocon. The signal anchor remains part of protein, usually in the first transmembrane domain.

protein, which is still in the process of translation, can enter the ER. The interaction between the protein's signal sequence and the translocon also helps determine how the protein is folded. The signal sequence in the SRP-dependent model functions by regulating SRP and then Sec61 binding. Signal peptidase recognizes the signal cleavage site of signal peptides and cleaves off the signal peptide, separating it completely from the protein (Figure 4). Oligopeptidases usually digest the cleaved signal peptide into free amino acids. However, sometimes certain signal peptides leak into the cytoplasm and bind to proteins like calmodulin (Martoglio et al., 1997). Therefore, signal peptides may have additional functions once cleaved from their original protein (von Heijne, 1998).

SRP-independent translocation can occur either cotranslationally or posttranslationally depending on the factors involved. In the absence of a highly hydrophobic region in bacteria and yeast, chaperone proteins translocate the translated proteins to the ER in a relaxed structure. In yeast, the nascent chain-associated complex can act as a chaperone by interacting with the ribosomal complex near the site the SRP binds and can interact with the SRP itself (Grallath et al., 2006). In Escherichia coli, the chaperone trigger factor translocates proteins independent of the SRP (Lee and Bernstein, 2001). During posttranslational translocation, the mRNA translates into a polypeptide chain on free cytosolic ribosomes and then is transported to the ER independent of SRP. The Sec62/63 complex can recognize a signal sequence and a chaperone (BiP) brings the polypeptide chain into the ER. Some SRP-independent translocation pathways may rely on mRNA complexes more than signal sequences (Kraut-Cohen and Gerst, 2010). In humans, Staufen1, Straufen2, PUM1, and PUM2 may also help direct mRNA to the ER without the use of SRP (Kiebler et al., 1999; Duchaine et al., 2002; Brendel et al., 2004;

Galgano et al., 2008). Although not fully developed, the SRP-independent pathways show that the SRP is not always necessary for ER targeting.

The importance of a functional signal peptide in membrane bound proteins can be illustrated with the type III splice variant of the parathyroid hormone (PTH)/PTH-related peptide (PTHrP) receptor gene, also known as PTH1. PTH1 has also been shown to associate with the RAMP2. The variant has a deletion in the hydrophobic region of the signal peptide, resulting in weak receptor expression in the plasma membrane and no detectable ligand binding. PTH and PTHrP induced a weak cAMP stimulation in COS-7 cells transfected with the type III PTH1 receptor when compared to COS-7 cells transfected with the type I PTH1 receptor. They both had similar EC_{50}s with PTH(1-34), PTH(1-84), and hPTHrP(1-36), however the type III PTH1 receptor expressing cells had a decreased maximum stimulation compared to COS-7 cells expressing type I (Joun et al., 1997).

Investigation of the splice variants of the pufferfish RAMP2s reveal changes in their signal peptide regions (Nag et al., 2006). Despite the deletion in the signal sequence of the pufferfish splice variant mfRAMP2b, the protein still retains a signal peptide and has similar cAMP accumulation as the nonvariant mfRAMP2a when coexpressed with a CL and stimulated with increasing concentrations of adrenomedullin. Alternatively, the expression of mfRAMP2a is relatively greater than mfRAMP2b in the kidney, gill and heart.

Dr. Rorabaugh first identified a rat RAMP2 splice variant, RAMP2b, in a rat aortic smooth muscle cell line (SV40LT-SMC), rat lung and rat vas deferens (Rorabaugh, 2002). RAMP2b has a 26 amino acid deletion in the signal peptide. Whether the

rRAMP2b retained a signal peptide or had any functional significance was not known.

Hypothesis

I hypothesize that the rat RAMP2 alternatively spliced variant, which has a modified signal peptide region, alters the activity of the AM_1 receptor.

Objectives

The overall goal of this investigation was to study the functional significance of alternative splice variants for the rat and human RAMP2. More specifically, it was accomplished by the following specific aims:

1. Identification of splice variants for the human RAMP2 and determine if the functional characteristics of AM_1 receptor changes with the human RAMP2 variant by performing a cAMP assay
2. Identify genomic splice sites for the rat RAMP2b splice variant and compare the putative protein sequence to that of the nonvariant rat RAMP2
3. Clone and express the rat RAMP2b splice variant in COS-7 cells and determine if the deletion in the signal peptide of the rat RAMP2b interferes with the protein's ability to traffic to the plasma membrane or form a functional AM_1 receptor

CHAPTER 2

IDENTIFICATION OF A SPLICE VARIANT AND A PCR ARTIFACT FOR THE HUMAN RAMP2

Abstract

The mammalian receptor activity-modifying protein (RAMP) family consists of three members (1-3) that have no known function when expressed by themselves. The RAMPs form heterodimers with GPCRs to create a functional receptor complex or exist as homodimers in the endoplasmic reticulum. Recently, RAMP splice variants have been identified in the rat and pufferfish. Therefore, RT-PCR was used to determine if there are any splice variants for the human RAMP2. During these experiments, both a PCR artifact, simulating a splice variant, and a valid human RAMP2 splice variant were discovered. The PCR artifact has a deleted region in the signal peptide and was most likely formed due to a secondary structure of the cDNA. PCR in the presence of DMSO eliminates the secondary structure of the DNA template and prevents the formation of the artifact. The non-artifact human RAMP2 splice variant I discovered contains an additional fifteen nucleotides, or five putative amino acid residues. This intron inclusion appears in the N-terminus of the protein, which is important for adrenomedullin stimulation of the receptor complex. An adrenomedullin receptor (AM_1) consists of the RAMP2 forming an oligomer with a CL homo-oligomer. A full-length human RAMP2 splice variant was constructed from the variant RT-PCR amplicon of the 5′ region of the gene, and the PCR product of the 3′ half of the gene. The human variant was cloned and coexpressed with the human CL in COS-7 cells but did not show any significant

difference in cAMP accumulation from the expression of the non-variant and human CL.

Introduction

RAMPs were first isolated by expressed sequence tags, short fragments sequenced from cloned mRNA (McLatchie et al., 1998). Since the discovery of RAMPs, many researchers use RT-PCR to determine if RAMPs are present in cell lines and tissues. RT-PCR uses the enzyme reverse transcriptase to generate cDNA using RNA as a template and uses a high fidelity thermostable DNA polymerase to amplify the cDNA and reduce errors in DNA replication. The PCR products can be visualized on an ethidium-stained agarose gel to establish the size of the product and, after the DNA amplicons are sequenced, one can determine if they represent RAMP products and if any nucleotide variations exist that might be evidence of splice variants.

Our laboratory studies the AM_1 in rat aortic smooth muscle cells. During this research, a RT-PCR revealed a rat RAMP2 splice variant (Rorabaugh, 2002). Further experiments were needed to verify that SK-N-MC cells, a human neuroblastoma cell line, have RAMP2 as previously shown by McLatchie et al. and to determine if any splice variants were present (McLatchie et al., 1998).

Even though pufferfish have five RAMPs (mfRAMP1-5), the mfRAMP2 and mfRAMP3 each have one splice variant (Nag et al., 2006). Both the mfRAMP2a and mfRAMP2b are functional, with different preferences to the three CLs and adrenomedullin peptides. The pufferfish has five endogenous adrenomedullin ligands, but only three of them were studied. The mfRAMP2a had relatively higher expression than the mfRAMP2b. To add more complexity, the mfCLs and mfRAMPs, including mfRAMP2a and mfRAMP2b, have different expression levels in seawater and freshwater

pufferfish. RAMP2 splice variants are also predicted for the chimpanzee (accession numbers XM_001160651.1 and XM_511520.2).

Materials and Methods

Chemicals and Reagents. SK-N-MC human neuroblastoma cells were kindly donated by Dr. Myron Toews of the University of Nebraska Medical Center (Omaha, NE). Human lung total RNA was purchased from Ambion (Austin, TX). Dulbecco's modified Eagle medium, antibiotic/antimycotic (containing 10,000 units/ml penicillin G, 10,000 μg/ml streptomycin and 25 μg/ml amphotericin B), TRIzol, *Taq* DNA polymerase, Platinum® *Pfx* DNA polymerase, 10 x PCR Buffer (200 mM Tris-HCl, pH 8.4, 500 mM KCl), amplification grade DNase I, 10 mM dNTP mix, T_4 DNA ligase, 100 base pair ladder, agarose, TA-cloning kit (containing with pCR® 2.1 vector and One Shot® INVαF′ Chemically Competent *E. coli*), pcDNA™ 3.1(+), *Xho*I, *BamH*I, *Eco*RI, and trypsin were purchased from Invitrogen (Grand Island, NY). Certified fetal bovine serum (FBS) was purchased from Invitrogen (Grand Island, NY) and Atlanta Biologicals (Lawrenceville, GA). Moloney murine leukemia virus reverse transcriptase, random hexamers, and oligo $d(T)_{16}$ were purchased from Applied Biosystems (Foster City, CA). RNasin was purchased from Promega (Madison, WI). A plasmid maxi kit and RNase A were purchased from QIAGEN (Valencia, CA). Isopropyl alcohol and DMSO were purchased from Sigma (St. Louis, MO).

Cell Culture. SK-N-MC cells were grown in Dulbecco's modified Eagle medium supplemented with fetal bovine serum (10%), penicillin G (100 units/ml), streptomycin (100 μg/ml), and amphotericin B (0.25 μg/ml). Cells were grown to confluency in 24 well plates or T-175 cell culture flasks at 37°C in a humidified incubator with an

atmosphere of 5% CO_2/ 95% air.

RNA Isolation and Analysis. The SK-N-MC cells were washed with ice-cold phosphate-buffered saline four times. TRIzol Reagent (15 ml) was added to the flasks. The cells were scraped and separated into 1 ml aliquots. Each aliquot had 200 µl of chloroform added. The tubes were vortexed and centrifuged in an IEC Micromax Centrifuge at 12,000 x g for 15 minutes at 4°C. The aqueous layer was added to an equal volume of isopropyl alcohol and incubated at room temperature for 10 minutes. The samples were centrifuged at 12,000 x g for 10 minutes at 4°C, washed with 75% ethanol, vortexed, and centrifuged at 7,500 x g for 5 minutes at 4°C. Supernatant was removed and the ethanol evaporated. RNA was dissolved in RNase free water, stored at -70°C, concentration determined by the OD at 260 nm, purity determined by the OD260/OD280 ratio and the integrity checked on a 1% agarose gel.

RT-PCR. A DNase treatment was performed to remove any contaminating DNA from the SK-N-MC RNA samples. RNA was incubated at room temperature for one hour in the presence of 1 unit of amplification grade DNase I in DNase I buffer and 10 units of RNasin. DNase inactivation was accomplished by heating the RNA to 75°C in the presence of 2.5 mM EDTA. cDNA synthesis occurred during reverse transcription in a 10 µl volume containing 1 X PCR Buffer, 2 µg RNA, 5 mM $MgCl_2$, 1 mM dNTP mix, 25 units Moloney murine leukemia virus reverse transcriptase, and either oligo d(T), random hexamers, or both. The first RT-PCR attempts used 25 pmoles antisense primer

Table 3. Primers used in the discovery and cloning of the human RAMP2 splice variant, identification of the PCR artifact, and screening colonies in the pCRII vector. Shaded regions indicate the primer overlap as shown in Figure 5.

Primer	Sequence
hUP1	5′-CTCCTCGCCTCCTTGCTG -3′
hDN1	5′-CAGGCAATCTCGCAGGGT-3′
hUP2	5′-CCTTATAGCACCCTGCGAG -3′
hDN2	5′-TGTTGAGAAGCTCGTGCC-3′
M13 For	5′- GTAAAACGACGGCCAG -3′
M13 Rev	5′- CAGGAAACAGCTATGAC -3′

(hUP1 in Table 3) as an anti-sense primer for the RT reaction but it yielded many nonspecific bands. Therefore, oligo d(T) and random hexamers were used for priming the RT reaction. The RT reaction was incubated for 50 minutes at 42°C and 5 minutes at 95°C. The polymerase chain reaction (PCR) contained the above RT reaction and 1 X PCR buffer, 3 mM $MgCl_2$, 0.2 mM dNTP mix, 50 pmoles antisense primer, 50 pmoles sense primer, 10 µl cDNA, and 2.5 units *Taq* DNA polymerase in a final volume of 100 µl. PCR conditions were as follows: 5 minute denaturation at 95°C, followed by 37 cycles of 30 seconds at 95°C, 30 seconds at 55°C, and 30 seconds at 72°C, and a final extension of 7 minutes at 72°C. The RT-PCR products were visualized on a 3% agarose gel stained with ethidium bromide and documented. Negative control reactions (minus reverse transcriptase reactions and reagents only reactions) were performed to ensure that there was no contamination.

PCR Products into a pCRII Vector. Deoxyadenosine nucleotide 3′ overhangs were added to PCR products by incubating dATP in the presence of *Taq* polymerase for 10 min at 72°C. In this procedure the non-template dependent activity of *Taq* polymerase adds single deoxynucleotides to 3′ ends of PCR products. The specific PCR product bands with the A overhang were excised on a 0.8% Nusieve gel. The PCR product was then cloned into the pCRII cloning vector with T overhangs using the TA Cloning Kit protocol (Invitrogen) by an in-gel ligation procedure in the presence of T_4 DNA ligase. Briefly, the PCR products are separated on an agarose gel by electrophoresis. The band of interest is cut out and incubated with a vector, T_4 DNA ligase, and buffer.
The colonies were screened using Xgal for blue/white screening or by PCR using the vector primers M13 For and M13 Rev to detect inserts. The clones were sequenced

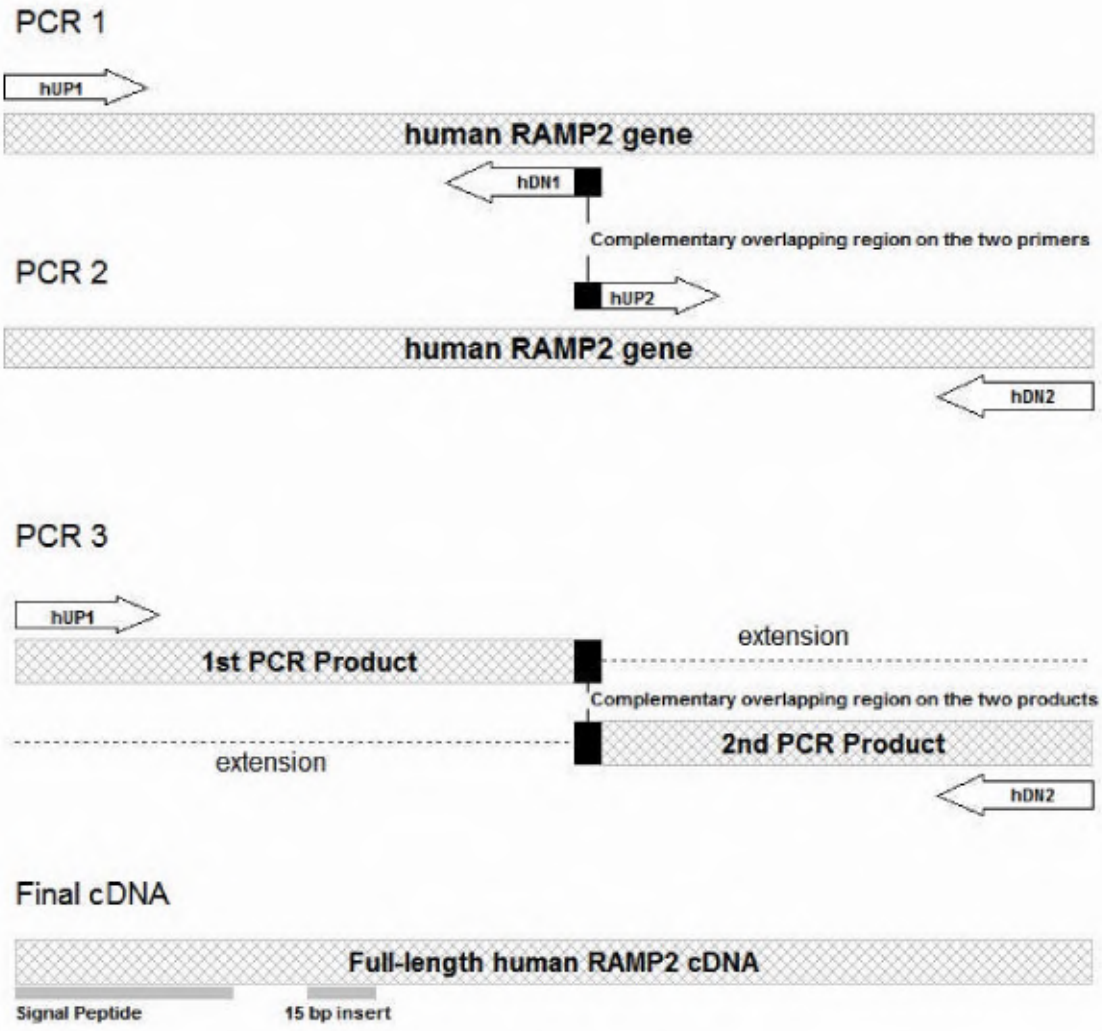

Figure 5. Creation of a full-length hRAMP2 by PCR. The 1st and 2nd PCR products are created with identical 3′ and 5′ ends (or overlapping sequences) from individual reactions. The complementary overlapping regions on the two primers are highlighted in black on the primers hDN1 and hUP2. The 3rd PCR amplification extends the original two PCR products into a full-length cDNA. The black highlighted regions on the 1st and 2nd PCR products indicate the complementary overlapping regions. The signal peptide and 15 nucleotide intron inclusion in the human RAMP2b and indicated below the full-length PCR product. This figure is adapted from *PCR Technology: Principles and Applications for DNA Amplification* (Higuchi, 1989).

using 3100 Avant Genetic Analyzer. DNA sequences were analyzed using the Wisconsin Package Version 10.1 (Genetics Computer Group, Madison, WI) software.

Creation of a Full-length hRAMP2 and Cloning in the pcDNA3.1 Vector. The PCR products of a full-length variant or nonvariant hRAMP2 were indistinguishable on a gel and thus were constructed from two halves of the cDNA using two PCR products with 5′ and 3′ complementary overhanging ends as templates (Figure 5) and the high fidelity DNA polymerase Platinum® *Pfx* DNA polymerase. The first half 5′ PCR product was generated with primers hUP1 and hDN1 and the second half 3′ PCR product was generated with primers hUP2 and hDN2. The products were separated and isolated from a 0.8% Nusieve gel, and joined in a final PCR reaction using the primers hUP1 and hDN2. The full-length PCR products were excised from a 0.8% Nusieve gel and were cloned into the pCRII cloning vector according to the TA Cloning Kit protocol (Invitrogen) and sequenced using 3100 Avant Genetic Analyzer.

The variant and nonvariant hRAMP2s were digested with *Xho*I and either *Eco*RI or *BamH*I and treated with shrimp alkaline phosphatase. The pcDNA3.1 + zeo (Invitrogen) vector was digested with *Xho*I, and *Eco*RI or *BamH*I and gel excised from a 0.8% Seaplaque gel. The cDNA was gel excised from a 0.8% NuSieve gel and ligated with T4 DNA ligase into the pcDNA3.1+zeo (Invitrogen) vector overnight. The recombinant DNA was transformed into bacteria. These new clones were sequenced and analyzed as described above.

Alkaline Lysis Miniprep. Briefly, a single colony was isolated and incubated in 5 ml LB medium in the presence of 50 μg/ml kanamycin overnight in a cell shaker at 37°C. The cells were pelleted and resuspended in a 100 μl solution I (50 mM glucose, 10 mM

EDTA, and 25 mM Tris, pH=8). The cells were lysed with a 200 µl 0.2 M NaOH and 1% SDS and the bacterial chromosomal-protein-SDS complex was precipitated out with 150 µl of potassium acetate (3 M potassium acetate, 2 M glacial acetic acid). The sample was digested with 3 µl of 10 mg/ml of DNase-free RNase to remove any contaminating RNA. The DNA was extracted with equal volumes of phenol/ chloroform/ isoamyl alcohol (25:24:1) and washed with ethanol. The DNA was resuspended in 10-20 µl sterile water.

PCR to Remove Secondary Structures with DMSO. The polymerase chain reaction (PCR), contained the above RT reaction, and 1 X PCR Buffer, 3 mM $MgCl_2$, 0.2 mM dNTP mix, 50 pmoles antisense primer hDN1 (Table 3), 50 pmoles sense primer hUP1, 10% DMSO, 2.5 units *Taq* DNA polymerase, and 10 ng cDNA. PCR conditions were as follows: 5 minute denaturation at 95°C, followed by 37 cycles of 30 seconds at 95°C, 30 seconds at 55°C, and 30 seconds at 72°C, and a final extension of 7 minutes at 72°C. Additional PCR products were amplified in 1% and 5% DMSO. The PCR products were visualized on a 3.5% MetaPhor agarose (Cambrex Bio Science Rockland, Inc. Rockland, Maine) gel stained with ethidium bromide.

Measurement of Intracellular cAMP Using the DPCI Radioassay. One day prior to transfection, COS-7 cells were plated into 24 well plates and were grown in Dulbecco's modified Eagle medium supplemented with fetal bovine serum (10%) in the absence of antibiotics and antimycotics, which may decrease transfection efficiency. Confluent cells were transfected using Lipofectamine™ 2000 (Invitrogen). Two days after transfection, the media was removed and the cells were washed twice with HEPES buffered Krebs solution containing isobutylmethylxanthine (HKI) (20mM HEPES, 4 mM

$NaHCO_3$, 11 mM dextrose, 1.25 mM NaH_2PO_4, 120 mM NaCl, 5.5 mM KCl, 2.5 mM $CaCl_2$, 1.2 mM $MgCl_2$, and 0.5 mM isobutylmethylxanthine) prepared by probe sonication. The cells were preincubated for 10 minutes with 450 µl HKI and then incubated with adrenomedullin, forskolin, or additional HKI (for basal levels) for 30 minutes at 37°C. The solution was removed and replaced with 100 µl of 90% ethanol to lyse the cells. The ethanol was evaporated in an oven for approximately 25 minutes. The cells were scraped in Tris-EDTA buffer provided by DPCI. Two-thirds of each sample was incubated with Tris-EDTA, [^{3}H]cAMP, and cAMP binding protein for 2 hours in an ice water bath refrigerated at 4°C. On a magnetic stir plate, charcoal-dextran suspension was stirred at least 20 minutes before use in the refrigerator at 4°C. Five hundred microliters of ice-cold charcoal-dextran suspension was added to all tubes. The tubes were vortexed and incubated for 10 minutes on ice in the refrigerator at 4°C. The tubes were centrifuged for 10 minutes at 5000 g. Immediately after centrifugation, 1 ml of supernatant was transferred to scintillation vials. Scintillation fluid was added and the samples were counted on a liquid scintillation counter. A standard curve was also generated using serial dilutions of a known concentration of cAMP.

Results

Identification of Multiple RT-PCR Products. RT-PCR was used to determine if any splice variants are present in human lung and human SK-N-MC cells. Several different sizes of PCR products resulted from the RT-PCR of SK-N-MC RNA where the quantity and size of the amplicons appeared to depend on the reverse transcription antisense primers used in the reverse transcriptase reaction (Figure 6). Antisense primers

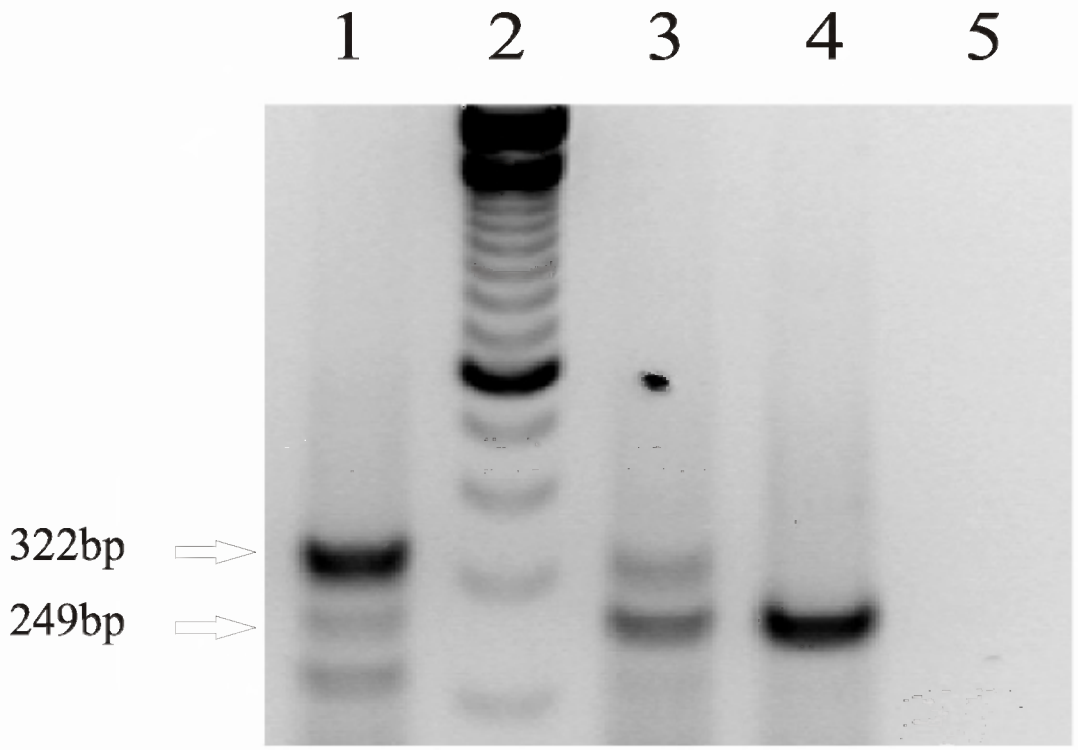

Figure 6. SK-N-MC RNA RAMP2 RT-PCR products on a 3% agarose gel stained with ethidium bromide. Oligo d(T) was the primer for cDNA synthesis (Lane 1), random hexamers were the primers for cDNA synthesis (Lane 3); and oligo d(T) and random hexamers were both used to prime the RT reaction for cDNA synthesis (Lane 4). DNase treated RNA was amplified by PCR without conversion to cDNA by reverse transcriptase (Lane 5). A 100 base pair ladder was used to reference the size of the products (Lane 2). The cDNA was amplified with primers hUP1 and hDN1 (Table 3). The 322 bp band represents the hRAMP2 and hRAMP2b and the 249 bp band represents the artifact PCR products with sizes around 249 to 259 bp.

used in the RT step for the PCR were oligo d(T)s, random hexamers, or a combination of the two. The PCR included both the hUP1 and hDN1 primers (Table 3). Using only oligo d(T)s, the reaction produced three distinct bands (Figure 6, Lane 1). The random hexamers reaction created two bands (Lane 3); whereas the reaction with both random hexamers and oligo d(T)s formed only one band (Lane 4). A RT-PCR using human lung total RNA and oligo d(T)s also produced two bands about the same size as the two bands (322 bp and 250 bp) created from the random hexamers reaction for the SK-N-MC RNA. However, these products were smeared and not distinctive bands. The bands corresponding to approximately 250 base pairs were cloned and sequenced. The sequences of two of the SK-N-MC and two of the human lung 250 bp cloned fragments were compared to the published human RAMP2 sequence (Figure 7). All of the approximately 250 bp RT-PCR products showed deletions in the signal peptide region of the human RAMP2. The signal peptide is responsible for protein transport to the endoplasmic reticulum, where it is then targeted for the plasma membrane. Interestingly, the human lung RAMP2 clone 2F and human SK-N-MC RAMP2 clone 3C have the same 68 nucleotide out of frame deletion. Missing 63 nucleotides, only the SK-N-MC RAMP2 clone 3B has an in frame deletion.

Despite multiple attempts to clone and sequence the lowest molecular weight band (Figure 6, Lane 1), I could not identify it as a product amplified from the RAMP2 gene. This band may represent non-specific truncated cDNAs formed by internal poly(A) priming (Nam et al., 2002).

Identification of a PCR artifact. The variability of the deleted region (63 to 73 bp) in the approximately 250 bp PCR products indicates that this might not be evidence of

```
            1                                                   50

Lung-2F     CTCCTCGCCT CCTTGCTGCA CGATGGCCTC .......... ..........
Lung-2E     CTCCTCGCCT CCTTGCTGCA CGATGGCCTC .......... ..........
BC027975    CTCCTCGCCT CCTTGCTGCA CGATGGCCTC GCTCCGGGTG GAGCGCGCCG
SK-N-MC-3B  CTCCTCGCCT CCTTGCTGCA CGATGGCCTC GCTCCG.... ..........
SK-N-MC-3C  CTCCTCGCCT CCTTGCTGCA CGATGGCCTC .......... ..........

            51                                                 100
Lung-2F     .......... .......... .......... .......... ..........
H Lung-2E   .......... .......... .......... .......... ........GC
BC027975    GCGGCCCGCG TCTCCCTAGG ACCCGAGTCG GGCGGCCGGC AGCGCTCCGC
SK-N-MC-3B  .......... .......... .......... .......... .........C
SK-N-MC-3C  .......... .......... .......... .......... ..........
            101                                                150
Lung-2F     ...CTCCTCC TGCTGGGCGC TGTCCTGAAT CCCCACGAGG CCCTGGCTCA
Lung-2E     CTCCTCCTTC TGCTGGGCGC TGTCCTGAAT CCCCACGAGG CCCTGGCTCA
BC027975    CTCCTCCTCC TGCTGGGCGC TGTCCTGAAT CCCCACGAGG CCCTGGCTCA
SK-N-MC-3B  CTCCTCCTTC TGCTGGGCGC TGTCCTGAAT CCCCACGAGG CCCTGGCTCA
SK-N-MC-3C  ...CTCCTCC TGCTGGGCGC TGTCCTGAAT CCCCACGAGG CCCTGGCTCA

            151                                                200
Lung-2F     GCCTCTTCCC ATCACAGGCA CACCAGGGTC AGAAGGGGGG ACGGTGAAAA
Lung-2E     GCCTCTTCCC ACCACAGGCA CACCAGGGTC AGAAGGGGGG ACGGTGAAGA
BC027975    GCCTCTTCCC ACCACAGGCA CACCAGGGTC AGAAGGGGGG ACGGTGAAGA
SK-N-MC-3B  GCCTCTTCCC ACCACAGGCA CACCAGGGTC NGAAGGGGGG ACGGTGAATA
SK-N-MC-3C  GCCTCTTCCC ATCACAGGCA CACCAGGGTC AGAAGGGGGG ACGGTGAAAA

            201                                                250
Lung-2F     ACTATGAGAT AGCTGTCCAA TTTTGCTGGA ATCATTATAA GGATCAAATG
Lung-2E     ACTATGAGAC AGCTGTCCAA TTTTGCTGGA ATCATTATAA GGATCAAATG
BC027975    ACTATGAGAC AGCTGTCCAA TTTTGCTGGA ATCATTATAA GGATCAAATG
SK-N-MC-3B  ACTATGAGAC AGCTGTCCAA TTTTGCTGGA ATCATTATAA GGATCAAATG
SK-N-MC-3C  ACTATGAGAT AGCTGTCCAA TTTTGCTGGA ATCATTATAA GGATCAAATG

            251                                                300
Lung-2F     GATCCTATCG AAATGGATTG GTGCGACTGG GCCATGATTA GCAGGCCTTA
Lung-2E     GATCCTATCG AAAAGGATTG GTGCGACTGG GCCATGATTA GCAGGCCTTA
BC027975    GATCCTATCG AAAAGGATTG GTGCGACTGG GCCATGATTA GCAGGCCTTA
SK-N-MC-3B  GATCCTATCG AAAAGGATTG GTGCGACTGG GCCATGATTA GCAGGCCTTA
SK-N-MC-3C  GATCCTATCG AAATGGATTG GTGCGACTGG GCCATGATTA GCAGGCCTTA

            301                 322
Lung-2F     TATCACCCTG CGAGATTGCC TG
Lung-2E     TAGCACCCTG CGAGATTGCC TG
BC027975    TAGCACCCTG CGAGATTGCC TG
SK-N-MC-3B  TAGCACCCTG CGAGATTGCC TG
SK-N-MC-3C  TATCACCCTG CGAGATTGCC TG
```

Figure 7. Nucleotide sequence of various RAMP2 RT-PCR products from human total RNA. Clones 2F and 2E represent cDNA from RT-PCR products from human lung total RNA. Clones 3B and 3C represent cDNA from RT-PCR products from SK-N-MC total RNA. Clone 3B has a deletion of 63 nucleotides (21 amino acids), which is the only sequence without a frameshift. The highlighted sequences represent the primers used for PCR and the underlined region represents a putative signal peptide region.

true splicing and the PCR products might represent an artifact of the RT-PCR process. To test this hypothesis increasing concentrations of DMSO were used to amplify the undeleted cloned RAMP2 cDNA (322 bp) and SK-N-MC clone 3C DNA with deleted nucleotides (259 bp) by PCR using the primers hUP1 and hDN1. DMSO relaxes secondary structure that can form in either the primers or template. DMSO concentrations of 1%, 5%, and 10% were used. PCR amplification of a cDNA template with no deletion or nonvariant hRAMP2 (322 bp) with the primers hUP1 and hDN1 in the absence of DMSO and the presence of 1% DMSO produced a smaller sized (259 bp) amplicons (Figure 8, Lane 2). PCR amplification of a cDNA template with no deletion or nonvariant hRAMP2 (322 bp) with the same primers hUP1 and hDN1 in the presence of 5% or 10% DMSO resulted in only one band, which was the size (322 bp) of the template or nonvariant hRAMP2 (Figure 9, Lane 4). This indicates that RT-PCR product with the human RAMP2 deletion was in fact a PCR artifact that was most likely due to a secondary structure formed by the cDNA. In the absence of DMSO, the plasmid hRAMP2 becomes the same size as the artifact in two different reactions with the primer combinations hUP1:hDN1 and hUP1:hDN2 (Figure 8, Lanes 2 and 7, respectively). The new PCR product was sequenced to confirm that the sequence was identical to the PCR product formed by RT-PCR of SK-N-MC RNA and thus the 259 bp product represents an artifact of the PCR reaction in the absence of DMSO.

Secondary Structure Analysis Using mfold. In order to verify that a secondary structure exists in the human RAMP2 DNA in the signal peptide region, the nucleic acid sequence was entered into the mfold web server. The mfold web server predicts the secondary structure of single stranded nucleic acids (Zuker, 2003). First created

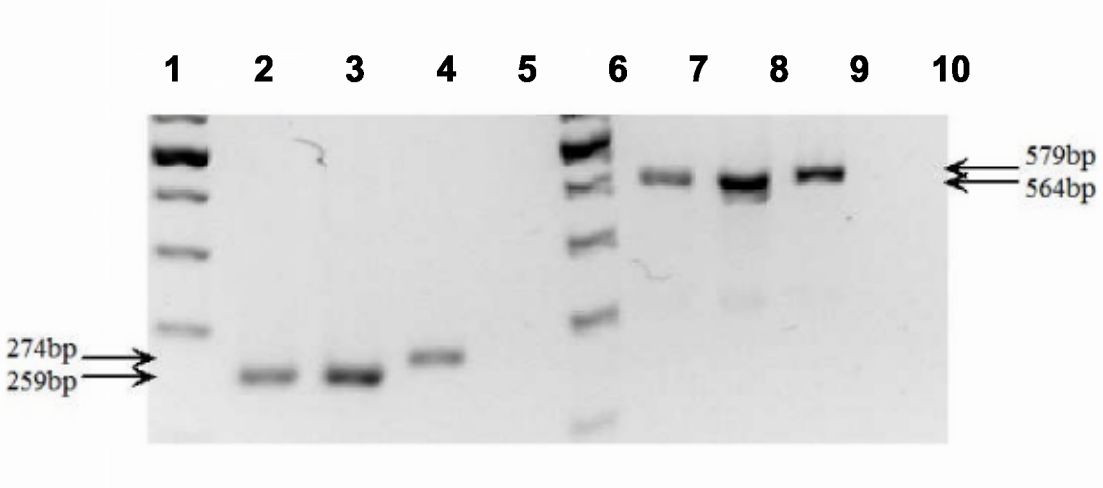

Figure 8. PCR of the hRAMP2 clones in the absence of DMSO. Human RAMP2 clones created from a RT-PCR in the absence of DMSO were sequenced and the products were visualized on a 3% agarose gel. The PCR products using primers hUP1 and hDN1 (Table 3) for the hRAMP2 (Lane 2) and artifact (Lane 3) were the same size (259 bp) even though the hRAMP2 size should be 322 bp. This suggests and was confirmed by sequencing the PCR product that the hRAMP2 has a deleted region. The hRAMP2b PCR product also has a deleted region (Lane 4). Another PCR in the absence of DMSO was performed using the hUP1 and hDN2 primers. The hRAMP2 (Lane 7) and artifact (Lane 8) produced the same size (564 bp) products. The hRAMP2b (Lane 9) also had missing nucleotides. A 100 base pair ladder was used as a reference (Lanes 1 and 6). Reactions without any DNA showed there was no contamination in the primer combinations hUP1:hDN1 and hUP1:hDN2 (Lanes 5 and 10, respectively).

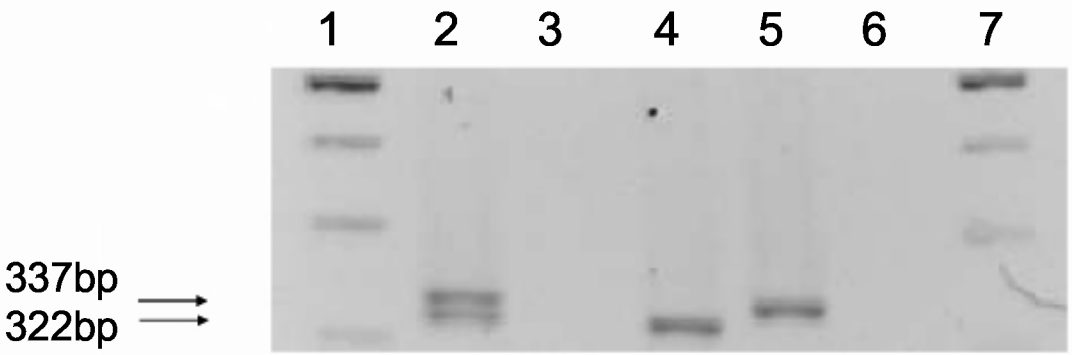

Figure 9. RT-PCR and PCR in the presence of 10% DMSO visualized on a 3.5% MetaPhor Agarose ethidium bromide stained gel. A RT-PCR of human SK-N-MC RNA using oligo d(T)s in the reverse transcription step and the primers hUP1 and hDN1 (Table 3) was repeated using 10% DMSO in the PCR step (Lane 2). The hRAMP2 and hRAMP2b could now be distinguished as two distinct bands (Lane 2). A similar reaction except without any reverse transcriptase shows there was no DNA contamination (Lane 3). A PCR of the hRAMP2 plasmid (Lane 4) and hRAMP2b plasmid (Lane 5) in the presence of 10% DMSO resulted in the expected band sizes. A PCR lacking any plasmid proves that there was no contamination of the reagents (Lane 6). A 100 base pair ladder was used as a reference (Lanes 1 and 7).

in the late 1980's to determine the folding of RNA based on minimum free energies, mfold also predicts DNA secondary structures. Although many secondary structures may occur in human RAMP2 DNA, one such folding repeatedly appears in the signal peptide region and this loop approximately corresponds to the nucleotides that are deleted during the PCR of 5′ half of the hRAMP2 (Figure 10). The inability to replicate this secondary structure of DNA by DNA polymerase most likely contributes to the formation of the PCR artifact.

Identification of a human RAMP2 splice variant. While cloning the 5′ half of the nonvariant human RAMP2, an unexpected RAMP2 splice variant was discovered. Using the primers hUP1 and hDN1, an intense band was detected at the expected size of 322 base pairs. After separating the RT-PCR product by electrophoresis on a horizontal Nusieve gel and extracting the band, the cDNA was ligated into the pCRII vector. Initial screening of the colonies with M13 primers from the vector did not show any discernable difference in the sizes of the cloned cDNA. However after sequence analysis of the cloned RT-PCR products in both directions with the M13 primers, it was determined that one of the recombinant DNA clones contained a human RAMP2 splice variant with a 15 bp insert. In order to confirm the validity of the PCR and show that the difference in size between the RT-PCR products of the nonvariant and splice variant human RAMP2s, the RT-PCR was repeated in the presence of 10% DMSO and analyzed on a 3.5% MetaPhor Agarose ethidium bromide stained gel (Figure 9). Two distinct bands at 322 and 337 bp were visible (Figure 9, Lane 2). A PCR using the primers hUP1 and hDN1 of the plasmids containing the nonvariant 322 bp hRAMP2 and variant hRAMP2 337 bp DNA in the presence of 10% DMSO still resulted in PCR products which represented the

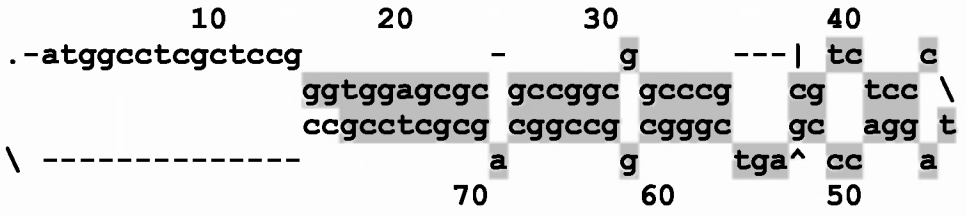

Figure 10. The mfold version 3.2 results of hRAMP2 cDNA sequence show a possible secondary structure (Zuker, 2003). This folding is near the deleted region in the hRAMP2 PCR artifact. The shaded nucleotides indicate the nucleotides not included in the SK-N-MC RAMP2 clone 3B PCR artifact.

starting templates at 322 and 337 base pairs, respectively (Figure 9, Lanes 4 and 5). Thus the PCR products are not an artifact.

I next constructed a full-length cDNA clone of the hRAMP2 splice variant which contained the 15 bp insert. The human RAMP2 variant was constructed by joining two PCR products representing the 5′ nonvariant and 3′ common halves (Figure 5). Because we already determined the sequences of the first portion of the hRAMP2 clones, we performed another PCR to amplify the last portion of the hRAMP2. This method was chosen because of the difficulty of detecting by gel electrophoresis the variant full-length cDNA (337 bp) from the nonvariant (322 bp), when using PCR primers from the 5′ and 3′ ends of the cDNA. The 5′ half was derived from the previously cloned PCR product with the 15 bp insert amplified by hUP1 and hDN1 primers (Figure 9, Lane 2 upper band). The 3′ half was amplified by RT-PCR with the hUP2 and hDN2 primers (Table 3) from SK-N-MC RNA. The hDN2 primer was based on a reported sequence that has been updated to show that it was missing a nucleotide after the stop codon. Therefore, our clones lack a nucleotide in the 3′ end of the cDNA.

The hUP2 and hDN1 primers had complementary sequences at their 3′ and 5′ ends, respectively, such that the two halves or PCR amplicons of the gene had overlapping sequences (Figure 5). I amplified the 5′ and 3′ halves together with PCR and the primer set hUP1 and hDN2 using the high fidelity DNA polymerase Platinum® *Pfx* DNA polymerase (Invitrogen) to prevent replication errors. This created a full-length hRAMP2b splice variant, which was sequenced and the sequence then was compared to the nonvariant hRAMP2 I cloned, an already published hRAMP2 (accession # BC027975), and the genomic DNA (NT 010755) (Figure 11).

```
            1                                                          50
NT 010755   CCTGCAGCTT GGGCTGGGGA TATAGGCGCC CCCACACCCG GGCCCGGCTC
BC027975    ~~~~~~~~~~ ~~~~~~~~~~ ~~~~~~~~~~ ~~~~~~~~~~ ~~~~~~~~~~
hRAMP2      ~~~~~~~~~~ ~~~~~~~~~~ ~~~~~~~~~~ ~~~~~~~~~~ ~~~~~~~~~~
hRAMP2b     ~~~~~~~~~~ ~~~~~~~~~~ ~~~~~~~~~~ ~~~~~~~~~~ ~~~~~~~~~~

            51                                                        100
NT 010755   AGCGCCGCCG CCGCTCCTCG CCTCCTTGCT GCACGATGGC CTCGCTCCGG
BC027975    ~~~~~~~~~~ ~~~~~~~~CG CCTCCTTGCT GCACGATGGC CTCGCTCCGG
hRAMP2      ~~~~~~~~~~ ~~~CTCCTCG CCTCCTTGCT GCACGATGGC CTCGCTCCGG
hRAMP2b     ~~~~~~~~~~ ~~~CTCCTCG CCTCCTTGCT GCACGATGGC CTCGCTCCGG

            101                                                       150
NT 010755   GTGGAGCGCG CCGGCGGCCC GCGTCTCCCT AGGACCCGAG TCGGGCGGCC
BC027975    GTGGAGCGCG CCGGCGGCCC GCGTCTCCCT AGGACCCGAG TCGGGCGGCC
hRAMP2      GTGGAGCGCG CCGGCGGCCC GCGTCTCCCC AGGACCCGAG TCGGGCGGCC
hRAMP2b     GTGGAGCGCG CCGGCGGCCC GTGTCTCCCT AGGACCCGAG TCGGGCGGCC

            151                                                       200
NT 010755   GGCAGCGCTC CGCCTCCTCC TCCTGCTGGG CGGTGAGCGC GGCGCCCCGA
BC027975    GGCAGCGCTC CGCCTCCTCC TCCTGCTGGG CG-------- ----------
hRAMP2      GGCAGCGCTC CGCCTCCTCC TTCTGCTGGG CG-------- ----------
hRAMP2b     GGCAGCGCTC CGCCTCCTCC TTCTGCTGGG CG-------- ----------

            201                                                       250
NT 010755   GGCCCGGGCG GGAGGCGCGA GAGGCCCCGG AGGGGAGAGG GGAGAGGGGA

            251                                                       300
NT 010755   GAGGGGCTGG ATGGCCGAGG CCGGAACGGG CCCTGGGGTG CGGGTTAGGA

            301                                                       350
NT 010755   CCGACGTACC TAGCAGCACT GGCCCTCGGA CGGTCCCTGA CCCCACCTCG

            351                                                       400
NT 010755   GGGCGGGCGC AGCATGAGCT GCTTCCCACC CAGGGAAAGC TGGGGTGCTG

            401                                                       450
NT 010755   GCCCCGGCCC CTCGAAGAGG GCTTAGGAGG ACGGAAGCTG GCCAGAGATG

            451                                                       500
NT 010755   AGGGGGCTTT GGGCCTGGGT GTGAGTGACA AGGAGCTGGT GCCAGCCCCT

            501                                                       550
NT 010755   CCCTCCCCGG CACTGAGGCG TCCGTGGGGG CTAGATTATT CCTCCTTTTC
```

Figure 11. Nucleotide sequences of the human Chromosome 17 (NT 010755) genomic region of human RAMP2, published hRAMP2 sequence (accession number BC027975), cloned hRAMP2 nonvariant (hRAMP2) and cloned variant hRAMP2b (EF687002). The bold ATG represents the methionine start site. The bold TAG represents the stop codon. The start and stop primers are underlined. The hRAMP2b partial intron inclusion is marked as (.) in the hRAMP2, the intron regions are noted as (-), and regions not cloned are illustrated as (~). The GT and AT splice sites for the cloned variant hRAMP2b (EF687002) are highlighted. The hRAMP2 and hRAMP2b were created from the primer hDN2, which is missing a nucleotide after the stop codon.

```
           551                                                  600
NT 010755  TTCCAAGGTA GCCTATTTTC GGAGGGTCTC AGTCCCCCAA CCCCCCTCGC

           601                                                  650
NT 010755  AGGCTCCACT GCCGGGGTCC CCGCTATGTT ACCCTCCTCT CCCGTTTCTT

           651                                                  700
NT 010755  CCCACAGCTG TCCTGAATCC CCACGAGGCC CTGGCTCAGC CTCTTCCCAC
BC027975   -------CTG TCCTGAATCC CCACGAGGCC CTGGCTCAGC CTCTTCCCAC
hRAMP2     -------CTG TCCTGAATCC CCACGAGGCC CTGGCTCAGC CTCTTCCCAC
hRAMP2b    -------CTG TCCTGAATCC CCACGAGGCC CTGGCTCAGC CTCTTCCCAC


           701                                                  751
NT 010755  CACAGGCACA CCAGGGTCAG AAGGTGGGTA CCCAGGGTGT GGAAGGGTGG
BC027975   CACAGGCACA CCAGGGTCAG AAG------- ---------- ----------
hRAMP2     CACAGGCACA CCAGGGTCAG AAG------- ---------- ----------
hRAMP2b    CACAGGCACA CCAGGGTCAG AAG------- ---------- ----------

           751                                                  800
NT 010755  CCGAGGGTAA GGACGAGAGC AAGTTCAGTG GGGAGGGTTC CTTTCCCACG

           801                                                  850
NT 010755  AGGCCTGCCC AACCCCAGCT GATGCCCCAC TACACTCCCC TCTGTTCTTT

           851                                                  900
NT 010755  CTTGGGGTTC CTCGTGGTCT TTCTCCCTGT CCTCCTACAA AGCCCCTGCA

           901                                                  950
NT 010755  CGGCTCTGAG CTGCCCACCT CACAAGTGGG CGAGAAGACC CCAGGAAAAG

           951                                                 1000
NT 010755  GTGTACGTGG AAGTTCTTAT CAGGCTGGGA TGGAAAGTGC TTAGCACATG

           1001                                                1051
NT 010755  GAAGTCATTA TAGGATTCCT GAGCTGGGAC TCTGTCCTCA GCCAGAATGT

           1051                                                1100
NT 010755  TTTGCTAGGG AAACTTTCTG AAGGGTTCCC ACGTTTGAAG ACAGGCAGTT

           1001                                                1150
NT 010755  CACCTTGCAA GCACCTGGGC AGGAGGGTTT GTAGGGAGGG GTAGGGGTGT

           1151                                                1200
NT 010755  GGTCATTGTG TAGCATCTGT ACCTACAGGG GGGACGGTGA AGAACTATGA
BC027975   ---------- ---......... ......GG GGGACGGTGA AGAACTATGA
hRAMP2     ---------- ---......... ......GG GGGACGGTGA AGAACTATGA
hRAMP2b    ---------- ---CATCTGT ACCTACAGGG GGGACGGTGA AGAACTATGA

           1201                                                1250
NT 010755  GACAGCTGTC CAATTTTGCT GGAATCATTA TAAGGATCAA ATGGATCCTA
BC027975   GACAGCTGTC CAATTTTGCT GGAATCATTA TAAGGATCAA ATGGATCCTA
hRAMP2     GACAGCTGTC CAATTTTGCT GGAATCATTA TAAGGATCAA ATGGATCCTA
hRAMP2b    GACAGCTGTC CAATTTTGCT GGAATCATTA TAAGGATCAA ATGGATCCTA
```

```
           1251                                                1300
NT 010755  TCGAAAAGGA TTGGTGCGAC TGGGCCATGA TTAGCAGGTA GGGGCAGTGA
BC027975   TCGAAAAGGA TTGGTGCGAC TGGGCCATGA TTAGCAG--- ----------
hRAMP2     TCGAAAAGGA TTGGTGCGAC TGGGCCATGA TTAGCAG--- ----------
hRAMP2b    TCGAAAAGGA TTGGTGCGAC TGGGCCATGA TTAGCAG--- ----------

           1301                                                1350
NT 010755  TGGAGGGTGG CTCAGGCCAG GGGGTGGACC TGCTCATTGC AGGTAGACCC

           1351                                                1400
NT 010755  TGAGTGAGAG TGGGGCACTC TTCTCCCTGG GTCCACCCCC TCTCTCACTC

           1401                                                1450
NT 010755  AAGTCCTCTT CTGCCCCTAG GCCTTATAGC ACCCTGCGAG ATTGCCTGGA
BC027975   ---------- ---------- GCCTTATAGC ACCCTGCGAG ATTGCCTGGA
hRAMP2     ---------- ---------- GCCTTATAGC ACCCTGCGAG ATTGCCTGGA
hRAMP2b    ---------- ---------- GCCTTATAGC ACCCTGCGAG ATTGCCTGGA

           1451                                                1500
NT 010755  GCACTTTGCA GAGTTGTTTG ACCTGGGCTT CCCCAATCCC TTGGCAGAGA
BC027975   GCACTTTGCA GAGTTGTTTG ACCTGGGCTT CCCCAATCCC TTGGCAGAGA
hRAMP2     GCACTTTGCA GAGTTGTTTG ACCTGGGCTT CCCCAATCCC TTGGCAGAGA
hRAMP2b    GCACTTTGCA GAGTTGTTTG ACCTGGGCTT CCCCAATCCC TTGGCAGAGA

           1501                                                1550
NT 010755  GGATCATCTT TGAGACTCAC CAGATCCACT TTGCCAACTG CTCCCTGGTG
BC027975   GGATCATCTT TGAGACTCAC CAGATCCACT TTGCCAACTG CTCCCTGGTG
hRAMP2     GGATCATCTT TGAGACTCAC CAGATCCACT TTGCCAACTG CTCCCTGGTG
hRAMP2b    GGATCATCTT TGAGACTCAC CAGATCCACT TTGCCAACTG CTCCCTGGTG

           1551                                                1600
NT 010755  CAGCCCACCT TCTCTGACCC CCCAGAGGAT GTACTCCTGG CCATGATCAT
BC027975   CAGCCCACCT TCTCTGACCC CCCAGAGGAT GTACTCCTGG CCATGATCAT
hRAMP2     CAGCCCACCT TCTCTGACCC CCCAGAGGAT GTACTCCTGG CCATGATCAT
hRAMP2b    CAGCCCACCT TCTCTGACCC CCCAGAGGAT GTACTCCTGG CCATGATCAT

           1601                                                1650
NT 010755  AGCCCCCATC TGCCTCATCC CCTTCCTCAT CACTCTTGTA GTATGGAGGA
BC027975   AGCCCCCATC TGCCTCATCC CCTTCCTCAT CACTCTTGTA GTATGGAGGA
hRAMP2     AGCCCCCATC TGCCTCATCC CCTTCCTCAT CACTCTTGTA GTATGGAGGA
hRAMP2b    AGCCCCCATC TGCCTCATCC CCTTCCTCAT CACTCTTGTA GTATGGAGGA


           1651                                                1700
NT 010755  GTAAAGACAG TGAGGCCCAG GCCTAGGGGG CCACGAGCTT CTCAACAACC
BC027975   GTAAAGACAG TGAGGCCCAG GCCTAGGGGG CCACGAGCTT CTCAACA~~~
hRAMP2     GTAAAGACAG TGAGGCCCAG GCCTAGGGGG C ACGAGCTT CTCAACA~~~
hRAMP2b    GTAAAGACAG TGAGGCCCAG GCCTAGGGGG C ACGAGCTT CTCAACA~~~
```

The hRAMP2b has the GT/AG splice site, which is the most common mammalian splice site. The nucleotide sequence was translated into the putative amino acid residue sequence and was compared to the hRAMP2 and an already published hRAMP2 (Figure 12). The cloned hRAMP2 variant was then inserted into the pcDNA3.1 expression vector for transfection into cell lines.

cAMP Production. The hRAMP2b was cotransfected with human CL in COS-7 cells to determine whether adrenomedullin stimulation of the proposed hRAMP2b-CL complex can increase cAMP production. COS-7 cells were transiently transfected with human CL and either human RAMP2 or its variant, human RAMP2b. A cAMP radioassay was performed in duplicate. The variant and nonvariant when coexpressed with the CL showed no difference in cAMP production upon stimulation of 100 nM adrenomedullin (Figure 13). Maximal stimulation of adrenomedullin receptors has been shown at 100nM adrenomedullin in COS-7 cells transfected with hCL and hRAMP2 (Hay et al., 2003).

Discussion

Many physiological and pathological conditions alter the expression levels of RAMP2 in selective tissues. RAMP2 expression elevates during pregnancy, congestive heart failure, cardiac hypertrophy, untreated hypertension, obstructive nephropathy, diabetes, obesity, and after a myocardial infarction (Oie et al., 2000; Totsune et al., 2000; Nishikimi et al., 2001; Qi et al., 2003; Thota et al., 2003; Wang et al., 2003; Hiragushi et al., 2004; Fukai et al., 2005; Nishikimi et al., 2005; Oie et al., 2005; Yoshihara et al., 2005). However, sepsis has been shown to cause a decrease in RAMP2 expression

```
           1                                                          50
BC027975   MASLRVERAG GPRLPRTRVG RPAALRLLLL LGAVLNPHEA LAQPLPTTGT
hRAMP2     MASLRVERAG GPRLPRTRVG RPAALRLLLL LGAVLNPHEA LAQPLPTTGT
hRAMP2b    MASLRVERAG GPCLPRTRVG RPAALRLLLL LGAVLNPHEA LAQPLPTTGT

           51                                                        100
BC027975   PGSE.....G GTVKNYETAV QFCWNHYKDQ MDPIEKDWCD WAMISRPYST
hRAMP2     PGSE.....G GTVKNYETAV QFCWNHYKDQ MDPIEKDWCD WAMISRPYST
hRAMP2b    PGSEASVPTG GTVKNYETAV QFCWNHYKDQ MDPIEKDWCD WAMISRPYST

           101                                                       150
BC027975   LRDCLEHFAE LFDLGFPNPL AERIIFETHQ IHFANCSLVQ PTFSDPPEDV
hRAMP2     LRDCLEHFAE LFDLGFPNPL AERIIFETHQ IHFANCSLVQ PTFSDPPEDV
hRAMP2b    LRDCLEHFAE LFDLGFPNPL AERIIFETHQ IHFANCSLVQ PTFSDPPEDV

           151                          180
BC027975   LLAMIIAPIC LIPFLITLVV WRSKDSEAQA
hRAMP2     LLAMIIAPIC LIPFLITLVV WRSKDSEAQA
hRAMP2b    LLAMIIAPIC LIPFLITLVV WRSKDSEAQA
```

Figure 12. Putative amino acid sequences of the hRAMP2 published sequence (accession number BC027975), the cloned hRAMP2 nonvariant (hRAMP2) and the cloned alternative splice variant hRAMP2b (EF687002).

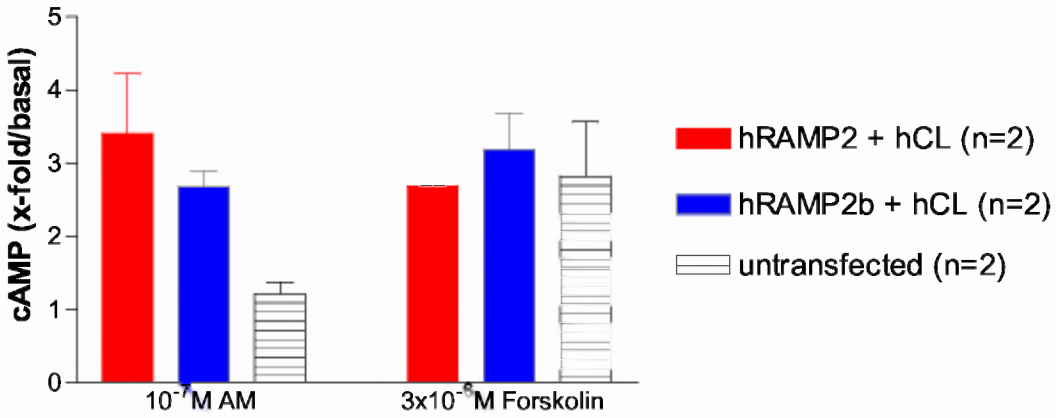

Figure 13. Stimulation of cAMP production in COS-7 cells. COS-7 cells were transfected with human CL and either human RAMP2 or the newly discovered hRAMP2b splice variant. Untransfected COS-7 cells were used as a negative control. Cells were stimulated with 100 nM adrenomedullin or 3 μM forskolin.

(Ono et al., 2000).

With the discovery of RAMP2 splice variants in rat and fish and the prediction in chimpanzee, an RT-PCR was performed on SK-N-MC RNA to determine if any human RAMP2 splice variants exist. Depending on the conditions used in the reverse transcription step the results were variable. For example, when oligo d(T) was used as the reverse transcription primer along with the two PCR primers hUP1 and hDN1, three bands were detected (approximately 322, 250 and 220 bp). The most intense band produced by the oligo d(T) reaction was the expected size of 322 base pairs along with a less intense band at 250 bp. The upper band actually contained the two different sized PCR products RAMP2 and RAMP2b (322 and 337 bp, respectively) and could be separated out on a MetaPhor agarose gel (Figure 9, Lane 2). A reaction using random hexamers yielded both the 322 bp band and 250 bp but now the most intense band was around 250 base pairs. However when both oligo d(T) and random hexamers were used in the reverse transcription step, a single band of 250 base pairs was present. Although oligo d(T) favors cDNA production at the 3′ end of the mRNA due to the lack of processivity of the reverse transcriptase enzyme and random hexamers favor transcription at the 5′ end, it is unclear to what extent oligo d(T) or random hexamers affect the amplification of the cDNA with secondary structures.

However, from the experiments where only the cDNA templates were amplified, it is evident that the PCR step alone was able to convert cDNA templates to a shortened PCR product artifact in the absence of DMSO (Figure 8, Lanes 2 and 7) but not in the presence of DMSO (Figure 9, Lane 2). Thus PCR serves as a powerful method for cDNA amplification, but limitations do occur as seen in the creation of the human

RAMP2 PCR artifact. This artifact was most likely due to folding of the cDNA, where *Taq* DNA polymerase skipped over the looped DNA. When this secondary structure was eliminated after the addition of 5% or 10% DMSO, the artifact was no longer present. DMSO is essential to proving the presence of an artifact because it promotes DNA strand separation in GC rich regions and elimination of secondary structures. The mfold web server results support the secondary structure of the DNA and the production of multiple PCR product sequences from only one cDNA template and one set of primers illustrates the potential for DNA templates with secondary structures to create artifacts during replication. Although RNA can exist without a secondary structure, RNA may require a hairpin loop for proper functioning of transcription termination and gene expression (Gollnick et al., 2005; Bevilacqua and Blose, 2008). Therefore, the hairpin loop formed in human RAMP2 may effect transcription and translation. For example, hairpin loops can stabilize the RNA polymerase complex during the initiation of transcription.

I have also used RT-PCR to identify a human RAMP2b splice variant that contains an additional 15 nucleotides and five putative amino acid residues in the N-terminus of the accessory protein between amino acid #54 and amino acid #55 (Figure 12) . The splice variant has partial intron inclusion of the second intron and uses the canonical GT/AG site with a 5' GT donor and a 3' AG acceptor. Although the splice variant does not have a specific known purpose, hRAMP2b is located in the N-terminus region, which is the most variable region between RAMP1, RAMP2, and RAMP3. The N-terminal region also contains the amino acid region crucial for adrenomedullin binding as shown in Figures 12 and 14 (Kuwasako et al., 2001).

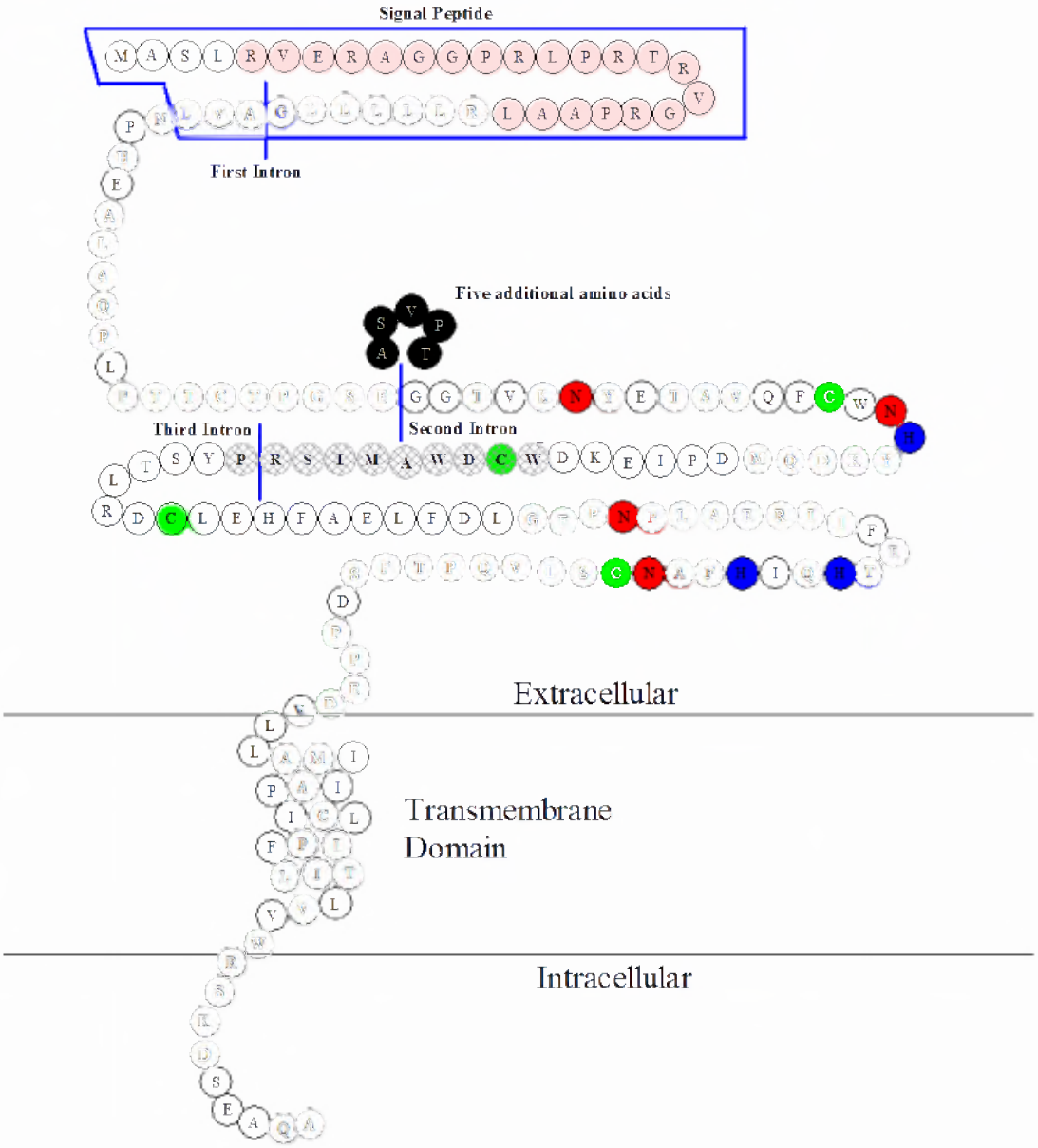

Figure 14. Human RAMP2 amino acid sequence. The pink highlighted regions are the amino acids deleted in the PCR artifact. The cysteines, histidine, and glycosylation sites are highlighted in green, blue and red, respectively. The shaded regions are amino acids critical for adrenomedullin binding (Kuwasako et al., 2001). The vertical lines indicate where the three introns are located. The hRAMP2b has fifteen nucleotides of the second intron left in the coding region to produce an additional five putative amino acid residues in the N-terminus, which are indicated by the five black amino acids at the second intron. The signal peptide has been boxed.

Adrenomedullin stimulation of COS-7 cells transfected with the human CL and RAMP2b can invoke a cAMP response (Figure 13). This cAMP response is not statistically different from COS-7 cells cotransfected with human RAMP2 and human CL. This data suggests that the hRAMP2b can form an adrenomedullin receptor similar to AM_1.

Careful examination of RT-PCR results for human RAMP2 yielded an artifact resulting from a secondary structure and the discovery of a RAMP2 splice variant. The presence of 5% or 10% DMSO prevents the formation of the artifact. This suggests that the human RAMP2 DNA can form a hairpin loop, which may alter replication and transcription rates. At first, the human RAMP2 splice variant was not detected because the size of the variant and nonvariant were so similar that their RT-PCR products appeared as one band. Sequencing of TA clones uncovered the fifteen nucleotide difference. The human RAMP2 splice variant has an intron inclusion resulting in a putative five amino acid addition in the N-terminus, which may be important for ligand binding. These findings require further investigation to determine their significance.

CHAPTER 3

IDENTIFICATION OF A SPLICE VARIANT IN RAT AORTIC SMOOTH MUSCLE CELLS AND RAT HEART BY REVERSE TRANSCRIPTION-POLYMERASE CHAIN REACTION (RT-PCR)

Abstract

An active adrenomedullin receptor is comprised of two CL (calcitonin receptor-like receptor) and the accessory protein RAMP2 (receptor activity-modifying protein 2). Activation of the receptor stimulates the production of cAMP. Receptor activity modifying proteins (RAMPs) consist of a signal peptide, an N-terminal domain, a single transmembrane domain, and a short intracellular C-terminal domain. Among mammals, there are three different types of RAMPs (1-3). While investigating the activity of adrenomedullin receptors in SV40LT-SMC (rat aortic smooth muscle) cells, evidence of an isoform of RAMP2, RAMP2b, was detected in these cells and rat heart when a partial cDNA molecule was cloned from a RT-PCR (reverse transcription-polymerase chain reaction) product. I confirmed the presence of the isoform by cloning both the full-length cDNA variant and nonvariant by RT-PCR both in the presence and absence of DMSO. Examination of the full-length RAMP2b sequence revealed it had a 26 amino acid deletion within a highly hydrophobic region of the signal peptide of the nonvariant RAMP2. Signal peptides target proteins for translocation to the endoplasmic reticulum, a requirement for cell surface expression. Analysis of the N-terminus of the RAMP2 and the RAMP2b by the SignalP 3.0 server predicted the presence and absence of a signal peptide, respectively. Kyte-Doolittle hydropathy plots also predicted a signal peptide for

the RAMP2 and not the RAMP2b. Both the rat RAMP2 and RAMP2b are expected to have a single transmembrane domain according to these plots. The server mfold was also used to determine if the cDNA was folded into a configuration that would prevent the nucleotides encoding the 26 amino acid region from being amplified by *TAQ* polymerase, but such a secondary structure configuration that was identical to this location could not be found. Thus these are further evidence for the existence of a novel splice variant for the rat RAMP2 with deletions in the putative signal peptide.

Introduction

Three RAMPs have been identified in mammals; however, five RAMPs have been discovered in pisces (fish). Additionally, a RAMP2 splice variant has been detected in pufferfish (Nag et al., 2006). Our laboratory amplified a cDNA fragment of the rat RAMP2 and discovered a splice variant (Rorabaugh, 2002). Examination of the RAMP2b sequence revealed it had a 26 amino acid deletion within the highly hydrophobic region of the signal peptide of the non-variant RAMP2. Signal peptides are the amino acids that target the protein to the endoplasmic reticulum (ER). Although they don't have a consensus sequence, signal peptides have a common structure: a short, positively charged amino-terminal region (N-region); a central hydrophobic region (h-region); and a more polar carboxy-terminal region (C-region) containing the cleavage site (von Heijne, 1985; von Heijne, 1998). Most signal peptides are then cleaved in the ER and are degraded. The protein enters the ER and the RAMP2 forms a homodimer to remain in the ER or forms a complex with the CL homo-oligomer and is targeted to the golgi complex and plasma membrane.

RAMP2 amino acid sequences are generally longer than the other RAMPs. For example, the rat RAMP2 (Accession number BAB03505) is 182 amino acids long, with 45 amino acids in the signal peptide and 106 amino acids in the N-terminus. The rat RAMP1 (NP_113833) and RAMP3 (NP_064485) have 148 and 147 amino acids, respectively. Both have about 27 amino acids in the signal peptide and 89 amino acids in the N-terminus. The N-terminal regions of RAMP1, 2, and 3 contain the amino acids (101-103, 86-92, 59-65 respectively) critical for ligand binding (Kuwasako et al., 2001; Kuwasako et al., 2003).

Human RAMP1 has a tryptophan at amino acid 74, which contributes to its higher hydrophobicity over other nonprimate RAMP1s. Both nonpeptide and peptide CGRP antagonists have been shown to be selective for primate CGRP receptors (Mallee et al., 2002; Taylor et al., 2006). Qi et al. transfected COS-7 cells with HA-CL and RAMP2-E101W, a mutant substituting a tryptophan in the position comparable to the RAMP1, to show that the receptor complex did not traffick to the plasma membrane and had no significant cAMP response upon AM, αCGRP, or βCGRP stimulation (Qi et al., 2008). When expressed with HA-CTa, the cAMP responses to AMY, αCGRP, or βCGRP were similar to control responses.

The crystal structure of the human RAMP1's extracellular domain shows that three disulfide bonds form a three-helix bundle (Kusano et al., 2008). Tryptophan at amino acid 74 is near the hydrophobic patch and helps form the binding site on the extracellular surface. The nonpeptide antagonist BIBN4096BS is selective for RAMP1 (Doods et al., 2000; Mallee et al., 2002). Recently, Miller et al. has shown that

BIBN4096BS interacts with tryptophan 74 on human RAMP1 and methionine 42 on CL (Miller et al., 2010).

Kuwasako et al. proved that some extracellular histidine residues on hRAMP2 and hRAMP3 are important for the RAMP-CL complex's function (Kuwasako et al., 2008). The hRAMP2-H71A can traffic hCL to the plasma membrane but had a lower percent specific binding and an increase EC_{50} with no change in maximal response when compared to the wildtype hRAMP2-CL complex. Cells transfected with CL and hRAMP2-H124A or H127A have a marked decrease in cell surface expression and cannot form a functional receptor complex. Despite being able to traffic to the cell surface, the hRAMP3-H97A and CL complex has decreased binding and cAMP response.

The rat RAMP2 has three *N*-glycosylation sites; whereas the rat RAMP3 has four glycosylation sites and RAMP1 lacks any glycosylation sites. *N*-glycosylation aids in the transportation to cell membrane (Rodriguez-Boulan and Gonzalez, 1999). RAMP2 and RAMP3 traffic to the plasma membrane by themselves, but RAMP1 can only traffic in the form of a heterodimer. Upon addition of glycosylation sites to mouse RAMP1 by site-directed mutagenesis, the accessory protein could traffic to the plasma membrane (Flahaut et al., 2002). Similarly, the *N*-glycosylation sites of RAMP2 and RAMP3 were mutated to serines and were not able to transport to the cell surface when expressed alone. However, the addition of the CL restored trafficking to the plasma membrane.

Both the RAMP1 and RAMP3 contain six cysteine residues, yet the RAMP2 only has four. In RAMP2, mutation of a cysteine to an alanine inhibits trafficking to the plasma membrane either by itself or when coexpressed with a CL (Kuwasako, 2003).

These are thought to be involved in disulfide bond formations. Although the crystal structure of human RAMP1 show a three helix bundle in its extracellular domain, the RAMP2 lacks the first disulfide bond between cysteine residues 27 and 82, which mutation analysis concludes is not critical for receptor function (Steiner et al., 2003). The second and third helices have a greater impact on receptor function than the first helix (Simms et al., 2009).

All RAMPs contain a single transmembrane domain (about 22 amino acids) and a short intracellular tail (about 9 amino acids) (Figure 14). Only the RAMP3 contains a PDZ (Post synaptic density, Disc large protein and ZO=1 proteins) binding domain in its C-terminal tail that allows the receptor complex to recycle to the plasma membrane (Bomberger et al., 2005a). The RAMP1 and RAMP2 target their receptor complexes to be degraded by lysosomes.

I wanted to further investigate the evidence for a rat RAMP2 splice variant by using primers for RT-PCR that would clone the full-length cDNA of the rat RAMP2 and RAMP2b. In addition, cloning of the full-length cDNA variant will enable an assessment of any other variations from the nonvariant in its putative amino acid sequence for the N-terminus, transmembrane domain, and C-terminus including glycosylation sites and cysteines.

Materials and Methods

Chemicals and Reagents. A rat aortic smooth muscle cell line (SV40LT-SMC cells) was purchased from the American Type Culture Collection (Manassas, VA). Dulbecco's modified Eagle medium, antibiotic/antimycotic (containing 10,000 units/ml penicillin G, 10,000 μg/ml streptomycin and 25 μg/ml amphotericin B), TRIzol, *Taq*

DNA polymerase, 10 X PCR Buffer (200 mM Tris-HCl, pH 8.4, 500 mM KCl), amplification grade DNase I, 10 mM dNTP mix, T_4 DNA ligase, 100 base pair ladder, agarose, TA-cloning kit (containing with pCR® 2.1 vector and One Shot® INVαF' Chemically Competent *E. Coli*), and trypsin were purchased from Invitrogen (Grand Island, NY). Certified fetal bovine serum (FBS) was purchased from Invitrogen (Grand Island, NY) and Atlanta Biologicals (Lawrenceville, GA). Moloney murine leukemia virus reverse transcriptase, random hexamers, and oligo $d(T)_{16}$ were purchased from Applied Biosystems (Foster City, CA). RNasin was purchased from Promega (Madison, WI). RNase A was purchased from QIAGEN (Valencia, CA). Isopropyl alcohol was purchased from Sigma (St. Louis, MO).

Cell Culture. SV40LT-SMC (rat aortic smooth muscle) cells were grown in Dulbecco's modified Eagle medium supplemented with fetal bovine serum (10%), penicillin G (100 units/ml), streptomycin (100 μg/ml), and amphotericin B (0.25 μg/ml). Cells were grown to confluency in T-175 cell culture flasks at 37°C in a humidified incubator with an atmosphere of 5% CO_2/ 95% air.

RNA Isolation. The cells were washed with ice-cold phosphate-buffered saline four times. Fifteen ml of TRIzol Reagent were added to the flask. The cells were scraped and separated into 1 ml aliquots. Previously collected rat heart tissue was pulverized with a hammer. The tissue was then homogenized with 1 ml of TRIzol Reagent. Insoluble material was removed from the homogenate by centrifugation at 12,000g for 10 minutes at 4°C. Then 200 μl of chloroform was added to each aliquot. The tubes were vortexed and centrifuged in an IEC Micromax Centrifuge at 12,000 g for 15 minutes at 4°C. The aqueous layer was added to an equal volume of isopropyl alcohol

and incubated at room temperature for 10 minutes. The samples were centrifuged at 12,000 g in the IEC Micromax centrifuge for 10 minutes at 4°C, washed with 75% ethanol, vortexed, and centrifuged at 7,500 g for 5 minutes at 4°C in the IEC Micromax Centrifuge. Supernatant was removed and the ethanol evaporated. RNA was dissolved in RNase free water, stored at -70°C, and the integrity checked on a 1% agarose gel.

RT-PCR. A DNase treatment was performed to remove any contaminating DNA from the RNA samples. RNA was incubated at room temperature for one hour in the presence of 1 unit of amplification grade DNase I in DNase I buffer and 10 units of RNasin. DNase inactivation was accomplished by heating the RNA to 75°C in the presence of 2.5 mM EDTA. cDNA synthesis occurred during reverse transcription in a 10 µl volume containing 1 X PCR Buffer, 2 µg RNA, 5 mM $MgCl_2$, 1 mM dNTP mix, 25 units Moloney murine leukemia virus reverse transcriptase, and 25 pmoles antisense primer. The reverse transcription (RT) reaction incubated for 50 minutes at 42°C and 5 minutes at 95°C. The polymerase chain reaction (PCR), contained the above RT reaction, and 1 X PCR Buffer, 3 mM $MgCl_2$, 0.2 mM dNTP mix, 50 pmoles antisense primer, 50 pmoles sense primer, 10 µl cDNA, and 2.5 units *Taq* DNA polymerase. PCR conditions were as follows: 5 minute denaturation at 95°C, followed by 37 cycles of 30 seconds at 95°C, 30 seconds at 55°C, and 30 seconds at 72°C, and a final extension of 7 minutes at 72°C. The RT-PCR products were visualized on a 3% agarose gel stained with ethidium bromide. Negative control reactions (minus reverse transcriptase reactions and reagents only reactions) were performed to ensure that there was no contamination.

Full-length cDNAs were cloned into a vector to confirm the sequence of the nonvariant and any alternatively spliced variants. The PCR product bands were gel

excised on a 0.8% Nusieve gel. They were cloned into the pCRII cloning vector according to the TA Cloning Kit protocol (Invitrogen). The recombinant plasmids were isolated using an alkaline lysis miniprep protocol (below) and sequenced using 3100 Avant Genetic Analyzer. DNA sequences were analyzed using the Wisconsin Package Version 10.1 (Genetics Computer Group, Madison, WI) software.

Alkaline Lysis Miniprep. Briefly, a single colony was isolated and incubated in 5 ml LB medium in the presence of 50 μg/ml kanamycin overnight in a cell shaker at 37°C. The cells were pelleted and resuspended in solution I (50 mM glucose, 10 mM EDTA, and 25 mM Tris, pH=8). The cells were lysed with freshly made 0.2 M NaOH and 1% SDS and the bacterial chromosomal-protein-SDS complex was precipitated out with potassium acetate (3 M potassium acetate, 2 M glacial acetic acid). The sample was digested with DNase-free RNase to remove any contaminating RNA. The DNA was extracted with phenol/ chloroform/ isoamyl alcohol, washed with ethanol, and resuspended in sterile water.

Secondary Structure, Signal Peptide, and Transmembrane Domain Prediction. Secondary structure prediction was performed using mfold version 3.2 from Rensselaer Polytechnic Institute as previously described in Chapter 2. Prediction of the probability that a signal peptide is present was done using Kyte-Doolittle hydropathy plots and SignalP version 3.0 (Kyte and Doolittle, 1982; Nielsen et al., 1997; Nielsen and Krogh, 1998; Bendtsen et al., 2004). Both methods calculate scores based on the amino acid residue sequence. If the scores are high or over a threshold, a signal peptide is anticipated. Kyte-Doolittle hydropathy plots also determine the probability of a transmembrane domain.

Results

Identification of a rat RAMP2 Splice Variant. Using primers (UP1 & DN1) that were within the rat RAMP2 coding sequence, Dr. Rorabaugh discovered a rat RAMP2 splice variant, which he called the RAMP2B and is now referred to as the RAMP2b (Rorabaugh, 2002). I designed primer pairs (UP2-DN2 and UP3-DN3) outside the coding region to clone the full-length rat RAMP2 (the nonvariant RAMP2) and the splice variant RAMP2b. The primer pair UP3 and DN2 was used to clone and sequence the RAMP2b and the primer pair UP3 and DN3 was used to clone and sequence the RAMP2 (Table 4 and Figure 15). Total rat heart RNA was used to clone both the full-length RAMP2 (642 bp) and RAMP2b (564 bp) (Figure 16). RNA from the rat aortic smooth muscle cell line, SV40LT-SMC, was a template for RT-PCR with UP3 and DN2 primers and the same size amplicons of the cDNA were produced, 642 bp and 564 bp, and represent the full-length RAMP2 and RAMP2b transcripts, respectively.

Further, all clones made from different primer combinations were sequenced in both directions resulting in only one sequence. In addition, PCR using templates with DNA plasmids containing the rat RAMP2 in the absence and presence of 10% DMSO resulted only in the amplification of a RAMP2 amplicon, in contrast to that observed with a template of human RAMP2 DNA where both RAMP2 and the resultant PCR artifact were amplified in the absence of DMSO (Chapter 2). Further, multiple sized amplicons were present in the human RAMP2 artifact as opposed to only one product for the rat

Table 4. Primers used to identify and clone the rat RAMP2 and RAMP2b. Primers UP1 and DN1 were designed by Dr. Rorabaugh (Rorabaugh, 2002). The last column represents the nucleotide numbers for the primer region on the RAMP2 gene (Figure 15).

Primer	Sequence	Location
UP1	5′-CGCTCCGGGTAGAGCGCGCC-3′	31-51
DN1	5′-CCAAGGAGCAGTTGGCAAAGTG-3′	1465-1486
UP2	5′-TCGCCATCTCGCCCAA-3′	2-17
DN2	5′-GTAAGTGGGTAGGGAGGGGAGG-3′	1670-1691
UP3	5′-TCTCGCCCAAGGCGTGATG-3′	8-26
DN3	5′-TCCAGCAGGGTACAGG-3′	1642-1657

```
          1                                                          50
NM_047339 GTCGCCATCT CGCCCAAGGC GTGATGGCTC CGCTCCGGGT AGAGCGCGCC
AB042888  ~TCGCCATCT CGCCCAAGGC GTGATGGCTC CGCTCCGGGT AGAGCGCGCC
rRAMP2    ~~~~~~~TCT CGCCCAAGGC GTGATGGCTC CGCTCCGGGT AGAGCGCGCC
rRAMP2b   ~~~~~~~TCT CGCCCAAGGC GTGATGGCTC CGCTCCGGGT AGAGCGCGCC

          51                                                        100
NM_047339 CCGGGTGGAT CACAGCTCGC TGTGACCAGC GCCCAGCGGC CCGCAGCGCT
AB042888  CCGGGTGGAT CACAGCTCGC TGTGACCAGC GCCCAGCGGC CCGCAGCGCT
rRAMP2    CCGGGTGGAT CACAGCTCGC TGTGACCAGC GCCCAGCGGC CCGCAGCGCT
rRAMP2b   CCGGGTGGAT CACAGCTCG. ..........  .......... ..........

          101                                                       150
NM_047339 CCGCCTCCCT CCGCTGTTAC TGCTGCTGTT GCTGCTGCTG CTGGGCGGTG
AB042888  CCGCCTCCCT CCGCTGTTAC TGCTGCTGTT GCTGCTGCTG CTGGGCG---
rRAMP2    CCGCCTCCCT CCGCTGTTAC TGCTGCTGTT GCTGCTGCTG CTGGGCG---
rRAMP2b   .......... .......... .......... .......... .......---

          151                                                       200
NM_047339 AGCACAGCGT TGGGGCCCGG GTGGGAGATG AGGGAGGTCC GGGAGGGGAA

          201                                                       250
NM_047339 GGGGCCTGCG CCATCGAGGC CAGCACGGGA CCACCCTGCG AGTGCCAACC

          251                                                       300
NM_047339 GACGTGAGGA GCAGCTCTGA CCTGCACATG GGTCCTGAAC ACATCTCTGG

          301                                                       350
NM_047339 TTTGGCGCAG GCCAGCTACT TAGGCTGCTT CGTACTTAAG AAAAGCTGGG

          351                                                       400
NM_047339 GTGCCTGCTC GGACCCCGCA GAGAAGTCTT AGGAGGTTCA GGACTGACAA

          401                                                       450
NM_047339 AGAGGGAGAG GGCTTTGGAC TCGGGAGTGA TTGGGACGCA TCTGGTACCA

          451                                                       500
NM_047339 GCCGTTCCCT TCCCTCAATA GGACAATCCC ATGGGGGAGG AGGGGAGATT

          501                                                       550
NM_047339 ATTCTTTTTG TTCCAAAGCA GTGCTGACTT CCCAGGGCCT TGCTCGCTAC

          551                                                       600
NM_047339 CCATAAACAG GTACTACTGT TCAGACCTCT CCCCATATCA CCCCACCCTT
```

Figure 15. Nucleotide sequences of the rat Chromosome 10 (NM_047339) genomic region of rat RAMP2, published rRAMP2 sequence (accession number AB042888), cloned rRAMP2 nonvariant (rRAMP2) and cloned rRAMP2 alternative splice variant rRAMP2b (EF595744). The bold ATG represents the methionine start site. The bold TAG represents the stop codon. The primers in Table 4 are underlined. The RAMP2b deletion is marked as (.), the intron regions are noted as (-), and regions not cloned are illustrated as (~).

```
          601                                                   650
NM_047339 CTGGTTCATT TCTTTATACA GCTGTCTCAA CCTCTCCGGA GTCCCTGAAT
AB042888  ---------- ---------- -CTGTCTCAA CCTCTCCGGA GTCCCTGAAT
rRAMP2    ---------- ---------- -CTGTCTCAA CCTCTCCGGA GTCCCTGAAT
rRAMP2b   ---------- ---------- -CTGTCTCAA CCTCTCCGGA GTCCCTGAAT

          651                                                   700
NM_047339 CAATCTCATC CTACTGAGGA CAGCCTTCTG TCAAAAGGTG AGTGCCTAAG
AB042888  CAATCTCATC CTACTGAGGA CAGCCTTCTG TCAAAAG--- ----------
rRAMP2    CAATCTCATC CTACTGAGGA CAGCCTTCTG TCAAAAG--- ----------
rRAMP2b   CAATCTCATC CTACTGAGGA CAGCCTTCTG TCAAAAG--- ----------

          701                                                   750
NM_047339 TCTGAGGGAG AATGACCTAG TGGGAAGGAT AAGCCCAGCA CGGGGGAGGA

          751                                                   800
NM_047339 GTCCTTTCAC AAGACAATCC TAGAACCAAC TGATGCCCGC TAACCTCTCT

          801                                                   850
NM_047339 GGTGTCTCTT GGGGTTCCTA TGGTCTTCCT CCCTATCATC CCACAAAGCC

          851                                                   900
NM_047339 ACAGTCCAGT GCCTTGGCCC AGTTGGCTAG GTAGAGCAAG ACTAGGTCTA

          901                                                   950
NM_047339 TGTGAATATC TTGCGGGGCT AGACAATATA ATTGCCATTG CAGGATTCCC

          951                                                  1000
NM_047339 GAGCCACAGA GTTCGGGGAG AGAATGCTCC TCTCGGCCAC AAGTGTCCTG

          1000                                                 1050
NM_047339 CTAGGGAGAT TTTCAGAGGG ATTCCCTTCT CTAAAGGCAG AAGACTGTAC

          1051                                                 1100
NM_047339 TCTGGAAATA CCTGGATCAG AAGGCTCGGA GGGAGGGCCA GGGGTGTGGT

          1101                                                 1150
NM_047339 CATTGGGAAG CCTCTGTCCC CACAGGGAAG ATGGAGGACT ACGAAACAAA
AB042888  ---------- ---------- -----GGAAG ATGGAGGACT ACGAAACAAA
rRAMP2    ---------- ---------- -----GGAAG ATGGAGGACT ACGAAACAAA
rRAMP2b   ---------- ---------- -----GGAAG ATGGAGGACT ACGAAACAAA


          1151                                                 1200
NM_047339 TGTCCTACCT TGCTGGTATT ATTACAAGAC TTCCATGGAC TCTGTCAAGG
AB042888  TGTCCTACCT TGCTGGTATT ATTACAAGAC TTCCATGGAC TCTGTCAAGG
rRAMP2    TGTCCTACCT TGCTGGTATT ATTACAAGAC TTCCATGGAC TCTGTCAAGG
rRAMP2b   TGTCCTACCT TGCTGGTATT ATTACAAGAC TTCCATGGAC TCTGTCAAGG

          1201                                                 1250
NM_047339 ACTGGTGCAA CTGGACTTTG ATTAGCAGGT AGGGGCAGTG TTGAAGGAGG
AB042888  ACTGGTGCAA CTGGACTTTG ATTAGCAG-- ---------- ----------
rRAMP2    ACTGGTGCAA CTGGACTTTG ATTAGCAG-- ---------- ----------
rRAMP2b   ACTGGTGCAA CTGGACTTTG ATTAGCAG-- ---------- ----------
```

```
          1251                                                1300
NM_047339 ATGGCTCAGG CCAGGAGTTG GATCTGACCT TTGTGGGTGG GGGGTGGGGG

          1301                                                1350
NM_047339 GTCATCCTTC TCCCTGGACC CAATCCTTCC CTCACTCGAA TCCCCTACTG

          1351                                                1400
NM_047339 CTCTCCAGGT ATTACAGCAA CCTGCGGTAT TGCTTGGAGT ACGAGGCAGA
AB042888  --------GT ATTACAGCAA CCTGCGGTAT TGCTTGGAGT ACGAGGCAGA
rRAMP2    --------GT ATTACAGCAA CCTGCGGTAT TGCTTGGAGT ACGAGGCAGA
rRAMP2b   --------GT ATTACAGCAA CCTGCGGTAT TGCTTGGAGT ACGAGGCAGA

          1401                                                1450
NM_047339 CAAGTTTGGC CTGGGCTTCC CAAATCCCTT GGCAGAAAGT ATCATCCTTG
AB042888  CAAGTTTGGC CTGGGCTTCC CAAATCCCTT GGCAGAAAGT ATCATCCTTG
rRAMP2    CAAGTTTGGC CTGGGCTTCC CAAATCCCTT GGCAGAAAGT ATCATCCTTG
rRAMP2b   CAAGTTTGGC CTGGGCTTCC CAAATCCCTT GGCAGAAAGT ATCATCCTTG


          1451                                                1500
NM_047339 AGGCTCACCT GATACACTTT GCCAACTGCT CCTTGGTGCA GCCTACCTTC
AB042888  AGGCTCACCT GATACACTTT GCCAACTGCT CCTTGGTGCA GCCTACCTTC
rRAMP2    AGGCTCACCT GATACACTTT GCCAACTGCT CCTTGGTGCA GCCTACCTTC
rRAMP2b   AGGCTCACCT GATACACTTT GCCAACTGCT CCTTGGTGCA GCCTACCTTC

          1501                                                1550
NM_047339 TCCGATCCCC CAGAGGATGT GCTTCTGGCC ATGATCATAG CCCCCATCTG
AB042888  TCCGATCCCC CAGAGGATGT GCTTCTGGCC ATGATCATAG CCCCCATCTG
rRAMP2    TCCGATCCCC CAGAGGATGT GCTTCTGGCC ATGATCATAG CCCCCATCTG
rRAMP2b   TCCGATCCCC CAGAGGATGT GCTTCTGGCC ATGATCATAG CCCCCATCTG

          1551                                                1600
NM_047339 CCTCATCCCT TTCCTCGTTA CGCTTGTGGT GTGGAGGAGT AAAGACGGCG
AB042888  CCTCATCCCT TTCCTCGTTA CGCTTGTGGT GTGGAGGAGT AAAGACGGCG
rRAMP2    CCTCATCCCT TTCCTCGTTA CGCTTGTGGT GTGGAGGAGT AAAGACGGCG
rRAMP2b   CCTCATCCCT TTCCTCGTTA CGCTTGTGGT GTGGAGGAGT AAAGACGGCG

          1601                                                1650
NM_047339 ATGCGCAGGC GTAGGCTCCG CCTCTCAGCA GCCATCTTTT CCCTGTACCC
AB042888  ATGCGCAGGC GTAGGCTCCG CCTCTCAGCA GCCATCTTTT CCCTGTACCC
rRAMP2    ATGCGCAGGC GTAGGCTCCG CCTCTCAGCA GCCATCTTTT CCCTGTACCC
rRAMP2b   ATGCGCAGGC GTAGGCTCCG CCTCTCAGCA GCCATCTTTT CCCTGTACCC

          1651                                                1700
NM_047339 TGCTGGAACC AGGATCTCTC CTCCCCTCCC TACCCACTTA CTCCCATCCT
AB042888  TGCTGGAACC AGGATCTCTC CTCCCCTCCC TACCCACTTA C~~~~~~~~~
rRAMP2    TGCTGGA~~~ ~~~~~~~~~~ ~~~~~~~~~~ ~~~~~~~~~~ ~~~~~~~~~~
rRAMP2b   TGCTGGAACC AGGATCTCTC CTCCCCTCCC TACCCACTTA C~~~~~~~~~
```

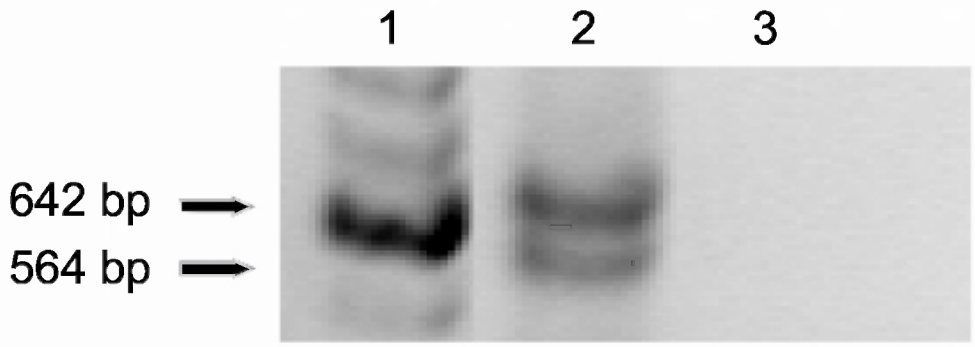

Figure 16. Full-length rat heart RAMP2 RT-PCR products on a 3% agarose gel stained with ethidium bromide. Rat heart RNA was used as a template in an RT-PCR reaction using DN2 for the antisense primer for the production of cDNA and the primers UP3 and DN2 for the PCR amplification of the cDNA (Lane 2). A PCR amplification with only rat heart RNA as a template was performed in the absence of reverse transcriptase (Lane 3). A 100 base pair ladder acted as the reference (Lane 1).

RAMP2b. Thus I have used different primer sets for RT-PCR and different sources of RNA, rat heart RNA and the SV40LT-SMC cell line used by Dr. Rorabaugh, to show evidence of the RAMP2b splice variant.

To further investigate the possibility of the rat RAMP2b being an artifact, the mfold version 3.2 was used to determine if there was a secondary structure in the region of the rat RAMP2 that might correspond to the region deleted in the rat RAMP2b variant, similar to that found for the human RAMP2 (Chapter 2). Although many secondary structures may be likely, there was only one such folding in the region deleted from the rRAMP2b (Figure 17). However, this structure does not correctly match the sequence excised in the variant. The secondary structure in Figure 17 is short 7 nucleotides on the N-terminus and extends 3 nucleotides on the C-terminus when compared to the deleted region of the variant.

Identification of a CT/AG Splice Site. The rat RAMP2 gene has four exons and three introns. Upon careful examination of the RAMP2 genomic (accession number AB042888), RAMP2 (AB042888) and RAMP2b (EF595744) sequences, the RAMP2b splice variant has a partial deletion of exon 1 (Figure 15). Most mammalian splice junctions have a 5' GT donor and a 3' AG acceptor. The rat RAMP2b has the rare CT/AG splice site, which has not yet been identified as a mammalian splice site. All other rat RAMP2 splice junctions contain the canonical GT/AG site.

Classification of the Rat RAMP2b Splice Variant. Since the splice variant has deletions in a region that might coincide to the signal peptide region, I investigated whether the rat RAMP2b had a signal peptide and could potentially traffic to the plasma membrane. There are many programs available that can identify signal peptides based on

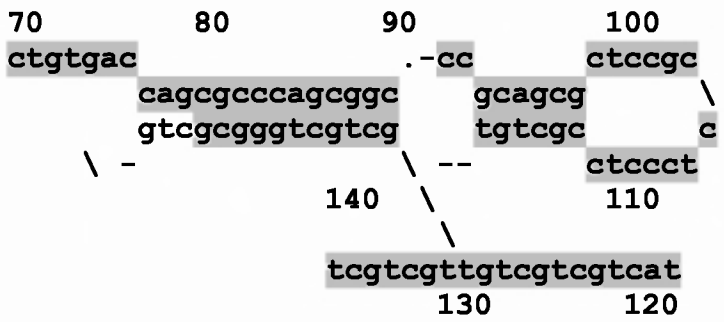

Figure 17. The mfold version 3.2 results of the rat RAMP2 cDNA sequence in the region of the rRAMP2b deletion. The shaded sections indicate the nucleotides deleted in the rRAMP2b splice variant. This shows a possible secondary structure of the rat RAMP2 cDNA but does not match the rRAMP2b's exon exclusion. The nucleotides are numbered according to Figure 15.

their predicted amino acid residue sequence. SignalP3.0 server uses the hidden Markov model to calculate the probability of whether a signal peptide is present and the position of the signal peptidase I (SPase I) cleavage site (Nielsen and Krogh, 1998; Bendtsen et al., 2004). Furthermore, this model also reports the probability of a signal anchor, previously named uncleaved signal peptides. The SignalP3.0 evaluates the sequence to determine an n-region, h-region, and c-region. SignalP3.0 predicts a signal peptide for the rat RAMP2 (99.9% probability) with a hydrophobic region consisting of 10 leucines (Figure 18a). There is a 74.4% probability that the cleavage site is between amino acids 45 and 46 (AVST/SP). SignalP3.0 does not predict a signal anchor for rRAMP2 (0.1% probability). The rRAMP2b does not have a predicted signal peptide (Figure 18b) or signal anchor (2.0% or less).

The Kyte-Doolittle hydropathy plots are also useful in prediction of signal peptides and transmembrane domains (Kyte and Doolittle, 1982). Hydrophobicity scores between -4.5 and 4.5 are assigned to each amino acid with 4.5 being the most hydrophobic and -4.5 being the most hydrophilic. Using the default window size of 9, the average hydrophobicity scores of nine amino acids are averaged and given to the middle amino acid. The averages are then graphed on the hydropathy plot. Peaks that are greater than 1.8 are signal peptides or transmembrane domains. Kyte-Doolittle hydropathy plots show that both the RAMP2 and RAMP2b have a single transmembrane domain, but only the RAMP2 has a signal peptide (Figure 19).

A.

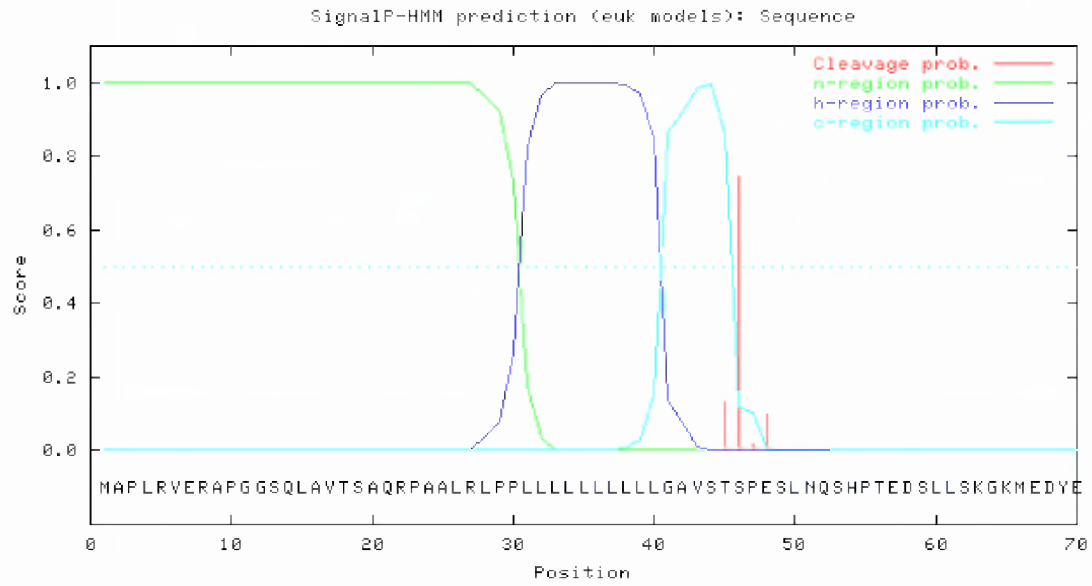

B.

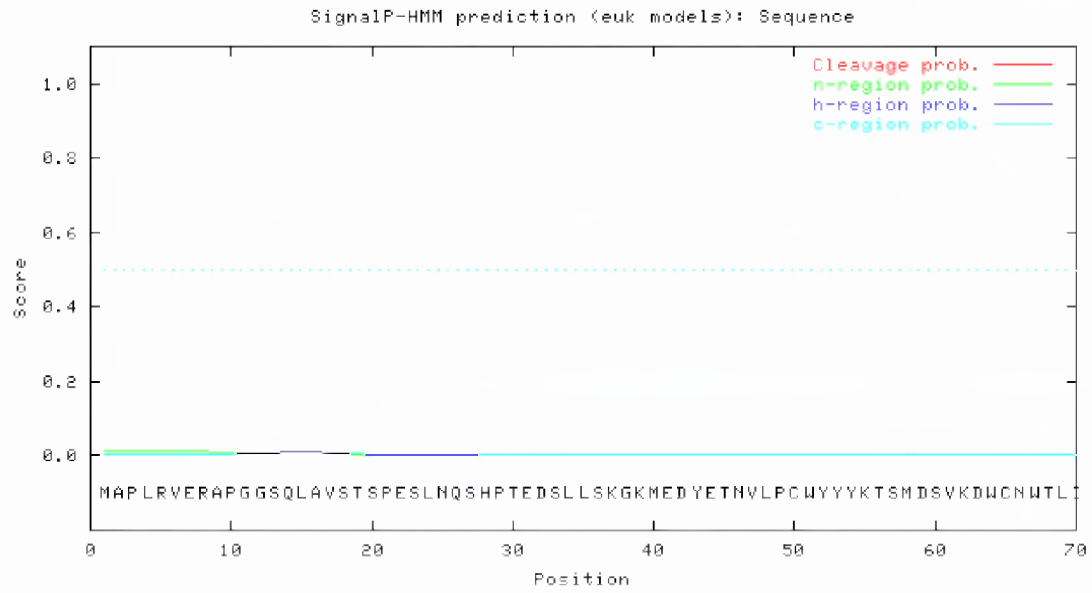

Figure 18. SignalP3.0 hidden Markov model signal peptide prediction results for the rat RAMP2 (A) and RAMP2b (B). A signal peptide is predicted for the rRAMP2 and not the rRAMP2b.

A.

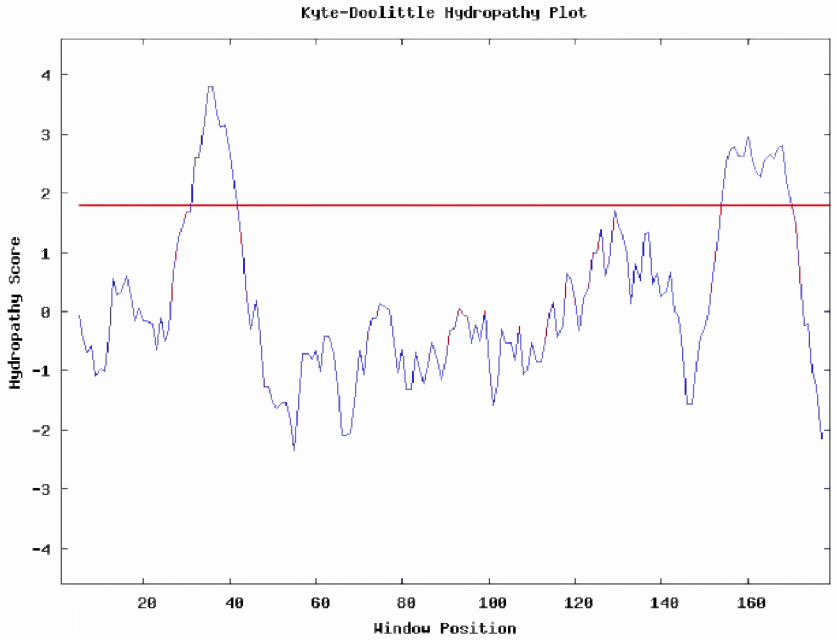

B.

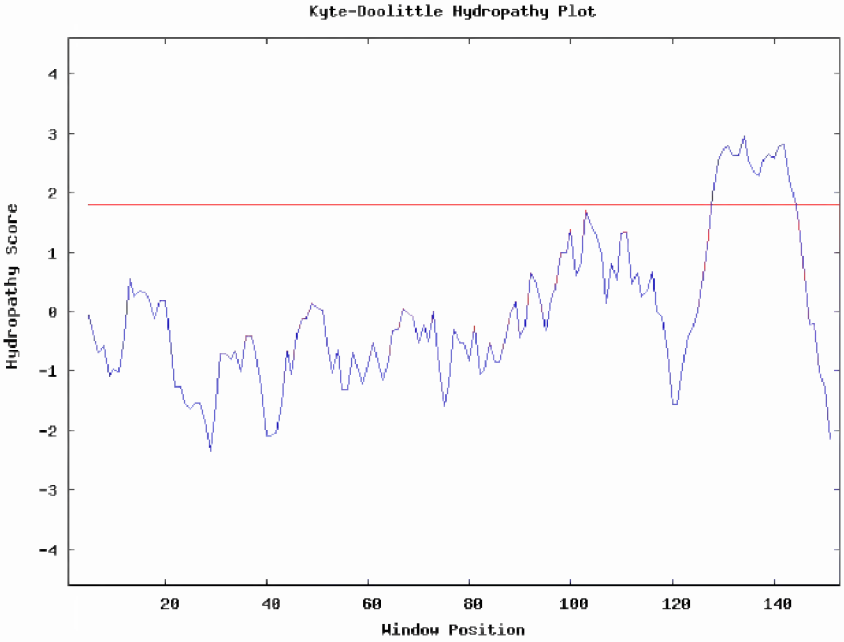

Figure 19. Kyte-Doolittle Hydropathy Plots for the rat RAMP2 (A) and RAMP2b (B). Although both the RAMP2 and RAMP2b have one transmembrane domain indicated by peaks at window position around 160 for RAMP2 and 135 for RAMP2b, a signal peptide is only predicted for the RAMP2 at window position 35. The red line indicates the cut-off value of 1.8 for significant signal peptide or transmembrane domain regions.

Discussion

While determining whether the SV40LT-SMC cells (a rat aortic smooth muscle cell line) has RAMP2 transcripts, Dr. Rorabaugh first discovered the rat RAMP2b (Rorabaugh, 2002). The rat RAMP2b is identical to the RAMP2 except it has a 78 nucleotide deletion. This deletion corresponds to the exclusion of 26 putative amino acids (A^{16} to G^{41}) in the signal peptide region (Figure 20). The remaining N-terminus including the amino acids important for ligand binding and glycosylation, transmembrane, and cytoplasmic domains are retained from the wildtype sequence.

The vast majority of splice sites follow the consensus sequence GT/AG. The intron has a GT at the 5′ end of the intron and an AG at the 3′ end. Other nonconsensus splice sites have also been identified. However, great care must be exhibited when looking through the literature and databases for splice sites.

The CT/AG splice site has been documented in several articles. However, many citations have been proven to be erroneous. For example, the statement "with the canonical sequence (CT/AG) present at each splice junction" does not make sense; yet clearly when you research the genomic sequence on NCBI (National Center for Biotechnology Information), the splice site is the true canonical splice site GT/AG (Holgate et al., 2003). Also, poorly scanned articles onto the web also show the GT/AG splice site as CT/AG in their summary on search engines (Foglio and Duester, 1996). Eden and Brunak detected a CT/AG splice site in human pre-RNA but a corrective shift of three nucleotides generates the consensus splice site, which the authors explained was due to errors in interpretation or typing (Eden and Brunak, 2004).

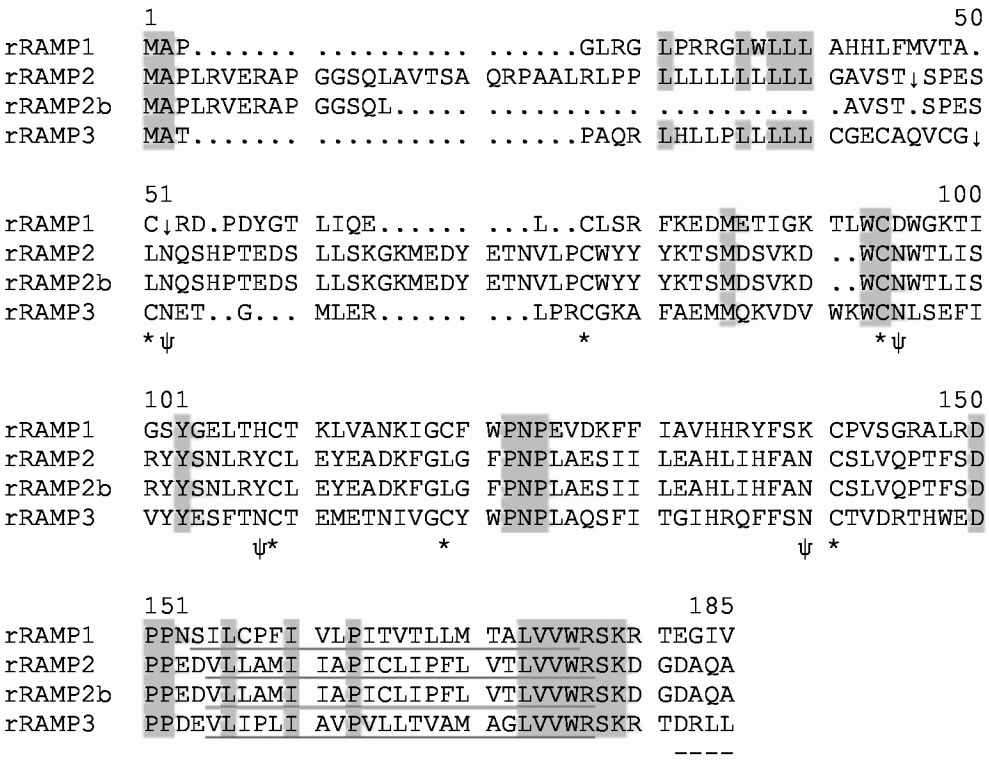

Figure 20. Comparison of the rat RAMP1 (Accession number NP_113833), RAMP2 (AB042888), RAMP2b (EF595744), and RAMP3 (NM_020100). Conserved amino acids are shaded and the transmembrane domains are underlined. Cysteine residues are indicated with a * and N-glycosylated residues are shown with a ψ. The PDZ domain in rat RAMP3 has dashes underneath it. An arrow (↓) indicates the most probable signal peptide cleavage site predicted with SignalP3.0.

Brunstein et al. found a CT/AG splice site in erythrovirus B19 using RT-PCR (Brunstein et al., 2000). However, this splice variant has not been found using other techniques and may mean that only RT-PCR can reveal small quantities of certain splice variants (Liu et al., 2004; Vashisht et al., 2004). During the discovery of the first example of an intron in *Giardia lamblia*, a flagellated protozoan, another CT/AG splice site was identified for the ferredoxin gene (Nixon et al., 2002). These findings show that CT/AG act as a splice site.

In Chinese Hamster Ovary cells, the dihydrofolate reductase mutant DS2 at the 5′ end of the intron 5 from GT to CT exhibited exon skipping of exon 5 (Mitchell et al., 1986). This data indicates that the CT/AG splice site is inactive under their conditions and the DS2 mutant, lacking exon 5, did not produce any dihydrofolate reductase activity. Although the group didn't further study the DS2 mutant, the same laboratory discovered additional mutations (reversions) that could partially reverse the inactivity of some of the previously found other (non CT/AG) dihydrofolate reductase mutants (Carothers et al., 1993).

A review by Sharma and Black discusses that the difficulty in prediction of alternative splicing is increased by intronic or exonic splicing silencer elements (ISS or ESS) and intronic or exonic splicing enhancer elements (ISE or ESE) (Sharma and Black, 2006). Silencer elements support exon skipping and enhancer elements encourage the inclusion of the exon. Sometimes these elements can act as silencers or enhancers depending upon the distance to the exon (Hui et al., 2005). These elements may also be bound to RNA-binding proteins (RBPs) (Black, 2003). Therefore, the consensus splice site GT/AG is not the only requirement for the splicing mechanism and the presence of

the splicing elements ISS, ESS, ISE, or ESE could influence the activity of the CT/AG splice site.

Unlike the human RAMP2 PCR artifact, the rat RAMP2b has a 78 nucleotide deletion due to alternative splicing. The human RAMP2 PCR artifact was most likely formed due to a secondary structure because addition of 5% or 10% DMSO in the reaction mix prevented formation of the extra "artifact" products. Addition of 5% or 10% DMSO in the rat RAMP2 PCR mix did not change the products. Additionally, the human RAMP2 PCR in the absence of DMSO created many different sequences; whereas the rat RAMP2 PCR in the absence and presence of DMSO produced one consistent nucleotide sequence suggesting site specific splicing in the rat RAMP2. Also mfold data show a longer region of consecutive hydrogen bonding in the human RAMP2 with an optimal energy of -225 kcal/mol. The rat RAMP2 secondary structure has an optimal energy of -202.9 kcal/mol. The rat RAMP2b is a splice variant and not an artifact of PCR.

All three of the RAMPs contain a signal sequence, which targets the protein for secretory vesicles, lysosomes, or the plasma membrane. Cytoplasmic proteins normally do not contain such a sequence. The signal peptide usually has a short, positively charged amino-terminal region, a central hydrophobic region and a polar carboxy-terminal region with the cleavage site. However, the rat RAMP2b lacks 26 amino acids in a highly hydrophobic region of the signal peptide; therefore prediction servers were used to determine the probability of the protein having a signal peptide.

SignalP3.0 and Kyte-Doolittle hydropathy plots predict that the nonvariant rat RAMP2 has a signal peptide, as previously reported. However, both also suggest an

absence of a signal peptide in the rat RAMP2b. Without a signal peptide or signal anchor, the signal recognition particle (SRP) may not recognize the protein as targeted for the ER and will likely remain in the cytosol. Further experimentation in chapter 4 explore whether the rat RAMP2b variant that lacks a recognizable signal peptide can traffic to the plasma membrane and can function as an adrenomedullin receptor when coexpressed with the CL.

CHAPTER 4

FUNCTIONAL EVIDENCE FOR THE RAT RAMP2 SPLICE VARIANT

Abstract

Receptor activity-modifying protein 2 (RAMP2) forms a hetero-oligomer with the calcitonin receptor-like receptor (CL) to produce an adrenomedullin receptor. Recently, splice variants in the signal peptide region of RAMP2 have been identified in the pufferfish and rat and predicted in the chimpanzee. The splice variant rat RAMP2b has a 26 amino acid deletion in a highly hydrophobic region of the signal peptide.

My goal was to determine whether or not the deletion of 26 amino acids from the signal peptide of RAMP2 (RAMP2b) affected the trafficking of the AM_1 receptor to the plasma membrane or the receptor activity. I transiently co-transfected COS-7 cells with an N-terminal HA-tagged CL and either the wildtype RAMP2, containing the intact signal peptide, or the RAMP2b. Forty-eight hours after transfection, non-permeabilized live cells were immunostained with HA and RAMP2 primary antibodies to determine if epitopes of the proteins were present on the outer surface of the plasma membrane. A RAMP2 mutant, lacking the entire signal peptide, was also constructed and tested. My studies showed that both the rat RAMP2 and RAMP2b was present at the cell membrane in the presence or absence of CL, but that the RAMP2 mutant without the signal peptide did not reach the plasma membrane, even though it was detected inside the cells. After determining that the rRAMP2b did traffic to the cell membrane, the adrenomedullin receptor function was tested by stimulating the co-transfected COS-7 cells with adrenomedullin and measuring the cAMP levels either directly or indirectly with

luciferase. The rRAMP2b and hCL transfected COS-7 cells showed a decrease in adrenomedullin receptor activity.

Introduction

Receptor activity-modifying protein 2 (RAMP2) was isolated from human neuroblastoma SK-N-MC based on expressed sequence tag sequences (McLatchie et al., 1998). When coexpressed with the CL, it forms a functional adrenomedullin receptor (AM_1). Adrenomedullin binds to AM_1 and dissociates the G protein complex followed by a release of $G_{\alpha S}$ which activates adenylyl cyclase and increases intracellular cAMP levels. A receptor component protein (RCP) may also be required for signal transduction (Prado et al., 2001).

All three of the RAMPs contain a signal sequence that targets the protein for the plasma membrane. The signal peptide usually has a short, positively charged amino-terminal region, a central hydrophobic region and a polar carboxy-terminal region with the cleavage site. The hydrophobic region is recognized by a ribonucleoprotein complex, the signal recognition particle (SRP). During protein synthesis, the SRP transports the ribosome to the ER membrane. A channel, called the translocon, opens so that the protein, which is still being translated, can enter the ER. Signal peptidase recognizes the signal cleavage site and cleaves off the signal sequence, separating it completely from the protein.

While studying the rat aortic smooth muscle cell line, we identified a RAMP2 splice variant, the rat RAMP2b (Rorabaugh, 2002). A RAMP2 splice variant was detected in the pufferfish and a chimpanzee sequence predicts a splice variant. These

variants show differences in the signal peptide. Signal peptides usually have about 20-30 nucleotides and contain an n, h, and c region (von Heijne, 1985). The h region, or hydrophobic region, is critical for function (Kaiser et al., 1987). Because the rat RAMP2b lacks 26 putative amino acids in the signal peptide, it may not be recognized by the SRP and thus not traffic to the ER and form a hetero-oligomer with CL. In order to determine if the presence of RAMP2b affects transport to the membrane or reduces AM receptor activity, COS-7 cells were transfected with the putative splice variant. COS-7 cells endogenously express the receptor coupling protein (RCP) but not the CL protein and thus are ideal to use in transfection studies (Evans et al., 2000).

Materials and Methods

Chemicals and Reagents. The African Green Monkey kidney cell line (COS-7 cells) was purchased from the American Type Culture Collection (Manassas, VA). Dulbecco's modified Eagle medium, antibiotic/antimycotic (containing 10,000 units/ml penicillin G, 10,000 μg/ml streptomycin and 25 μg/ml amphotericin B), 100 base pair ladder, agarose, pcDNA™ 3.1(+), pcDNA™ 3.1/ Zeo(+), shrimp alkaline phosphatase, *Xho*I, *BamH*I, phenol, Lipofectamine™ 2000, OptiMeM 1 reduced serum medium, mouse anti-HA antibody and trypsin were purchased from Invitrogen (Grand Island, NY). Certified fetal bovine serum (FBS) was purchased from Invitrogen (Grand Island, NY) and Atlanta Biologicals (Lawrenceville, GA). Luciferase Assay System and Luciferase Cell Culture Lysis 5X Reagent were purchased from Promega (Madison, WI). A plasmid maxi kit and RNase A were purchased from QIAGEN (Valencia, CA). Adrenomedullin was purchased from Peninsula Laboratories (San Carlos, CA).

Forskolin, isopropyl alcohol, and isobutylmethylxanthine were purchased from Sigma (St. Louis, MO). RAMP2 (H-139, sc-11380) and CRLR (V-20, sc-18007) antibodies were purchased from Santa Cruz Biotechnology (Santa Cruz, CA).

Cell Culture. COS-7 cells were grown in Dulbecco's modified Eagle medium supplemented with fetal bovine serum (10%) in the absence of antibiotics and antimycotics, which decrease transfection efficiency. COS-7 cells were grown to confluency in 24 well culture plates at 37°C in a humidified incubator with an atmosphere of 5% CO_2/ 95% air.

Creation of a RAMP2 Mutant Lacking the Signal Peptide. PCR was used to create a rat RAMP2 mutant (RAMP2-NSP) that lacks the signal peptide. The polymerase chain reaction (PCR) contained 1 X PCR Buffer, 3 mM $MgCl_2$, 0.2 mM dNTP mix, 50 pmoles rDN3 antisense primer, 50 pmoles rUP-NSP sense primer (Table 5), 2.5 units *Taq* DNA polymerase and 10 ng cDNA. PCR conditions were as follows: 5 minute denaturation at 95°C, followed by 37 cycles of 30 seconds at 95°C, 30 seconds at 55°C, and 30 seconds at 72°C, and a final extension of 7 minutes at 72°C. The PCR products were visualized on a 2% agarose gel stained with ethidium bromide.

PCR Products into an Expression Vector. The pcDNA3.1/zeocin(+) vector was digested with *Xho*I and *BamH*I and treated with shrimp alkaline phosphatase. The vectors were gel excised from a 0.8% SeaPlaque gel. The nonvariant RAMP2 and splice variant RAMP2b were digested with *Xho*I and or *BamH*I. The clones were gel excised from a 0.8% NuSieve gel. These clones were ligated into the pcDNA3.1/zeocin(+) vector

Table 5. Primers used in the creation of the rat RAMP2 mutant (RAMP2-NSP) and in the confirmation of CL transfection into the COS-7 cell line. Human CL primers were previously designed by Dr. Boyd Rorabaugh (Rorabaugh, 2002).

Primer	Sequence
rUP-NSP	5′-GGATCCGCCACCATGGCTGTCTCAAC-3′
rDN3	5′-TCCAGCAGGGTACAGG-3′
hCLUP	5′-GGATCCGGATCCGCCACCATGGAGAAAAAGTGTA-3′
hCLDN	5′-CTCGAGCTCGAGTCAATTATATAAATTTTCT-3′

overnight. The recombinant DNA was transformed into bacteria. A maxi-prep (Qiagen) purified the plasmid DNA for transfection. These new clones were sequenced and analyzed as described above.

QIAGEN Maxi Preparation. A QIAGEN-tip 500 was used to purify plasmid DNA for transfections. Briefly, 250 ml of plasmid culture was harvested by centrifugation at 4°C for 10 minutes at 6000 g. The bacterial pellet was resuspended in 10 ml of buffer P1 (50 mM Tris/HCl, 10 mM EDTA 100 μg/ml RNase A). The solution was incubated at room temperature for 30 minutes. Freshly made buffer P2 (200 mM NaOH, 1% SDS) was added, gently mixed, and incubated at room temperature for 5 minutes. Then, 10 ml of chilled buffer P3 (3.0 M KAc, pH 5.5) was immediately added, gently mixed, and incubated on ice for 20 minutes. The sample was centrifuged at 4°C for 30 minutes at 20,000 g. The supernatant was promptly removed and was filtered through a QIA-filter.

The QIAGEN-tip 500 was equilibrated by applying 10 ml of buffer QBT (750 mM NaCl, 50 mM MOPS, 15% ethanol, pH 7.0 -.15% Triton X-100). The column emptied by gravity flow. The supernatant was then applied to the column. Two washes of 30 ml buffer QC (1.0 M NaCL, 50 mM MOPS, 15% ethanol, pH 7.0) were then added. The DNA was eluted with 15 ml buffer QF (1.25 M NaCl, 50 mM Tris/HCl, 15% ethanol, pH 8.5). This sample was collected and precipitated with 0.7 volumes of isopropanol, vortexed, and immediately centrifuged at 15,000 g for 30 minutes at 4°C. The supernatant was removed and the pellet was washed with 15 ml of cold 70% ethanol and centrifuged at 15,000 g for 15 minutes at 4°C. The supernatant was removed and the pellet was air dried and resuspended in sterile water.

Lipofectamine Transfection. One day prior to transfection, COS-7 cells were plated into 6 and 24 well plates and were grown in Dulbecco's modified Eagle medium supplemented with fetal bovine serum (10%) in the absence of antibiotics and antimycotics, which may decrease transfection efficiency. Confluent cells were transfected using Lipofectamine™ 2000 with the following plasmid combinations:

1. CRE-Luc + hCL + rRAMP2
2. CRE-Luc + hCL + rRAMP2b
3. CRE-Luc + hCL + rRAMP2-NSP
4. CRE-Luc + rRAMP2
5. CRE-Luc + rRAMP2b
6. CRE-Luc + rRAMP2-NSP
7. CRE-Luc + hCL
8. CRE-Luc
9. CRE-Luc + HA-CL + rRAMP2
10. CRE-Luc + HA-CL + rRAMP2b
11. CRE-Luc + HA-CL
12. pcDNA3.1

RAMP2 refers to the nonvariant RAMP2 whereas RAMP2b refers to the splice variant. A RAMP2 mutant was made (RAMP2-NSP) without a signal peptide to serve as a negative control. HA-CL is the human calcitonin receptor-like receptor in the pcDNA3.1 vector containing a HA-epitope tag between the signal peptide and the N-terminal region of the receptor. This cDNA was kindly provided by Dr. James Porter (University of North Dakota). The CRE-Luc is the pADneo2 C6-BGL luciferase cDNA was generously

supplied by Dr. Yaping Tu (Creighton University). pcDNA3.1 refers to the empty vector containing no inserted DNA. First, plasmid DNA concentrations were determined by spectrophotometry and diluted so that each DNA had a concentration around 750 ng/μl. DNA concentrations were confirmed by gel electrophoresis. COS-7 cells were transfected with 0.75 μg of plasmid CRE-Luc DNA per well for a 6 well plate and 150 ng per well for a 24 well plate. In addition, 1.625 μg of HA-CL, hCL, RAMP2, RAMP2b, and/or RAMP2-NSP plasmid DNAs were transfected per well for a 6 well plate and 325 ng per well for a 24 well plate. For each transfection, empty vector pcDNA3.1 DNA was added to bring the total amount of DNA up to 4 μg per well for a 6 well plate and 800 ng per well for a 24 well plate. The DNAs were diluted in OptiMeM.

Before use, Lipofectamine™ 2000 was gently mixed and diluted in OptiMeM. The plasmid DNA complex was incubated for 5 minutes at room temperature. The diluted Lipofectamine™ 2000 was combined with the diluted DNA, gently mixed, and incubated at room temperature for 20 minutes. The DNA complexes were then added to each plate and mixed gently by slowly rocking the plate back and forth. The cells incubated at 37°C in a CO_2 incubator. The medium (DMEM with FBS) was replaced after 5 hours. RNA isolation and RT-PCR using the CL primers (Table 5) was performed to verify that the cDNA was transfected into the cells and being transcribed into RNA. The CL primers derived from human sequences did not detect any CL transcripts in the untransfected COS-7 cells.

Measurement of Intracellular cAMP Using the DPCI Radioassay. COS-7 cells were grown and transfected in 24 well plates. The media was removed and the cells were washed twice with HEPES buffered Krebs solution containing isobutylmethylxanthine

(HKI) (20mM HEPES, 4 mM $NaHCO_3$, 11 mM dextrose, 1.25 mM NaH_2PO_4, 120 mM NaCl, 5.5 mM KCl, 2.5 mM $CaCl_2$, 1.2 mM $MgCl_2$, and 0.5 mM isobutylmethylxanthine) prepared by probe sonication. The cells were preincubated for 10 minutes with 450 µl HKI and then incubated with adrenomedullin, forskolin, or additional HKI (for basal levels) for 30 minutes at 37°C in a humidified incubator with an atmosphere of 5% CO_2/ 95% air. The solution was removed and replaced with 100 µl of 90% ethanol to lyse the cells. The ethanol was evaporated in an oven for approximately 25 minutes.

The cells were scraped in Tris-EDTA buffer provided by DPCI. Two-thirds of each sample was incubated with Tris-EDTA, [^{3}H]cAMP, and cAMP binding protein for 2 hours in an ice water bath refrigerated at 4°C. On a magnetic stir plate, charcoal-dextran suspension was stirred at least 20 minutes before use in the refrigerator at 4°C. Five hundred microliters of ice-cold charcoal-dextran suspension was added to all tubes. The tubes were vortexed and incubated for 10 minutes on ice in the refrigerator at 4°C. The tubes were centrifuged for 10 minutes at 5000 g. Immediately after centrifugation, 1 ml of supernatant was transferred to scintillation vials. Scintillation fluid was added and the samples were counted on a liquid scintillation counter. A standard curve was also generated using serial dilutions of a known concentration of cAMP.

Measurement of Intracellular cAMP Using a Luciferase Assay. COS-7 cells were grown and transfected in 24 well plates. Approximately 18 hours after transfection, the cells were stimulated. Cells were washed three times with PBS. Groups of transfected cells were stimulated with 100 nM adrenomedullin, 3 µM forskolin, or Dulbecco's modified Eagle medium (DMEM) for five hours in the presence of DMEM without any fetal bovine serum. Concentration response curves were stimulated with varying

concentrations of adrenomedullin. A vehicle control with ethanol was also performed. Cells were washed twice with PBS and lysed with 100 µl cell culture lysis reagent. Cells were scraped with a pipette tip on ice. The lysate was stored on ice and centrifuged for 10 minutes at 12,000 g. The supernatant was removed and used for the luciferase and protein assay. Twenty microliters of supernatant was added to 100 µl luciferase assay substrate and briefly vortexed. Sirius Luminometer V3.1 measured the activity in relative light units. The supernatant was stored at -80°C.

RC DC Protein Assay. Frozen supernatant samples used for the luciferase assay were thawed to room temperature. Twenty-five microliters of sample was added to 125 µl of *RC* Reagent I, vortexed, and incubated at room temperature for 1 minute. Then, 125 µl of *RC* Reagent II was added to each tube, vortexed, and centrifuged at 15,000 g for 5 minutes. The supernatant was discarded by inverting the tubes. Reagent A′ was prepared by adding 20 µl of reagent S to each ml of reagent A required for the assay. The pellet was resuspended in 127 µl of reagent A′. The pellet was vortexed and incubated for 5 minutes at room temperature. One milliliter of reagent B was added to each tube and vortexed immediately. After a 15 minute incubation, the absorbances were read at 750 nm. A standard curve using bovine serum albumin was also generated each time an assay was preformed according to the above procedure.

Immunocytochemistry. Twenty-four hours after transfection in 6 well plates, the cells were split onto glass coverslips and allowed to grow for an additional twenty-four hours. The cells were washed three times with PBS. Coverslips were then divided into two groups: "cells stained prior to fixation" and "cells stained after fixation". The "cells stained prior to fixation" group represented cells where receptors were labeled only at the

extracellular cell surface. These cells were incubated with primary antibodies in DMEM with bovine serum albumin on ice for 10 minutes. The primary antibodies were washed off by three rinses of PBS. The cells were then fixed with fresh 4% paraformaldehyde for 45 minutes on ice. The cells were washed three times with PBS- 0.1% tween and blocked with 1% donkey serum in PBS- 0.1% tween for 20 minutes. The "cells stained after fixation" group represented receptors both at the cells surface and in the cytosol and were fixed with 4% paraformaldehyde for 45 minutes on ice. The cells were washed three times with PBS- 0.1% tween and permeabilized with PBS- 0.1% tween-0.05% Triton-X for 5 minutes on ice. The cells were rinsed once with PBS-tween and blocked with 1% donkey serum in PBS-tween for 20 minutes. The cells were then incubated with primary antibodies for 1 hour in 1% donkey serum in PBS- 0.1% tween and washed three times with PBS- 0.1% tween. The "no primary antibodies" controls were treated as "cells stained after fixation" except that they were not incubated with any primary antibodies. Mouse anti-HA (Invitrogen), RAMP2 (H-139, sc-11380) and CRLR (V-20, sc-18007) (Santa Cruz Biotechnology) were used as primary antibodies.

All cells stained with the primary antibody for RAMP2 (H-139, sc-11380) were washed, fixed and blocked as above and incubated for an hour with an additional antibody (e.g. goat anti-rabbit), washed three times with PBS- 0.1% tween and incubated for an hour with Alexa antibodies (Alexa Fluor® 568-donkey anti-goat or as required Alexa Fluor® 488-goat anti-rabbit) to amplify the RAMP2 fluorescence. This additional amplification step using the extra secondary antibody as well as the Alexa antibodies was necessary because studies using the RAMP2 antibody and only one secondary antibody did not produce consistent, strong fluorescence. After staining with Alexa antibodies, the

cells were washed three times with PBS- 0.1% tween and stained for 10 minutes with DAPI to identify the nucleus. The cells were washed three times with PBS- 0.1% tween and post-fixed for 30 minutes with 4% paraformaldehyde. The cells were then rinsed three times with PBS- 0.1% tween and mounted on glass slides with n-propyl gallate in 90% glycerol and 10% PBS. The slides were stored in aluminum foil covered boxes or microscope slide cases at 4°C.

Images were captured using the Zeiss LSM 510 META NLO system at the Nebraska Center for Cell Biology. The Coherent Chameleon XR (for multi-photon excitation) was used to detect DAPI staining. Amplification of the cells was aided by a 63x oil immersion objective.

Transfection Efficiency. Transfection efficiency was measured by immunocytochemistry. Briefly, transfected cells were stained with rabbit anti-RAMP2 after fixation and permeabilization (as described above). The cells' nuclei, labeled by DAPI, were counted under low objective power using the Coherent Chameleon XR. Then the RAMP2 positive cells were counted in this same field. The number of RAMP2 positive cells divided by the total number of cells as determined with DAPI nuclear staining yielded the transfection efficiency for RAMP2 and RAMP2b transfected cells.

Data Analysis. All calculations were done with GraphPad Prism (San Diego, CA). Three to four luciferase assays were performed in duplicate for each transfection and ligand or basal combination. Relative light units (RLU) were measured and divided by the amount of protein in mg. The RLU/mg protein duplicates for each condition were averaged and divided by the basal RLU/mg protein average for the transfection to yield

(RLU/mg protein)/basal levels. Statistical analysis was performed using an analysis of variance (ANOVA) and the Newman-Keuls Multiple Comparison Test.

Results

Identification of COS-7 cells lacking endogenous RAMP2 and CL proteins. Transfection assays with CL and the RAMPs usually use the COS-7 cell line (African green monkey kidney cells) because they endogenously express RCP and not CL or the RAMPs (Evans et al., 2000). However, some batches of COS-7 cells have been shown to express endogenous CL and RAMPs. For example, RT-PCR has amplified low levels of mRNA transcripts for RAMP1, RAMP2, and RAMP3 in COS-7 cells; however, Northern analysis did not yield any endogenous RAMP mRNA expression in these same cells (Tilakaratne et al., 2000). Northern blot analysis by Buhlmann et al. showed a weak signal of endogenous RAMP2 mRNA in COS-7 cells (Buhlmann et al., 1999). Most labs have shown that RAMPs were not detected by RT-PCR in COS-7 cells (Bouschet et al., 2005).

Using primers (hUP2, hDN2, hCLUP, and hCLDN) based on human RAMP2 and CL sequences (Tables 3 and 5, respectively), no endogenous RAMP2 or CL mRNA were detected by RT-PCR in our batch of untransfected COS-7 cells. Unfortunately, the African green monkey's CL and RAMPs were not cloned at the time of this study nor was a positive control from African green monkey RNA performed. Figure 21 shows that the human RAMP2 primers are similar to the predicted sequences of the chimpanzee and rhesus monkey, which are the closest related species with known or predicted sequences. RNA from transfected COS-7 cells produced a positive CL RT-PCR product

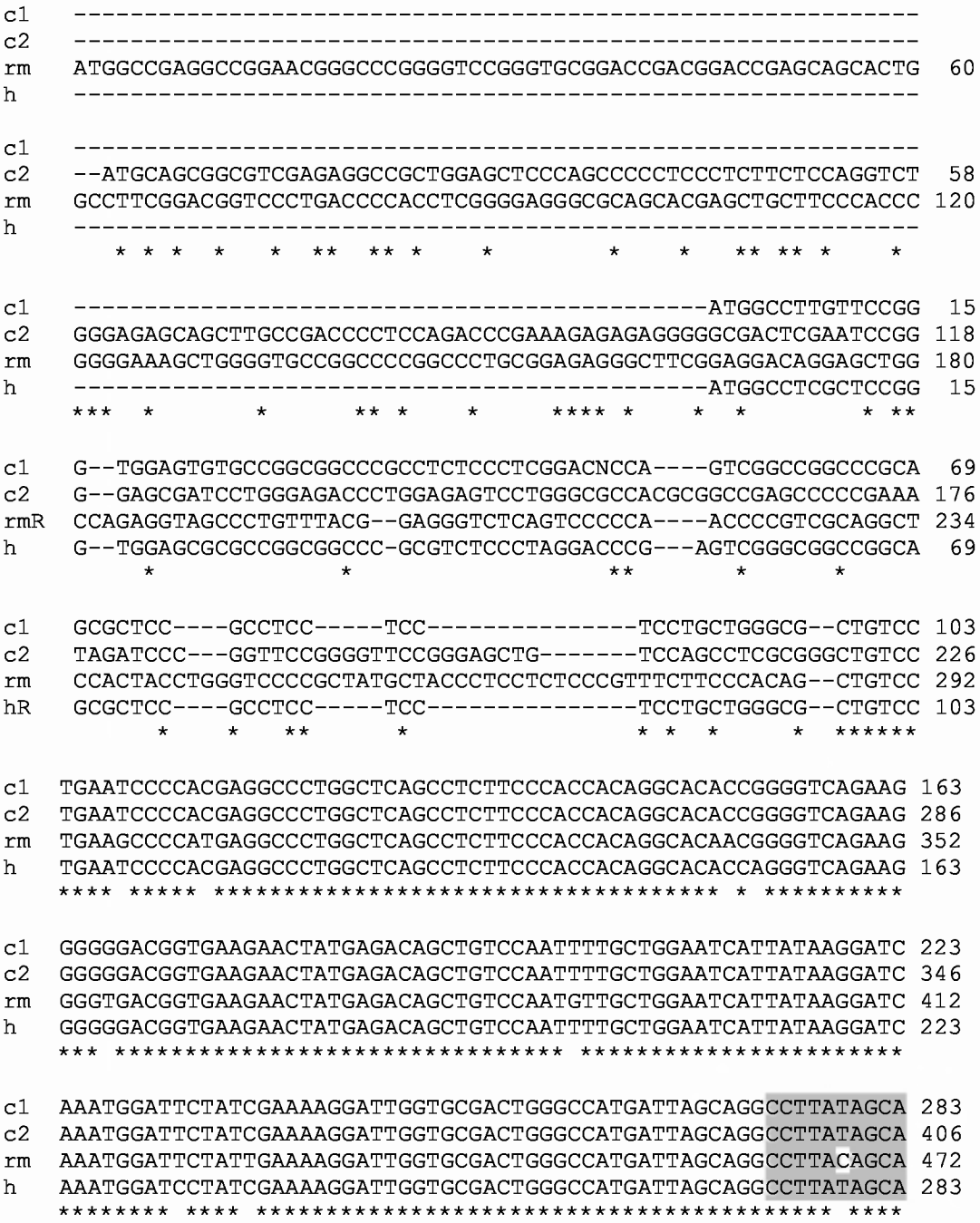

Figure 21. Comparison of the primate RAMP2 nucleotide sequences. Highlighted regions indicate the forward and reverse human primers used to determine if RAMP2 RNA is endogenously expressed in untransfected COS-7 cells. c1, c2, and rm RAMP2s are predicted sequences (XM_001160651.1 GI:114667125, XM_511520.2 GI:114667127, and XM_001096145.1 GI:109115419 respectively). The asterisks indicate identical nucleotides and the dashes represent gaps in sequence (c: chimpanzee, h: human, rm: rhesus monkey).

```
c1  CCCTGCGAGATTGCCTGGAGCACTTTGCAGAGTTGTTTGACCTGGGCTTCCCCAATCCCT 343
c2  CCCTGCGAGATTGCCTGGAGCACTTTGCAGAGTTGTTTGACCTGGGCTTCCCCAATCCCT 466
rm  CCCTGCGAGAATGCCTGGAGCACTTTGCGGAGTTGTTTGACCTGGGCTTCCCCAATCCCT 532
h   CCCTGCGAGATTGCCTGGAGCACTTTGCAGAGTTGTTTGACCTGGGCTTCCCCAATCCCT 343
    ********** ********** ********** ********** ********** ******

c1  TGGCAGAGAGGATCATCTTTGAGACTCACCAGATCCACTTTGCCAACTGCTCCCTGGTGC 403
c2  TGGCAGAGAGGATCATCTTTGAGACTCACCAGATCCACTTTGCCAACTGCTCCCTGGTGC 526
rm  TGGCAGAGAGGATCATCTTTGAGACTCACCAGATCCACTTTGCCAACTGCTCCCTGGTGC 592
hR  TGGCAGAGAGGATCATCTTTGAGACTCACCAGATCCACTTTGCCAACTGCTCCCTGGTGC 403
    ************************************************************

c1  AGCCCACCTTCTCCGACCCCCCAGAGGATGTACTCCTGGCCATGATCATAGCCCCCATCT 463
c2  AGCCCACCTTCTCCGACCCCCCAGAGGATGTACTCCTGGCCATGATCATAGCCCCCATCT 586
rm  AGCCCACCTTCTCTGACCCCCCAGAGGATGTACTCCTGGCCATGATCATAGCCCCCATCT 652
h   AGCCCACCTTCTCTGACCCCCCAGAGGATGTACTCCTGGCCATGATCATAGCCCCCATCT 463
    ************* ********** ********** ********** ********** ***

c1  GCCTCATCCCCTTCCTCATCACTCTTGTAGTATGGAGGAGTAAAGACAGTGAGGCCCAGG 523
c2  GCCTCATCCCCTTCCTCATCACTCTTGTAGTATGGAGGAGTAAAGACAGTGAGGCCCAGG 646
rm  GCCTCATCCCCTTCCTTATCACTCTTGTAGTATGGAGGAGTAAAGACAGTGAGGCCCAGG 712
h   GCCTCATCCCCTTCCTCATCACTCTTGTAGTATGGAGGAGTAAAGACAGTGAGGCCCAGG 523
    ********** ********** ********** ********** ********** ******

c1  CCTAGGGGGCCACGAGCTTCTCAACAACCATGTTACTCCACTTCCCCACCCCC 576
c2  CCTAGGGGGCCACGAGCTTCTCAACAACCATGTTACTCCACTTCCCCACCCCC 699
rm  CCTAGGGAGCCACGAGCTTCTCTATAACCACCTTACTCCACTTCCCCACACCA 765
h   CCTAGGGGGCCACGAGCTTCTCAACAACCATGTTACTCCACTTCCCCACCCCC 576
    ******* ********** * ***** ********** **
```

(1416 bp), which indicates that the CL cDNA was transfected into the cells and transcribed into RNA (Figure 22a). Untransfected COS-7 cells did not yield any CL transcripts with the hCL primers. Predicted chimpanzee CL variants 1-5 and 7 have 99% identity to the human CL nucleotide sequence. Predicted variant 6 of chimpanzee CL has an additional 54 nucleotide insert, which is not near the primers. A partial sequence of the rhesus monkey has also been predicted. It has 98% nucleotide sequence identity. Additionally, untransfected COS-7 cells were stained with human RAMP2 and CL antibodies during the immunocytochemistry studies and showed that the cells do not endogenously express either epitopes (Figures 23c and 24a, respectively).

Hay et al. as well as others have shown that COS-7 cells do not have any functional RAMPs or CL (Hay et al., 2003). Because different batches of COS-7 cells have been shown to either express or not express CL and the RAMPs, it was important to show that the batch purchased from American Type Culture Collection used in our studies did not endogenously express functional levels of CL or the RAMPs. Therefore, cAMP radioassays using two concentrations of adrenomedullin (100 nM and 1 nM) and CGRP (10 nM and 0.1 nM) were used to determine if the untransfected COS-7 cells endogenously expressed functional adrenomedullin or CGRP receptors. Maximal stimulation of adrenomedullin and CGRP receptors has been shown with 100 nM AM and 10 nM CGRP, respectively (Hay et al., 2003). HEK 293 cells, which have also been used to study adrenomedullin receptors, were also examined to determine if their endogenous level of AM_1 was low enough to be used as a cell line to study the AM_1 receptor activity. Forskolin acted as a positive control to show that the cells were viable and that the cAMP assay was working. Untransfected COS-7 cells were stimulated with

A.

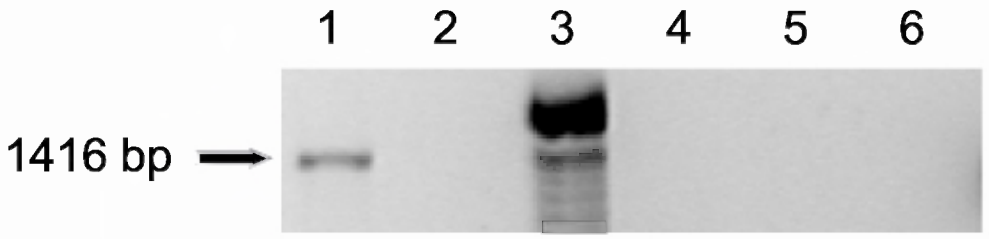

B.

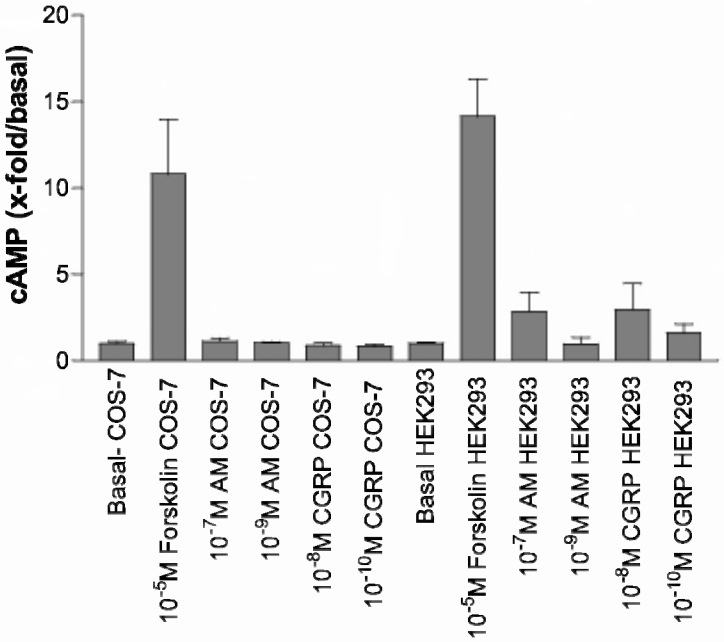

Figure 22. COS-7 cells lack endogenous AM or CGRP activity. (A) RT-PCR results show that COS-7 cells transfected with human CL cDNA transcribe CL RNA; whereas, untransfected COS-7 cells do not transcribe CL RNA (Lanes 1 and 4, respectively). Reactions without reverse transcriptase were performed to ensure that there was no DNA contamination in either transfected or untransfected COS-7 cells (Lanes 2 and 5, respectively). The reference marker was a 100 base pair ladder (Lane 3). A reaction without any RNA proved there was no contamination (Lane 6). (B). A cAMP assay of untransfected COS-7 and HEK 293 cells determines which cell line has the least endogenous AM or CGRP receptor activity. Basal levels were determined by incubation with buffer in the absence of drug. Forskolin (10^{-5} M) was used as a positive control to verify that the cAMP assay was working and that the cells were viable. COS-7 cells produced only basal levels of cAMP when stimulated with AM or CGRP. HEK 293 cells produced a 3-fold stimulation when incubated with AM or CGRP.

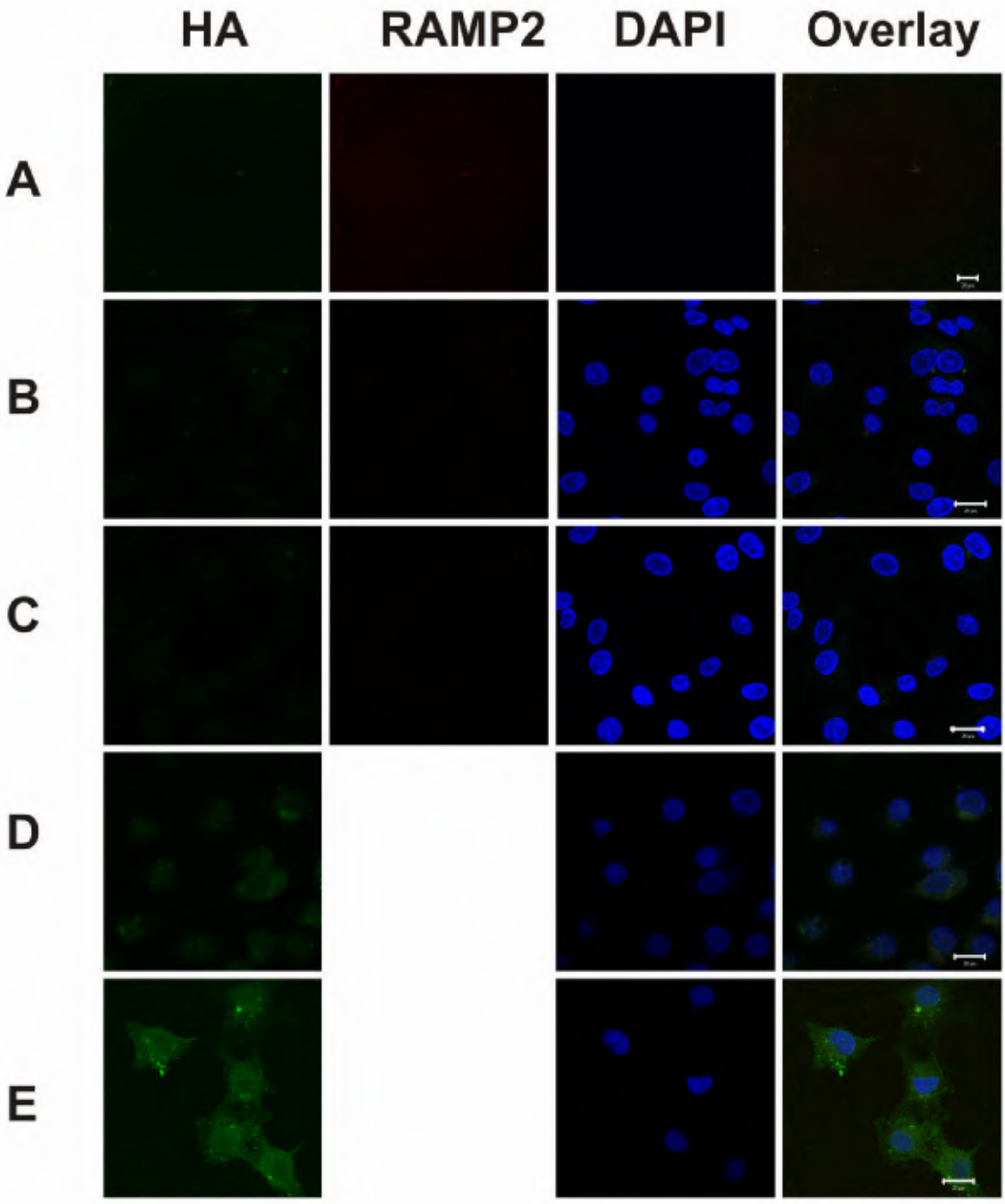

Figure 23. Confocal microscopy control experiments using COS-7 cells. A. Untransfected COS-7 cells in the absence of any antibodies or DAPI staining. B. COS-7 cells transfected with rRAMP2 and HA-CL stained with DAPI and ALEXA antibodies without any primary antibodies. C. Untransfected COS-7 cells stained with HA, RAMP2, goat anti rabbit, ALEXA and DAPI antibodies shows there is no expression of HA-CL or RAMP2. D. COS-7 cells transfected with HA-CL stained with anti-HA prior to fixation shows minor expression of HA-CL at the plasma membrane. E. COS-7 cells transfected with HA-CL stained with anti-HA after fixation shows expression of HA-CL. The scale bar represents 20 μm.

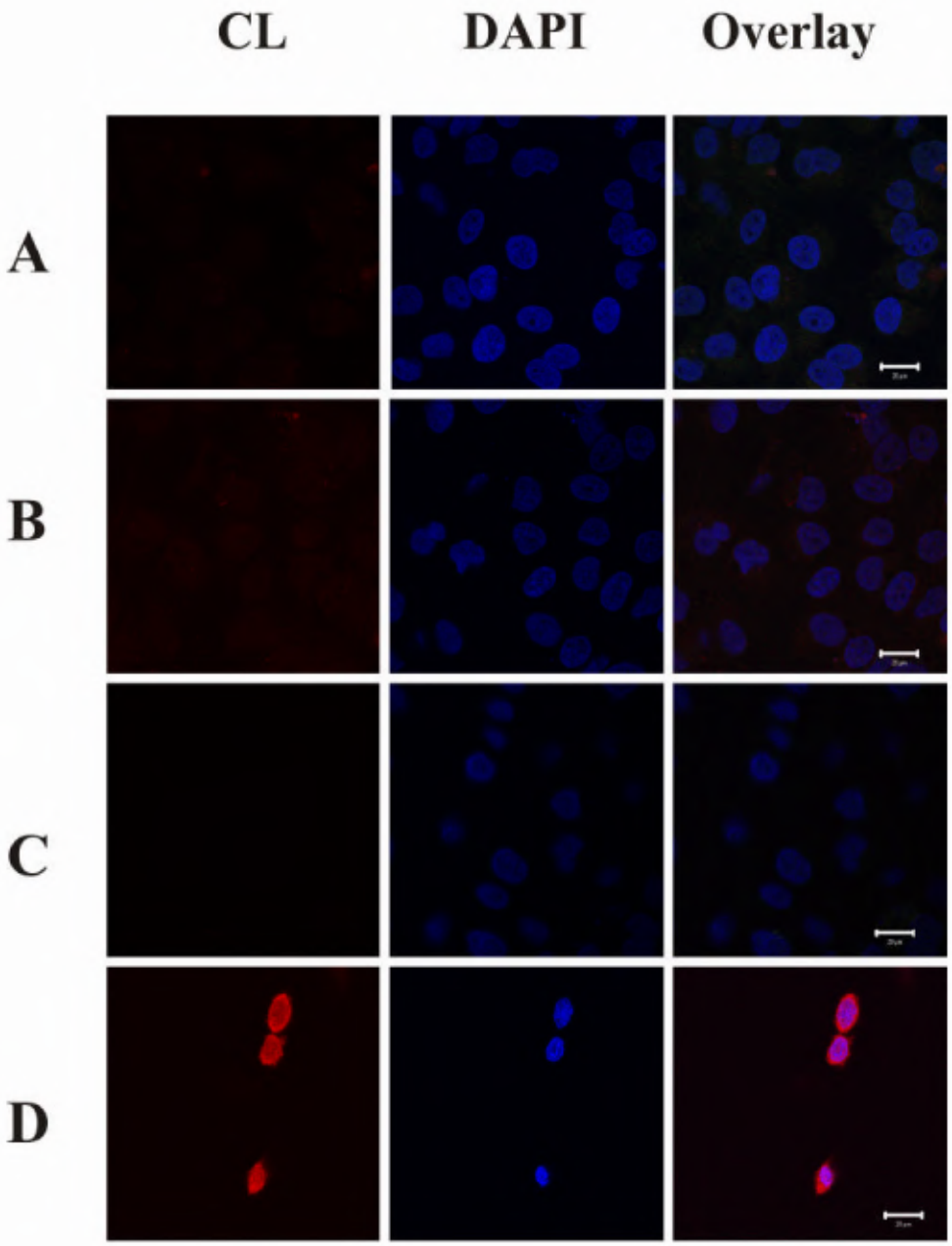

Figure 24. CL antibody targeting intracellular domain of CL does not penetrate the plasma membrane before fixation. A. Untransfected fixed COS-7 cells stained with CL primary and secondary antibodies. B. Rat RAMP2 and human CL transfected COS-7 cells stained without CL primary antibody. C. COS-7 cells transfected with rat RAMP2 and human CL and immunostained before fixation. D. COS-7 cells transfected with rat RAMP2 and human CL and immunostained after fixation, which shows the antibody labeling the interior cell surface and/ or cytosol. The scale bar represents 20 μm.

both AM and CGRP with no cAMP activity over basal (Figure 22b). However, AM and CGRP elicited cAMP responses that were approximately 3-fold over basal in HEK 293 cells, a result similar to other published values (Kuwasako et al., 2002). This increase in cAMP indicates that endogenous CL and RAMPs are present in HEK 293 cells, which makes them a poor candidate for RAMP2 transfections. COS-7 cells, however, lack the expression of any functional endogenous CL or RAMPs.

Detection of RAMP2 and HA-CL on the extracellular plasma membrane. In order to detect RAMP2 and CL proteins on the plasma membrane by immunocytochemistry, the antibodies must target the N-terminus of these proteins. A commercial polyclonal antibody for the human N-terminus of RAMP2 was purchased from Santa Cruz Biotechnology. The amino acid sequences from human, chimpanzee, rhesus monkey, and rat were compared to show similarity in the epitope region of the human RAMP2 antibody (Figure 25). However, there were no commercial antibodies available at the time of this study that targeted the N-terminus of the CL; therefore, a human CL with an N-terminal HA-tag was obtained from Dr. James Porter (University of North Dakota). Special care is required when using a HA-tagged receptor because an N-terminal HA-tagged CL was initially purchased from University of Missouri-Rolla (Guthrie Institute) but the HA-tag was fused upstream to the N-terminus of the signal peptide. Studies using this HA- tagged protein yielded no HA staining because the HA-tag was most likely removed after cleavage of the signal peptide at the polar carboxy-terminal region. The HA-CL cDNA pCDNA3.1 plasmid from Dr. Porter has the N-terminal HA-tag after the signal peptide cleavage site and upon transfection into COS-7 cells was detected at the plasma membrane (Figure 23d).

```
c1    MALFRVECAG---GPP-----------LPRTP---------------------------- 18
c2    MQRRREA-AG---APSPLPLLQVWESSLPTPPD----------------PKERGGDSNPG 40
h     MASLRVERAG---GPR-----------LPRTR---------------------------- 18
rm    MAEAGTGP-GSGCGPTDRAALAFG-RSLTPPRGGRSTSCFPPGESWGAGPGPAERASEDR 58
r2    MAPLRVERAP---GGS----------QLAVTS---------------------------- 19
r2b   MAPLRVERAP---GGS----------QL-------------------------------- 15
      *       *                  *

c1    -----------VGRPAALRLLLLLG-------------AVLNPHEALAQPLPTTGTPGSE 54
c2    SDPGRPWRVLGATRPSPRNRSRFRGSGSCPA-----SRAVLNPHEALAQPLPTTGTPGSE 95
h     -----------VGRPAALRLLLLLG-------------AVLNPHEALAQPLPTTGTPGSE 54
rm    SWPEVALFTEGLSPPTP-SQAPLPGSPLCYPPLPFLPTAVLKPHEALAQPLPTTGTTGSE 117
r2    -----------AQRPAALRLPPLLLLLLLLLLG-----AVSTSPESLNQSHPTEDSLLSK 63
r2b   ------------------------------------AVSTSPESLNQSHPTEDSLLSK 37
                  *                         **    * * *  **     *

c1    GGTVKNYETAVQFCWNHYKDQMDSIEKDWCDWAMISRPYSTLRDCLEHFAELFDLGFPNP 114
c2    GGTVKNYETAVQFCWNHYKDQMDSIEKDWCDWAMISRPYSTLRDCLEHFAELFDLGFPNP 155
h     GGTVKNYETAVQFCWNHYKDQMDPIEKDWCDWAMISRPYSTLRDCLEHFAELFDLGFPNP 114
rm    GVTVKNYETAVQCCWNHYKDQMDSIEKDWCDWAMISRPYSTLRECLEHFAELFDLGFPNP 177
r2    G-KMEDYETNVLPCWYYYKTSMDSVK-DWCNWTLISRYYSNLRYCLEYEADKFGLGFPNP 121
rb    G-KMEDYETNVLPCWYYYKTSMDSVK-DWCNWTLISRYYSNLRYCLEYEADKFGLGFPNP 95
      *     *** *  **  **  **    *** *  *** ** ** ***  *  * ******

c1    LAERIIFETHQIHFANCSLVQPTFSDPPEDVLLAMIIAPICLIPFLITLVVWRSKDSEAQA 175
c2    LAERIIFETHQIHFANCSLVQPTFSDPPEDVLLAMIIAPICLIPFLITLVVWRSKDSEAQA 216
h     LAERIIFETHQIHFANCSLVQPTFSDPPEDVLLAMIIAPICLIPFLITLVVWRSKDSEAQA 175
rm    LAERIIFETHQIHFANCSLVQPTFSDPPEDVLLAMIIAPICLIPFLITLVVWRSKDSEAQA 238
r2    LAESIILEAHLIHFANCSLVQPTFSDPPEDVLLAMIIAPICLIPFLVTLVVWRSKDGDAQA 182
r2b   LAESIILEAHLIHFANCSLVQPTFSDPPEDVLLAMIIAPICLIPFLVTLVVWRSKDGDAQA 156
      *** ** * * ********************************** *********  ***
```

Figure 25. Comparison of RAMP2 amino acid sequences from various species. The amino acid sequences from the chimpanzee, human, rhesus monkey, rat RAMP2 and rat RAMP2b were compared to show the similarity of amino acids for the polyclonal antibody's (RAMP2 H-139 from Santa Cruz) epitope (highlighted). cRAMP2-1, cRAMP2-2, and rmRAMP2 are predicted sequences (XM_001160651.1 GI:114667125, XM_511520.2 GI:114667127, and XM_001096145.1 GI:109115419 respectively). (c: chimpanzee, h: human, r: rat, rm: rhesus monkey). Identical amino acids are designated with a *. Dashes indicate gaps in sequence homology.

Initial studies to detect proteins on the cell membrane were conducted with COS-7 cells transfected with RAMP2 and HA-CL but were not successful because the cells became permeabilized during the fixation process with 4% paraformaldehyde. In order to distinguish between extracellular protein on the plasma membrane and intracellular proteins, primary antibody staining was done prior to fixation. Some cells designated "cell surface" were stained for 10 minutes on ice with primary antibodies in the presence of BSA prior to fixation to label only exterior cell surface antigens. Other cells designated "cell surface + cytosol" were stained for 1 hour after fixation and permeabilization to label all antigens.

Negative controls ensured that the COS-7 cells had no autofluorescence or endogenous RAMP2, HA or CL epitopes (Figures 23a, c and Figure 24a). COS-7 cells were analyzed in the absence of any antibodies (including DAPI) to show that the cells do not have autofluoresence (Figure 23a). Untransfected cells were stained with the CL antibody targeted to the intracellular region of the CL or were stained with RAMP2 or HA antibodies targeted to the N-terminus of the RAMP2 or HA-CL protein in the presence of DAPI to show that the cells do not endogenously express the epitopes (Figures 24a and 23c, respectively). COS-7 cells transfected with RAMP2 and hCL were also stained with secondary and tertiary antibodies in the absence of the primary antibodies (Figures 23b and 24b, respectively).

COS-7 cells were transfected with the HA-CL and either rRAMP2, rRAMP2b or rRAMP2-NSP and stained with HA and RAMP2 primary antibodies. Primary antibody staining was performed before (cell surface) and after (cell surface + cytosol) fixation,

which caused permeabilization of the plasma membrane, while DAPI was used to stain the nucleus.

COS-7 cells transfected with rRAMP2 and HA-CL were stained before and after fixation with the CL antibody, which targets an intracellular region of the CL protein (Figure 24c and d, respectively). The CL protein was only detected after fixation, indicating that the antibody did not enter the plasma membrane prior to fixation.

Either rat RAMP2b or RAMP2-NSP was transfected into COS-7 cells in the absence of a CL protein to determine if the RAMPs could traffic to the plasma membrane by itself. In COS-7 transfected cells stained with primary RAMP2 antibody before fixation, the rRAMP2b was at the cell surface, but the rRAMP2-NSP was not (Figure 26a and b, respectively). Both the rRAMP2b and rRAMP2-NSP were expressed in the absence of the CL (Figure 26c and d, respectively).

The HA antibody staining also detected expression of HA-CL at the plasma membrane, when coexpressed with rRAMP2, rRAMP2b or rRAMP2-NSP (Figure 27a, b, and c, respectively). In addition, the rRAMP2 and rRAMP2b were expressed at the plasma membrane (Figure 27a and b, respectively). The rRAMP2-NSP was not expressed at the cell surface, but was translated into a protein that remains in the cytosol (Figures 27c and f, respectively).

These images were taken at different depths and should only be used for quantitative analysis. Future experiments should also use the z-stack method, which can give the cell a 3D projection. Prolonged exposure, however, may cause photobleaching.

Measurement of Transfection Efficiency. Transfection efficiency of rRAMP2 and rRAMP2b was measured by immunocytochemistry. COS-7 cells were transfected with

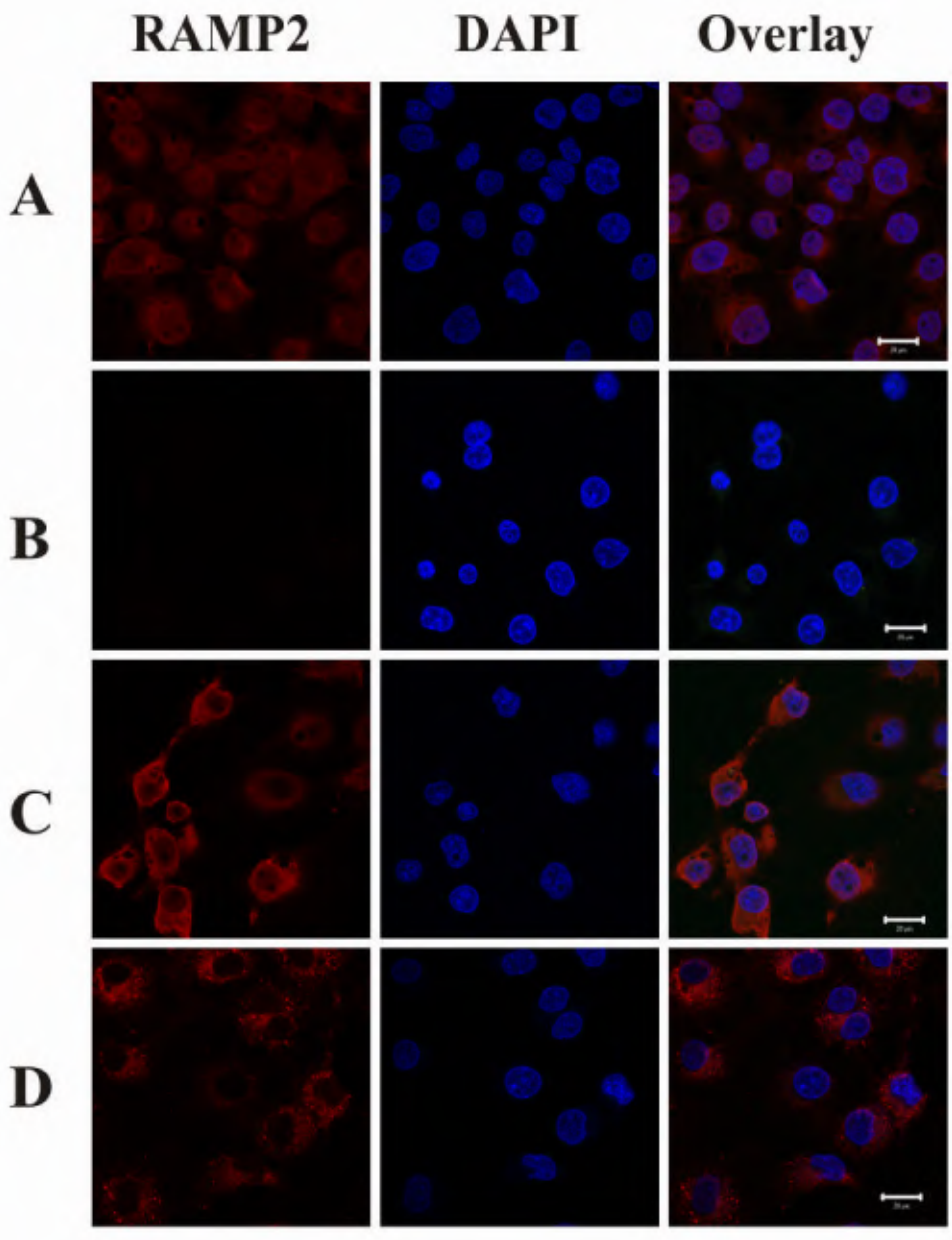

Figure 26. COS-7 cells transfected with rRAMP2b or rRAMP2-NSP stained with RAMP2 primary antibody before and after fixation. A. Rat RAMP2b transfected COS-7 cells stained prior to fixation. B. Rat RAMP2-NSP transfected COS-7 cells stained before fixation. C. COS-7 cells transfected with rRAMP2b stained after fixation in order to label cell surface and cytosolic proteins. D. Staining of rRAMP2-NSP in COS-7 cells after fixation. The scale bar represents 20 μm.

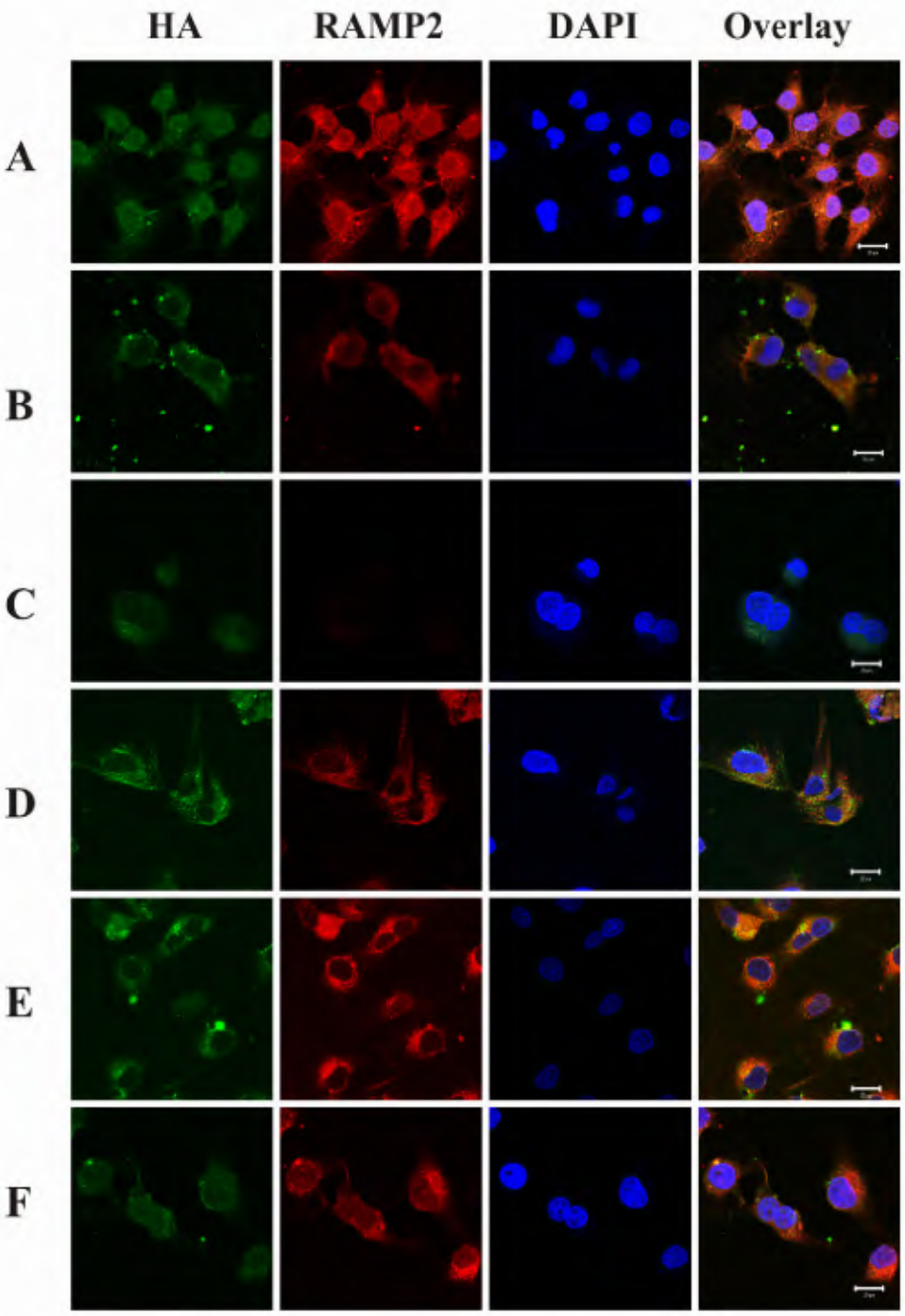

Figure 27. Transfected COS-7 cells stained with RAMP2 and HA primary antibodies before and after fixation. A. COS-7 cells transfected with rRAMP2 and HA-CL stained prior to fixation labeling proteins at the cell surface. B. rRAMP2b and HA-CL transfected COS-7 cells stained prior to fixation to indicate proteins at the cell surface. C. COS-7 cells transfected with rRAMP2-NSP and HA-CL stained prior to fixation labeling proteins at the cell surface. D. COS-7 cells transfected with rRAMP2 and HA-CL stained after fixation labeling proteins at the cell surface and in the cytosol. E. COS-7 cells transfected with rRAMP2b and HA-CL stained after fixation. F. COS-7 cells transfected with rRAMP2-NSP and HA-CL after fixation. The scale bar represents 20 μm.

HA-CL and either rRAMP2 or rRAMP2b using Lipofectamine™ 2000. This reagent is known to have high transfection efficiency in COS-7 cells with little cell death and no autofluoresence. The average transfection efficiency for three separate transfections of rRAMP2 and rRAMP2b were 87% and 85%, respectively. Both the wildtype and variant RAMP2s had similar levels of transfection efficiency.

Adrenomedullin Stimulation of the rRAMP2b and hCL Hetero-oligomer. The activity of the resultant AM_1 receptor formed after CL and RAMP2 or RAMP2b transfection was determined by a luciferase assay which measured the cAMP concentration after stimulation with adrenomedullin or forskolin. Basal levels were also measured for each transfection to account for any changes of CRE-Luc transfection efficiency. Luciferase induction of COS-7 cells transfected with the AM_1 receptor showed a 3.6 fold increase over basal; whereas the hCL hetero-oligomer with the rRAMP2b only had a 2.0 fold increase over basal, which is significantly different (Figure 28). The hCL and rRAMP2b hetero-oligomer, however, did have a significant increase in cAMP activity over COS-7 cells transfected with the empty vector control (pcDNA3.1) and the COS-7 cells transfected with hCL and the signal peptide mutant RAMP2-NSP. Forskolin stimulated cAMP activity was not significantly different between COS-7 cells transfected with CRE-Luc, hCL, and either the rRAMP2 or rRAMP2b. However, COS-7 cells transfected with the empty vector (pcDNA3.1) in the absence of the CRE-Luc did not produce any luciferase activity, indicating that the COS-7 cells have no endogenous luciferase activity.

A mutant cDNA was created to determine if the absence of the signal peptide reflects a change in expression at the protein at the plasma membrane. The rRAMP2-

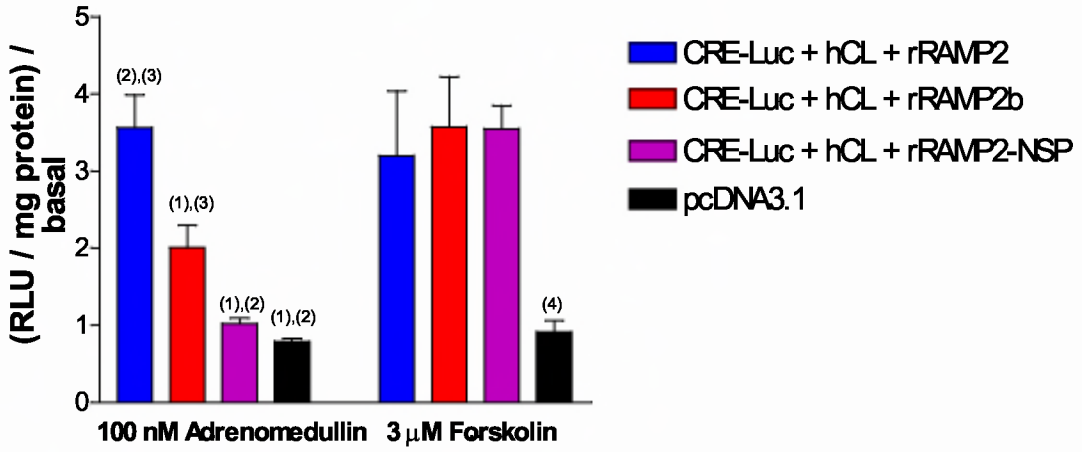

Figure 28. Luciferase assay measuring cAMP concentrations in COS-7 cells transfected with CRE-Luc, hCL and either rRAMP2, rRAMP2b or rRAMP2-NSP. As a negative control, COS-7 cells were transfected with the pcDNA3.1 vector in the absence of CRE-Luc. Cells were stimulated with either 3 μM forskolin or 100 nM adrenomedullin (AM) and cAMP was measured in relative light units (RLU). Data are means ± SEM of four experiments done in duplicate (ANOVA using Newman-Keuls Multiple Comparison Test, $P < 0.05$). cAMP stimulation of CRE-Luc + hCL + rRAMP2b transfected cells by 100 nM AM is statistically greater than cells transfected with only the pcDNA3.1 vector or cells transfected with CRE-Luc + hCL + rRAMP2-NSP. Also these cells have a significantly lower luciferase induction than cells transfected with the CRE-Luc + hCL + rRAMP2.

(1) Significantly different from AM stimulated CRE-Luc + hCL + rRAMP2 transfected COS-7 cells.
(2) Significantly different from AM stimulated CRE-Luc + hCL + rRAMP2b transfected COS-7 cells.
(3) Significantly different from AM stimulated CRE-Luc + hCL + rRAMP2-NSP and pcDNA3.1 transfected COS-7 cells.
(4) Significantly different from forskolin stimulated pcDNA3.1 transfected cells in the absence of CRE-Luc. There is a significant increase for forskolin stimulated COS-7 cells transfected with the CRE-Luc, hCL and either rRAMP2, rRAMP2b, or rRAMP2-NSP. Forskolin stimulation of these transfected cells is not different from each other.

NSP, a rat RAMP2 mutant created by RT-PCR, lacks the signal peptide. Luciferase cAMP assays were performed to determine whether it would form a functional adrenomedullin receptor when co-expressed with HA-CL or hCL (Figures 28 and 29, respectively). The mutant expressed with a CL did not significantly increase intracellular levels of cAMP upon adrenomedullin stimulation.

Experimental controls included COS-7 cells transfected with CRE-Luc, HA-CL and either rRAMP2 or RAMP2b to determine if the HA-tag interfered with the signal transduction of the AM_1 (Figure 29). The CRE-Luc + HA-CL + rRAMP2 transfected COS-7 cells produced a functional AM_1 indicating that the HA-tag does not interfere with the receptor's activity. Negative controls showed that there are insufficient amounts of endogenous CL or RAMP2 protein expressed by COS-7. The vehicle control confirmed that forskolin and not the ethanol vehicle stimulates the cells.

Concentration response curves were performed for COS-7 cells expressing CRE-Luc, hCL, and either the rRAMP2 or rRAMP2b (Figure 30). The maximal response of adrenomedullin stimulated CRE-Luc, hCL and rRAMP2b transfected COS-7 cells is not stastically different from basal cAMP levels; however, this response was shown to be significant when a greater number of experiments were performed (Figure 28). The EC_{50} for rRAMP2 is 1.2 nM and the EC_{50} for rRAMP2b is 1.9 nM. The maximal response for CRE-Luc, hCL and rRAMP2 is greater than the CRE-Luc, hCL and rRAMP2b cAMP even though they have the same potency.

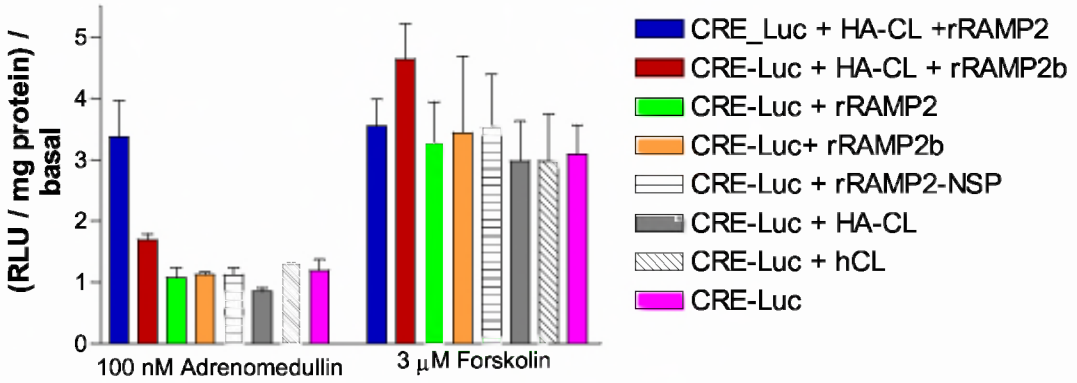

Figure 29. Efficiency of HA-tagged CL signal transduction. COS-7 cells were transfected with CRE-Luc, HA-CL and either rRAMP2 or RAMP2b to determine if the HA-tag interfered with the signal transduction of the AM_1. COS-7 cells were transfected with negative controls. Cells were stimulated with either 3 µM forskolin, 100 nM AM or a vehicle control and cAMP was measured in relative light units (RLU). Data are means ± SEM of three to four experiments done in duplicate. The CRE-Luc + HA-CL + rRAMP2 transfected COS-7 cells produced a functional AM_1 indicating that the HA-tag does not interfere with the receptor's activity. Negative controls showed that there are insufficient amounts of endogenous CL or RAMP2 protein expressed by COS-7.

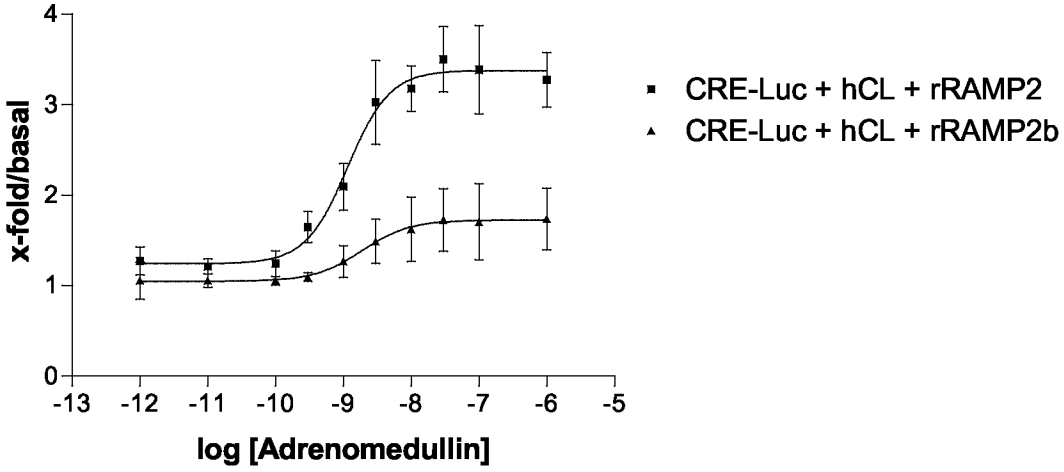

Figure 30. Concentration response curves for adrenomedullin stimulated COS-7 cells transfected with CRE-Luc, hCL, and either rRAMP2 or rRAMP2b. The EC_{50} for rRAMP2 is 1.2 nM and the EC_{50} for rRAMP2b is 1.9 nM.

Discussion

My study has shown that the presence of the signal peptide is essential for the trafficking of the rat RAMP2 to the cellular membrane and for the production of a functional AM_1 receptor. However, the deletion of a 26 amino acid region from within the critical hydrophobic region of the RAMP2 signal peptide (RAMP2b) still allows the RAMP2 protein to traffic to the COS-7 cell membrane in the presence or absence of the CL protein, but the cAMP functional response is diminished. This endogenous RAMP2alternative splice variant and its mutant signal peptide could play an important role in modulating the signal transduction of receptors requiring RAMP2 for functional activity.

Most studies have not investigated the role of the RAMP2 signal peptide in cellular function and trafficking since experiments are generally performed with a RAMP2 transfection plasmid with an epitope tag to follow the RAMP2 within the cell and a more efficient generic signal peptide is substituted for the wild type signal peptide (Kuwasako et al., 2000). Christopoulos et al. did investigate the native signal peptide in humans by designing a human RAMP2 construct with the native signal peptide but the peptide was fused to a double hemagglutinin (HA) tag (Christopoulos et al., 2003). Their results show that this construct had a lower cell surface expression than that of a c-Myc RAMP2 construct with an artificial signal peptide. However it is not clear if this difference in trafficking is due to the presence of different signal peptides or the choice of the epitope tag. The choice of the epitope tag can also determine the extent of cell surface expression. This was shown for the CL receptor where the HA-tagged CL

expresses at the plasma membrane in HEK293T cells; whereas the Myc-tagged CL does not (Hilairet et al., 2001b).

In my experiments I have been able to investigate both the RAMP2 cell surface expression and signal transduction in the absence of an epitope tag by using a RAMP2 antibody directed against the extracellular N-terminus of RAMP2. To my knowledge, my data shows the first use of this RAMP2 antibody (sc-11380 from Santa Cruz Biotechnology Inc.) in immunofluorescent studies. Previous laboratories have had success with this antibody to detect protein levels in western blots. However, multiple bands have been detected (Uzan et al., 2004; Uzan et al., 2006), which may indicate both monomers and homodimers as suggested by Sexton et al. (Sexton et al., 2001). Zhao et al. also found two bands in RAMP2 transfected COS-7 cells using the RAMP2 antibody; however, they also found the larger molecular weight band thought to correspond to the RAMP2 homodimers or a RAMP2 heterodimer complex in untransfected COS-7 cells (Zhao et al., 2006). They also conclude that the RAMP2 antibody, as well as the CL (sc-18007), RAMP1 (sc-11379) and RAMP3 (sc-11381) antibodies from Santa Cruz Biotechnology Inc., may detect proteins unrelated to the RAMP-CL complex. However, multiple bands for RAMP2 western blots are not unusual. Fernandez-Sauze et al. raised antibodies against the RAMP2 and obtained multiple bands on their western blots, indicating a monomer, a dimer, and possibly a deglycosylated form of RAMP2 (Fernandez-Sauze et al., 2004). To confirm the specificity of the antibody, they performed an absorption assay, which abolished the bands. In my experiments, the RAMP2 antibody (sc-11380) did not detect any RAMP2 staining in untransfected cells

but was able to detect immunostaining in RAMP2 transfected cells thus adding validity to the specificity of this antibody.

I detected the CL protein with the CL (sc-18007) antibody obtained from Santa Cruz Biotechnology Inc. and it has been previously used in immunofluorescent studies. Previous experiments by Takhshid et al. have shown the antibody to be specific for the CL by performing a preadsorption control with CL antisera (Takhshid et al., 2006). This CL antibody is directed to an epitope on the C-terminus of the CL, which is located on the intracellular portion of the heptahelical protein. In my experiments the CL antibody only stained permeabilized cells that were transfected with CL and rat RAMP2 and could not distinguish between the nonmembrane bound CL protein as well as membrane bound protein (Figure 24). The exclusively membrane bound CL fraction was detected in non-permeabilized cells transfected with CL plasmid constructs where an HA tag was added to the N-terminus of the CL protein and the cells were stained with an HA antibody (Figure 27).

My immunocytochemistry experiments have shown the rat RAMP2 and RAMP2b traffic to the plasma membrane in the presence and absence of the CL protein (Figures 26 and 27). Non-permeabilized cells that are stained with the RAMP2 and HA antibodies and transfected with HA-CL and RAMP2 or RAMP2b showed a convergence of the two stains on the cell membrane. Although these experiments are not quantitative to indicate the levels of cell surface protein expression, the rat RAMP2b does traffic to the plasma membrane even though it is predicted to not have a signal peptide.

The functional activity of the AM_1 receptor was determined by cAMP stimulation. These experiments confirmed that the N-terminal HA-tag on the CL protein obtained

from Dr. Porter had no effect on the AM_1 receptor's activity (Figure 29). In addition, the function of rRAMP2b was examined by performing cAMP assays using the luciferase gene. There was a decrease in cAMP response of rRAMP2b compared to that of the rRAMP2 transfected cell models which, in combination with the presence of the rRAMP2b on the cell membrane, indicates that the predicted hydrophobic deficient signal peptide does not entirely compromise receptor activity or cell membrane trafficking. However, the presence of a signal peptide was essential to these two events since the RAMP2 construct lacking the signal peptide, rRAMP2-NSP, did not traffic to the cell membrane nor did it show any AM_1 receptor activity in the presence of the CL protein.

From these experiments it is not clear if the trafficking of the RAMP2 to the cell membrane might be slightly impaired by the absence of the complete signal peptide and thus diminishes cAMP activity, or if the deficient signal peptide might be retained in the rRAMP2b protein as it traffics to the membrane and thus might interfere with AM_1 agonist binding and/or signal transduction. It is also not clear how this signal peptide deficient in a hydrophobic region actually allows the protein to traffic to the cell membrane. The function of this endogenous alternatively spliced RAMP2 variant may play a role in other receptor trafficking and may play a role as a negative modulator of AM_1 or other receptor function.

CHAPTER 5

CONCLUSION

Summary

The discovery of receptor activity modifying proteins (RAMPs) in 1998 has changed our understanding of receptor complexes (McLatchie et al., 1998). GPCRs were thought to mostly be monomeric proteins, but now have been to shown to form dimers with other GPCRs and accessory proteins, like RAMPs. RAMP1 can form hetero-oligomers with the CL homo-oligomer in the endoplasmic reticulum and they are transported together to the Golgi apparatus and plasma membrane (Heroux et al., 2007). The receptor complex remains together during lysosomal degradation or recycling. Recent evidence suggests that RAMPs1-3 interact with transmembranes 1-5 of the CL for efficient cell surface translocation (Kuwasako et al., 2009). The RAMP2 also requires an association with the CL homo-oligomer's extracellular domain, third intracellular loop, and sixth transmembrane domain.

The calcitonin family of receptors is not the only case of receptor dimerization. In fact, many GPCRs form heterodimers. The endogenous $GABA_B$ receptor requires two GPCRs, the $GABA_BR1$ and $GABA_BR2$. The CL protein has been shown to form a homo-oligomer, which mostly remains in the endoplasmic reticulum until it interacts with a RAMP. The α_{1D}-adrenergic receptor also has poor expression at the cell surface. Once coexpressed with the α_{1B}-adrenergic receptor, the α_{1D}-adrenergic receptor exhibits greater cell surface expression (Hague et al., 2004).

Three known mammalian RAMPs have been identified, RAMPs 1-3. RAMPs form dimers with GPCRs to act as a functional receptor. In the absence of this dimerization, the GPCR could have a different signal transduction pathway or no function at all. Other accessory proteins include the Drosophila cyclophilin gene *ninaA* (neither inactivation nor afterpotential A) and the mammalian RanBP2-encoding gene (RanBP2 for Ran binding protein 2), which translocates opsins to the plasma membrane (Colley et al., 1991; Ferreira et al., 1996).

As shown in Figure 31, RAMPs interact with CL and CTR or form homodimers that are retained in the ER. RAMPs also form complexes with vasoactive intestinal peptide/pituitary adenylate cyclase activating peptide (VPAC) 1 receptor, the parathyroid hormone (PTH) receptor 1, PTHR2, calcium sensing (CalS) receptor, glucagon and secretin receptor (Christopoulos et al., 2003; Bouschet et al., 2005; Harikumar et al., 2009). The β-adrenergic receptor may also be affected by RAMP expression (Tilakaratne et al., 2002). Increased levels of RAMP1 in Parkinson induced cells treated with dopamine may suggest an association of RAMP1 with the dopamine receptors (Lee et al., 2008).

Implications

The discovery of RAMP2 splice variants increases the complexity of an already elaborate system. Table 6 shows the updated list of calcitonin family receptors. Because RAMPs interact with not only the CL and CTR, the impact of the RAMP2 splice variants has not fully been determined. Further experiments will be needed to determine if the RAMP2b interacts with other receptors.

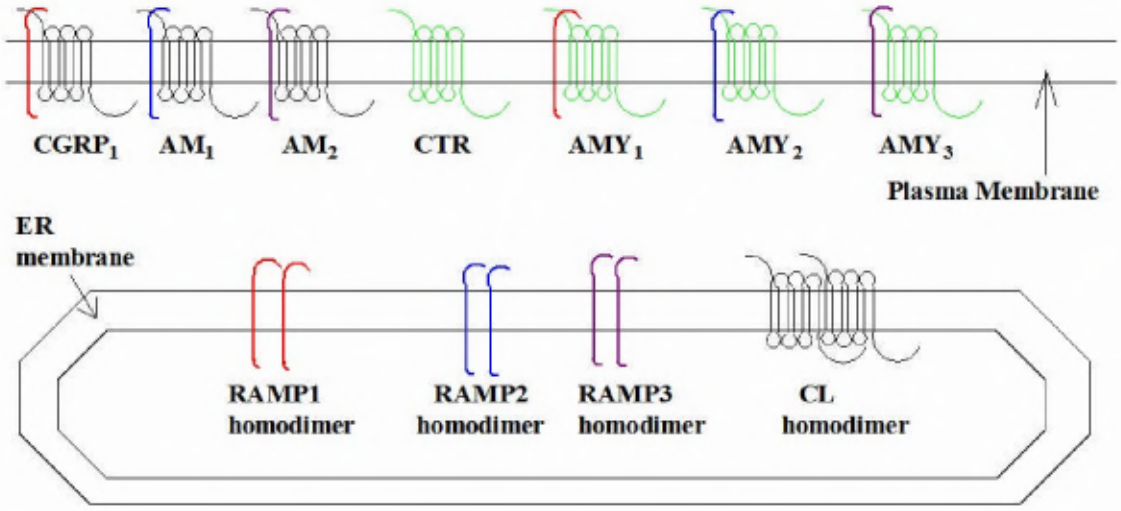

Figure 31. RAMPs associate with certain G protein coupled receptors (GPCRs) or form homodimers. These complexes originate in the endoplasmic reticulum and may traffic to the plasma membrane. The RAMP1, RAMP2, RAMP3, and CL can form homodimers or homo-oligomers that are retained in the ER. The CL and CTR can form complexes with all three RAMPs. The CTR can also act as a receptor independent of the RAMPs. This figure was adapted from Hay et al. (Hay et al., 2006).

Table 6. Updated list of the calcitonin family of receptors, including splice variants.

Calcitonin Receptors	Amylin Receptors	CGRP Receptor	Adrenomedullin Receptors
CTR_a	CTR_a + RAMP1	CLs + RAMP1	CLs + RAMP2
CTR_b	CTR_a + RAMP2		CLs + RAMP2b*
	CTR_a + RAMP2b*		CLs + RAMP3
	CTR_a + RAMP3		
	CTR_b + RAMP1		
	CTR_b + RAMP2		
	CTR_b + RAMP2b*		
	CTR_b + RAMP3		

The calcitonin receptor family consists of four types of receptors: calcitonin, amylin, CGRP (calcitonin gene-related peptide), and adrenomedullin. The calcitonin receptors consist of the calcitonin receptor (CTR) and a splice variant. Splice variants located near the translation start codon, untranslated regions, or incomplete receptors of CTR are not classified. Amylin receptors include the CTR and RAMPs and their splice variants. The CGRP receptor is a receptor complex of a CL (calcitonin receptor like) homo-oligomer and the RAMP1. A CGRP receptor subtype ($CGRP_2$) has not been cloned and proven not to exist (Rorabaugh et al., 2001). Adrenomedullin receptors are divided into two subtypes AM_1 (CL+CL+RAMP2) and AM_2 (CL+CL+RAMP3). The asterisks indicate the new RAMP2b and the proposed interactions, but there has been no data to support that it can form an amylin receptor. The human and rat RAMP2b splice variants also form an adrenomedullin receptor.

Although the function of the human RAMP2b has not been established, the hRAMP2b contains fifteen extra nucleic acids retained from an intron, which corresponds to an additional five putative amino acid residues. The RAMP2 N-terminus contains this variable region. The N-terminal region of the RAMPs includes amino acids critical for ligand specificity and trafficking to the plasma membrane (Rodriguez-Boulan and Gonzalez, 1999; Kuwasako et al., 2001; Flahaut et al., 2002; Kuwasako et al., 2008; Qi et al., 2008). Preliminary data shows that hRAMP2b forms an adrenomedullin receptor when coexpressed with the hCL (Figure 13).

Because RAMP2 can form dimers with many GPCRs, it is possible that the new human RAMP2 splice variant might affect the function of the other receptor complexes. RAMP2 splice variants identified in the pufferfish have variable regions in the signal peptide (Nag et al., 2006). The rat RAMP2b discovered and cloned in our laboratory also has differences in the signal peptide (Rorabaugh, 2002). Unlike the pufferfish, the rat variant has a deletion of 26 amino acids in its long 46 amino acid signal peptide. The pufferfish splice variants have different first exons, creating two distinct signal peptides. The variance in the signal peptide may cause one protein to be expressed at the plasma membrane in greater quantity than the other.

Signal sequences act as indicators that a protein will go to the ER and either stays there or traffic to the plasma membrane, secretory vesicles or lysosomes. Proteins lacking signal sequences usually remain in the cytoplasm. The two types of signal sequences are signal anchors and signal peptides. A signal anchor sequence remains in the mature protein, usually in the first transmembrane domain. All membrane proteins that have an intracellular N-terminus utilize signal anchors.

A signal peptide sequence translates with the protein at the N-terminus and then signal peptidase cleaves it off after it enters the ER. The signal peptide usually consists of a short, positively charged amino-terminal region, central hydrophobic region and a polar carboxy-terminal region containing the cleavage site. Many signal peptides have between 20 and 30 amino acid residues, with about 7 to 13 residues in the hydrophobic core. During SRP-dependent translocation, the signal recognition particle (SRP) recognizes the hydrophobic core and transports the new complex to the SRP receptor on the ER (Walter and Blobel, 1980). The SRP pauses translation until the ribosome complex reaches the translocase complex and SRP is released. Therefore, membrane bound protein expression occurs at the ER while the protein embeds into the ER membrane.

Missing 26 amino acids from the long wildtype RAMP2 signal peptide, the rat RAMP2b has 19 amino acids before the wildtype mature protein. SignalP3.0 and Kyte-Doolittle hydropathy plots do not predict a signal peptide for the rat RAMP2b (Figures 18b and 19b). The rRAMP2b retains half of the amino-terminal region and most of the polar carboxyl-terminal region containing the wildtype predicted cleavage site. However, the hydrophobic region of 10 leucines as predicted by SignalP3.0 in Figure 18a is missing from the rat RAMP2b. A study by Kaiser et al. shows that the biggest requirement of a signal peptide is the hydrophobic core (Kaiser et al., 1987).

The rRAMP2b has 26 putative amino acid residues deleted from its signal peptide including 10 hydrophobic leucines. Chou and Kendall have shown that mutating 10 amino acids in the natural hydrophobic core region of the secretory protein PhoA to amino acid residue stretches of leucines, isoleucines, valines or alanines could change the

rate of transport. For example, the natural, 10 leucine, and 15 leucine hydrophobic cores all had very rapid and complete transport at 1 min, (96%, 95%, and 97%, respectively). The 10 isoleucine stretch also was rapid but the 10 valine and 10 alanine hydrophobic cores were slow and weak. Increasing the length of the core helped the valine and alanine groups increase transport. Increasing the core to 20 leucines caused translocation to the ER, but anchored the protein in the membrane. Hydrophobic cores with 16-20 amino acid residues can act as anchors creating transmembrane domains (Davis and Model, 1985; Davis and Hsu, 1986). SiganlP3.0 predicts that the rRAMP2 also contains a 10 leucine hydrophobic core (Figure 18a). Based solely on the hydrophobic core, the rRAMP2 may also have a rapid and complete translocation.

In order to determine whether the rat RAMP2b traffics to the plasma membrane, COS-7 cells were transfected with rat RAMP2 or RAMP2b in the presence and absence of human HA-tagged CL. Protein expression experiments using confocal microscopy show that both rat RAMP2 and RAMP2b express independently at the plasma membrane in the presence and absence of CL. Therefore, the rat RAMP2b translocates to the ER before being processed to the cell membrane.

Even though the rat RAMP2b does not have a predictable signal peptide sequence, a signal anchor may be present. Signal anchors, usually located in the first transmembrane domain, target the protein to the ER after the N-terminus of the mature protein has been translated. Some proteins have both a cleavable signal peptide and a signal anchor (Wallin and von Heijne, 1995). Unfortunately, signal anchors do not have a consensus sequence or a reliable prediction pattern.

A rat RAMP2 mutant was constructed to establish whether the rat RAMP2 has a signal anchor. The rRAMP2-NSP lacks most of the signal peptide and only has five amino acid residues including the leading methionine residue before the predicted cleavage site (Figure 18). The rRAMP2-NSP was not expressed at the plasma membrane in the presence or absence of human CL. However, the rRAMP-NSP expresses intracellularly. Therefore, it is likely that the rRAMP2-NSP does not have an efficient signal sequence (peptide or anchor) that targets it to the ER and it becomes a cytosolic protein. Conversely, the rRAMP2-NSP may undergo SRP-independent translocation and be released into the cytosol or remain trapped in the ER.

Because the rRAMP2b does not have a predicted signal peptide (Figures 18b and 19b) and has been shown at the cell surface (Figure 26a and 27b), trafficking to the ER may require chaperone proteins in the absence of SRP binding (Hegde and Bernstein, 2006). The SRP binds to the hydrophobic region of the signal sequence; however, in the absence of a highly hydrophobic region in bacteria and yeast protein, chaperone proteins translocate the translated proteins to the ER in a relaxed structure. In yeast, SRP-deficient cells survived but grew poorly, showing the cells can function in its absence (Hann and Walter, 1991). Schlenstedt et al. show that the posttranslational polypeptide chain, preprocecropin A, can translocate in the absence of SRP, docking proteins, ribosomes and ribosome receptors (Schlenstedt et al., 1990). The same protein can also translocate cotranslationally in the presence of the SRP and its components.

A cAMP dependent luciferase assay of COS-7 transfected cells examined the function of the rat RAMP2 and RAMP2b. Activation of the CL and rat RAMP2 or RAMP2b complex leads to AM_1 receptor activation of both sets (Figure 28).

Concentration response curves showed that both have similar EC_{50}s, but the hCL-rRAMP2b complex has a 47% lower maximal stimulation than does the hCL-rRAMP2 complex (Figure 30).

The exact method of how rRAMP2b decreases the adrenomedullin receptor's function is unknown. The rRAMP2b may translocate to the ER using a SRP-independent pathway, which can have cotranslational or posttranslational translocation. Although one of the proteins studied was efficiently processed using the SRP-dependent or SRP-independent pathways, another protein was less efficiently processed using posttranslational proteins in the SRP-independent translocation (Schlenstedt et al., 1990). Schlenstedt et al. suggest that the folding of the translated domain may cause the decrease. Because the rRAMP2b likely uses a different translocation pathway, the protein may fold differently than the wildtype rRAMP2.

Chaperones keep the protein in a loosely folded structure. This suggests that the long N-terminus of the RAMP2b may have misfoldings. This new configuration may result in a shape that is more likely to form a dimer with one protein over another. For example, the rRAMP2b may be more prone to form homodimers with themselves in the ER, making them less likely to interact with the CL homo-oligomer. The new rRAMP2b folding may also be less favorable for the CL homo-oligomer creating a weaker attraction. In the absence of other RAMPs, the rRAMP2b may cause less adrenomedullin receptor complexes to be present at the cell surface than in the presence of rRAMP2.

The rat RAMP2b, lacking 26 amino acids from the signal peptide, traffics to the plasma membrane in the presence and absence of CL. Luciferase cAMP experiments on transfected COS-7 cells show that rRAMP2b and CL form an adrenomedullin receptor.

Concentration response curves suggest that less rat RAMP2b-CL and more rat RAMP2-CL complexes traffic to the cell surface. Further studies can determine the exact mechanism of translocation of the rat RAMP2b splice variant to the ER and whether it forms complexes with other GPCRs.

Because adrenomedullin, CL, and RAMP2 expression changes in different disease states, there are many implications of splice variants in this field. Research thus far has shown both rat RAMP2 and RAMP2b mRNA in the rat tissues examined (Rorabaugh, 2002). Future research can determine the whether protein expression of the RAMP2 or RAMP2b changes during pathological states.

APPENDIX

MOLECULAR AND PHARMACOLOGICAL CHARACTERISTICS OF THE GERBIL α_{1a}-ADRENERGIC RECEPTOR

Abstract

The gerbil α_{1A}– adrenergic receptor mediates vasoconstriction of the gerbil spiral modiolar artery, which provides blood to the inner ear. Since the gerbil is used as a mammalian model for hearing, we wanted to clone and express the gerbil α_{1a}-adrenergic receptor in order to compare its pharmacological properties to other mammalian α_{1a}-adrenergic receptors. Translation of the cDNA clone revealed a putative extra amino acid in the third intracellular loop, which could produce unique receptor pharmacology. We transiently transfected the cDNA into COS-1 cells and determined the pharmacological characteristics by [^{3}H]prazosin competition binding experiments. The K_i values for the α_{1A}-adrenergic receptor selective antagonists 5-methylurapidil and WB-4101 were 4.9 ± 1 nM and 1.0 ± 0.1 nM, respectively. BMY 7378, an α_{1D}-adrenergic receptor selective antagonist, bound with low affinity (260 ± 60 nM). Unlabeled prazosin had a K_i of 0.89 ± 0.09 nM. The 91.6% amino acid sequence identity and K_is of the cloned gerbil α_{1a}-adrenergic receptor are similar to the human cloned α_{1a}-adrenergic receptor. Therefore, the above data suggests that the gerbil α_{1a}-adrenergic receptor is representative of the human α_{1a}-adrenergic receptor lending validity to the use of the gerbil as a hearing model.

Introduction

The inner ear transmits sound vibrations into nerve impulses, which after traveling to the brain gives us the sensation of hearing. The inner ear receives its blood flow from the labyrinthine artery, which branches into the vestibulocochlear and spiral modiolar artery (SMA). Vasospasms of the SMA can cause inner ear ischemia, which may lead to certain types of hearing loss.

SMA blood flow is controlled by the sympathetic nervous system and adrenergic receptors (ARs). Sympathetic nerve fibers have been shown to innervate the SMA and Laser Doppler flowmetry has determined that the α_1-ARs control cochlear blood flow (Carlisle et al., 1990; Ohlsen et al., 1991). Wangemann and Wonneberger have also shown that the branch points of the SMA have sympathetic innervation (Wangemann and Wonneberger, 2005).

The α_1–ARs mediate the constriction of various blood vessels and are therapeutic targets in the treatment of hypertension and other cardiovascular diseases. The α_1–ARs are further separated into the subtypes α_{1A}, α_{1B}, and α_{1D} based on their pharmacology and molecular structure. It is conventional to refer to pharmacologically characterized endogenous α_1–ARs as uppercase letters and cloned subtypes as lowercase letters (Hieble et al., 1995).

The Mongolian gerbil has become a commonly used mammalian hearing model because of its large ear parts and thin cochlear bone, which makes cochlear blood flow measurements extremely consistent (Mom et al., 1999). Previous studies in the gerbil have shown that α_{1A}–AR mediates the vasoconstriction of the SMA (Gruber et al., 1998). Interestingly, in gerbil functional studies by Gruber et al., prazosin and 5-methylurapidil

(5-MU) have high affinities values. In view of this atypical functional data, we felt compelled to investigate the possibility that the α_{1a}-AR gene itself might have a variant sequence that would explain the discrepancies in the pharmacology observed for the gerbil α_{1A}-AR. Thus we cloned and expressed the complete coding region of the gerbil α_{1a}–AR to determine if the receptor is different from the α_{1a}–AR of other species with respect to molecular and pharmacological properties.

Materials and Methods

Chemicals and reagents. BMY 7378 dihydrochloride, 5-methylurapidil, phentolamine methanesulfonate, prazosin hydrochloride, and WB-4101 hydrochloride were obtained from Sigma-Aldrich, and [7-methoxy-^{3}H]prazosin ([^{3}H]prazosin) (70–87 Ci/mmol) was obtained from PerkinElmer Life and Analytical Sciences (Boston, USA). Dulbecco's modified Eagle medium, fetal bovine serum, agarose, and *Eco*R I were purchased from Invitrogen. *Not* I was purchased from New England Biologicals (Beverly, USA). Tris hydroxymethyl aminomethane and ScintiVerse scintillation fluid were obtained from Fisher Scientific (Suwanee, USA).

Tissue isolation and total RNA extraction. Gerbils were anaesthetized with sodium pentobarbital (50 mg kg^{-1}, i.p.). The animals were cared for in accordance with the Guide to the Care and Use of Laboratory Animals (1996, published by National Academy Press, 2101 Constitution Ave. NW, Washington, DC 20055, USA) and by a protocol approved by the Creighton University Institutional Animal Care and Use Committee. The brain, spiral modiolar artery, and various other tissues were quickly

removed, frozen in liquid nitrogen, and stored at -70°C. Total RNA was extracted with TRIzol Reagent (Invitrogen, Carlsbad, USA).

Amplification of the gerbil α_{1a}-AR cDNA sequence by RT-PCR. The reverse transcription (RT) reaction used 25 pmol antisense gene specific primer and 50 units Moloney murine leukemia virus reverse transcriptase (Applied Biosystems, Foster City, USA). The polymerase chain reaction (PCR) contained 25 pmol of the sense primer and 2.5 units *Taq* DNA polymerase (Invitrogen). PCR conditions were as follows: 5 minutes of denaturation at 95°C, followed by 39 cycles of 1 minute at 95°C, 1 minute at 58°C, and 3 minutes at 72°C, and a final extension of 10 minutes at 72°C.

Oligonucleotide sense and antisense primers were designed based on the rat α_{1a}-AR cDNA (Scofield et al., 1995) and the third intracellular loop of the gerbil α_{1a}-AR (Gruber et al., 1998). RT-PCR was performed using these primers, which are listed in Table 7. Similarly, a degenerative primer was used to amplify the 5′ region of the gerbil α_{1a}-adrenergic receptor. Then a 3′ RACE using the FirstChoice® RLM-RACE Kit (Ambion, Austin, USA) and gerbil specific primers from regions already sequenced was performed to obtain the C-terminal sequence.

All cDNA PCR and 3′ RACE products were then cloned into the pCRII cloning vector according to the TA Cloning Kit protocol (Invitrogen). The clones were sequenced (ABI model 373, Applied Biosystems). DNA sequences were analyzed using the Wisconsin Package Version 10.1 (Genetics Computer Group, Madison, USA) software.

Cloning of full-length gerbil α_{1a}-AR cDNA into a mammalian expression vector. The full-length gerbil α_{1a}-AR from gerbil total RNA was amplified by RT-PCR with primers UP4 and DN3 (Table 7 and Figure 32). The RT-PCR conditions were the same as

above except that Platinum® *Pfx* DNA polymerase (Invitrogen) with 2.5 mM $MgSO_4$ was used for PCR amplification. Restriction digest sites and a Kozak sequence were then added by performing another PCR with the sense primer UP-EcoRI containing two *Eco*R I digest sites and a Kozak sequence GCCACC and the antisense primer DN-NotI containing two *Not* I digest sites (Table 7) (Kozak, 1987). The PCR product was cloned into the pcDNA3.1+ vector (Invitrogen) using the restriction digest sites *Eco*R I and *Not* I. The DNA was sequenced and analyzed.

Transfection of recombinant gerbil α_{1a}-AR. COS-1 cells, African green monkey kidney cells, were obtained from American Type Culture Collection and grown in Dulbecco's modified Eagle medium that was supplemented with fetal bovine serum (10%). Cells were grown to confluency in T-75 cell culture flasks at 37°C in a humidified incubator with an atmosphere of 5% CO_2/ 95% air. Recombinant gerbil α_{1a}-AR was transfected into several flasks of COS-1 cells using FuGENE 6 Reagent with a 2:1 ratio according to the manufacturer's protocol (Roche, Indianapolis, USA).

Cell membrane preparation and radioligand binding. Cell membrane preparation and radioligand binding was performed as described previously (Bockman et al., 2004). Forty-eight hours after transfection, media were removed and the cells were rinsed twice with phosphate-buffered saline (137 mM NaCl, 2.7 mM KCl, 5.4 mM Na_2HPO_4, and 1.8 mM KH_2PO_4, pH = 7.4). The cells were scraped and harvested by centrifugation at 4°C for 15 minutes at 1000 g. The pellet was suspended in ice-cold 50 mM Tris buffer (pH 7.4). The cells were homogenized twice using a Janke and Kunkel Ultra-Turrax T25 homogenizer (Janke and Kunkel, Staufen, Germany) for 10 seconds. The homogenate was centrifuged at 4°C for 20 minutes at 30,000 g and the pellet was

Table 7. Sequence and species specificity of α_{1a}-adrenergic receptor oligonucleotide primers. Y=C/T, K=T/G, and R=A/G.

Primer	Sequence	Species
P1	5′-GTAGCCAAGAGAGAAAGCCG-3′	Rat/ Mouse
DN1	5′-CAACCCACCACGATGCCCAG-3′	Rat
UP2	5′-ATGGTGYTTCTYTCKGRAAA-3′	Rat/Mouse/ Human/Cow
DN2	5′-GCAGCAGACCTGCAAAAAG-3′	Rat
UP3	5′-AGGGATCGGCCAGGATTACA-3′	Rat/ Gerbil
DN3	5′-ATCAGCAGGACCTAGCGTCAA-3′	Gerbil
UP4	5′-ATGGTGTTTCTTTCGGAAAATGC-3′	Gerbil
UP-EcoRI	5′-GAATTCGAATTCGCCACCATGGTGTTTCTTTCGGAAAA-3′	Gerbil
DN-NotI	5′-GCGGCCGCGCGGCCGCCTAGACTTCCTCCCCGTTTTCG-3′	Gerbil

recovered. After resuspending the membrane pellet in Tris buffer, it was washed and centrifuged twice and stored at -70°C. The pellet was resuspended in 50 mM Tris buffer and homogenized just prior to analysis. Protein concentrations were determined by the Bradford assay (Pierce, Rockford, USA) (Bradford, 1976).

Transfected proteins were incubated with [^{3}H]prazosin in the presence of increasing concentrations of unlabeled drugs for 30 minutes in a 37°C water bath with light shaking. Assay tubes were pretreated with Sigmacote (Sigma-Aldrich, St. Louis, USA) as specified by the manufacturer. The bound protein was separated by vacuum filtration through a Whatman GF/B glass microfiber filter and rinsed three times with approximately 5 ml of ice-cold 50 mM Tris buffer (pH 7.4). The filters were transferred into scintillation vials with scintillation fluid. The vials were vortexed and counted in a scintillation counter. Data analysis was performed using GraphPad Prism. K_i values were calculated from IC_{50} values (Cheng and Prusoff, 1973).

Results

Amplification of the gerbil α_{1a}-AR cDNA sequence by RT-PCR. Previous amplification of 175 nucleotides of the third intracellular loop for the gerbil α_{1a}-AR in the SMA showed a putative extra amino acid and a nucleotide percent identity of 90.9, 92.5, and 85.7% when compared similar regions of the rat, mouse, and human α_{1a}-AR, respectively (Gruber et al., 1998). We used the primers from Gruber et al., UP1 and DN1, and primers (Figure 32 and Table 7) that were designed based on α_{1a}-AR sequences from other species to clone portions of the gerbil α_{1a}-AR. In addition, a high fidelity DNA polymerase, Platinum® *Pfx* DNA polymerase from Invitrogen, was used to prevent

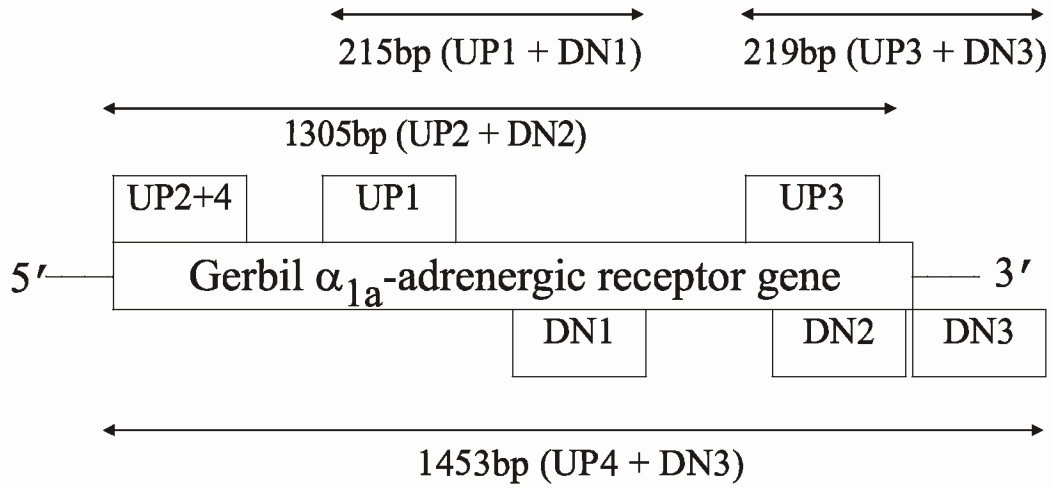

Figure 32. Oligonucleotide primers and the corresponding PCR product. Sense primers are UP1, UP2, UP3, and UP4 and their sequence location with respect to the gene is indicated. Antisense primers are DN1, DN2, and DN3 and their respective sequence location is shown. Primer sequences and species specificity are listed in Table 1. The size of the PCR products for the primer combinations is indicated and the arrows correspond to the respective regions of the gerbil α_{1a}-adrenergic receptor.

any errors during the amplification of the cDNA. Consequently, the 5′ region was cloned with a degenerate primer (UP2) from the open reading frame start site based on consensus sequences for the α_{1a}-AR from the rat, mouse, human, and cow. The RT-PCR product for UP2 and DN2 is shown in Figure 33. The 3′ region of the gerbil α_{1a}-AR was amplified by a 3′ RACE using the gene specific primer UP3. The complete cDNA sequence was amplified by RT-PCR with the primers UP4 and DN3 and the product was cloned and sequenced (Figure 34). The nucleotide percent identity for the complete gerbil α_{1a}-AR sequence was 93.0, 93.1, and 881% when compared to the rat, mouse, and human α_{1a}-AR, respectively (Figure 35). The coding region contained 467 amino acid residues with an additional amino acid in the third intracellular loop. The amino acid percent identities of the full-length gerbil α_{1a}-AR versus the rat, mouse, and human α_{1a}-AR were 96.8, 96.4 and 91.6%, respectively (Figure 36). None of the amino acid differences between the gerbil and other species were within published agonist or antagonist binding sites (Figure 37) (Hwa et al., 1995; Hamaguchi et al., 1996; Hwa and Perez, 1996; Porter et al., 1996; Zhao et al., 1996; Waugh et al., 2000; Piascik and Perez, 2001; Waugh et al., 2001; Pedretti et al., 2004; Kinsella et al., 2005). However, because the binding sites for many of the antagonists such as prazosin or 5-MU and the residues that interact with the agonist α-hydroxyl group have not all been clearly defined (Piascik and Perez, 2001; Pedretti et al., 2004), we cannot determine from the sequence alone whether or not the gerbil α_{1a}-AR might have residue substitutions at antagonist binding sites that might result in an atypical pharmacology.

Radioligand Binding. In order to directly compare the pharmacological properties of the recombinant gerbil α_{1a}-AR to those of other species, we determined the K_i values

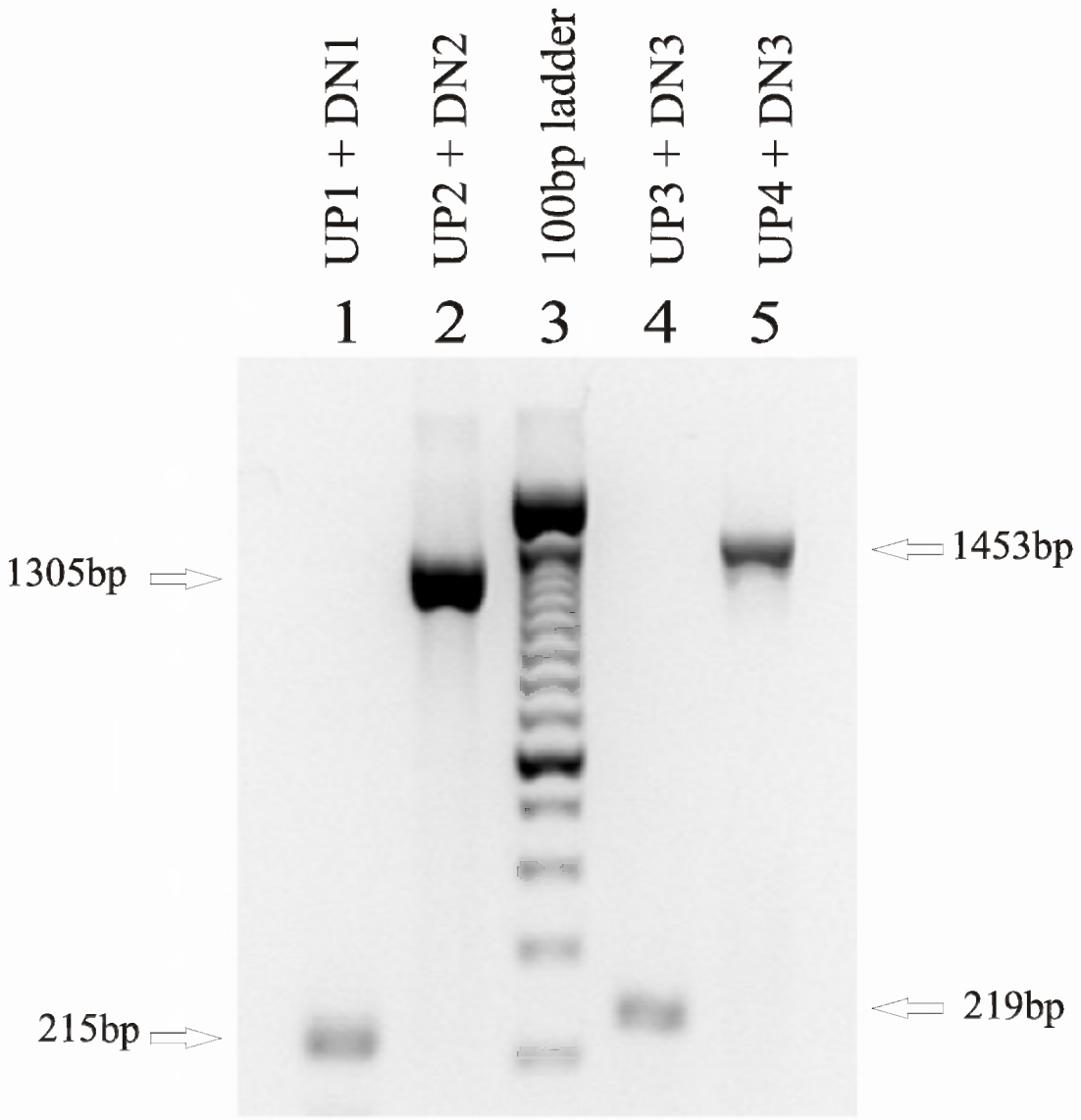

Figure 33. RT-PCR products from gerbil brain total RNA were amplified with indicated sense (UP) and antisense (DN) primers from Table 1 and visualized on a 3% agarose gel stained with ethidium bromide. Negative control reactions (minus reverse transcriptase reactions and reagents only reactions) were also performed to ensure that there was no contamination.

```
1    ATGGTGTTTCTTTCGGAAAATGCTTCCGAAGGCTCCAACTGCACCCACCAGCCAGCACCG   60
     M  V  F  L  S  E  N  A  S  E  G  S  N  C  T  H  Q  P  A  P

71   GTGAACATTTCTAAGGCCATTCTGCTTGGGGTAATCTTGGGGGGCCTCATCATCTTCGGG  120
     V  N  I  S  K  A  I  L  L  G  V  I  L  G  G  L  I  I  F  G

91   GTGCTGGGGAACATCTTAGTGATCCTTTCGGTCGCCTGTCATCGGCACCTGCACTCAGTG  180
     V  L  G  N  I  L  V  I  L  S  V  A  C  H  R  H  L  H  S  V

181  ACTCACTACTACATAGTCAACCTGGCCGTCGCCGACCTCCTCCTCACCTCCACCGTGCTG  240
     T  H  Y  Y  I  V  N  L  A  V  A  D  L  L  L  T  S  T  V  L

241  CCCTTCTCCGCCATCTTTGAGATCCTGGGCTACTGGGCCTTTGGCAGGGTCTTCTGCAAC  300
     P  F  S  A  I  F  E  I  L  G  Y  W  A  F  G  R  V  F  C  N

301  ATCTGGGCTGCGGTGGACGTCCTGTGCTGCACGGCGTCCATCATGGGCCTCTGCATCATC  360
     I  W  A  A  V  D  V  L  C  C  T  A  S  I  M  G  L  C  I  I

361  TCCATCGACAGATACATTGGCGTGAGCTACCCGCTGCGCTACCCTGCCATTGTCACCCAG  420
     S  I  D  R  Y  I  G  V  S  Y  P  L  R  Y  P  A  I  V  T  Q

421  AGGAGGGGCGTCAGGGCTCTGCTCTGCGTCTGGGCGCTTTCCCTGGTCATCTCCATCGGA  480
     R  R  G  V  R  A  L  L  C  V  W  A  L  S  L  V  I  S  I  G

481  CCGTTGTTCGGCTGGAGGCAGCCGGCTCCTGAGGATGAGACAATCTGCCAGATCAATGAG  540
     P  L  F  G  W  R  Q  P  A  P  E  D  E  T  I  C  Q  I  N  E

541  GAGCCTGGCTACGTGCTGTTCTCCGCGCTGGGCTCTTTCTACGTGCCCCTGGCCATCATC  600
     E  P  G  Y  V  L  F  S  A  L  G  S  F  Y  V  P  L  A  I  I

601  CTGGTTATGTACTGTCGGGTCTACGTGGTAGCCAAGAGGGAAAGCCGGGGCCTCAAGTCC  660
     L  V  M  Y  C  R  V  Y  V  V  A  K  R  E  S  R  G  L  K  S

631  GGCCTCAAGACCGACAAGTCGGACTCAGAGCAAGTGACGCTCCGTATCCACCGGAAAAAT  720
     G  L  K  T  D  K  S  D  S  E  Q  V  T  L  R  I  H  R  K  N

721  GTCCCCGCAGAAGGCGGCGGAGGGCTGAGCAGTGCCAAGAATAAGACTCACTTCTCCGTG  780
     V  P  A  E  G  G  G  G  L  S  S  A  K  N  K  T  H  F  S  V

781  CGGCTGCTCAAGTTTTCCCGGGAGAAAAAAGCGGCCAAGACGCTGGGCATCGTGGTGGGT  840
     R  L  L  K  F  S  R  E  K  K  A  A  K  T  L  G  I  V  V  G

841  TGCTTTGTCCTCTGCTGGCTGCCCTTCTTCCTAGTGATGCCCATTGGGTCCTTCTTCCCG  900
     C  F  V  L  C  W  L  P  F  F  L  V  M  P  I  G  S  F  F  P

901  GATTTCAAGCCTCCGGAAACCGTTTTCAAAATAGTGTTTTGGCTCGGGTACCTCAACAGC  960
     D  F  K  P  P  E  T  V  F  K  I  V  F  W  L  G  Y  L  N  S
```

Figure 34. Nucleotide and putative amino acid sequences of the gerbil α_{1a}-adrenergic receptor (accession number HM754402).

```
961  TGCATCAACCCCATCATATACCCATGCTCCAGCCAAGAGTTCAAGAAAGCCTTTCAGAAT 1020
     C  I  N  P  I  I  Y  P  C  S  S  Q  E  F  K  K  A  F  Q  N

1021 GTCCTGAGAATCCAGTGTCTCCGCAGAAGGCCGTCTTCCAAGCATGCCCTGGGCTACACC 1080
     V  L  R  I  Q  C  L  R  R  R  P  S  S  K  H  A  L  G  Y  T

1081 CTGCACCCGCCCAGCCAGGCTGTAGAAGGACAGCACAGAGGCATGGTGCGTATCCCGGTG 1140
     L  H  P  P  S  Q  A  V  E  G  Q  H  R  G  M  V  R  I  P  V

1141 GGCTCGGGAGAGACTTTCTATAAGATCTCCAAAGCGGACGGAGTCTGTGAATGGAAGCTT 1200
     G  S  G  E  T  F  Y  K  I  S  K  A  D  G  V  C  E  W  K  L

1201 CTCTCTTCCATGCCCCAGGGGTCAGCCAGGATTACAGTGCCGAAGGACCAATCTGCCTGC 1260
     L  S  S  M  P  Q  G  S  A  R  I  T  V  P  K  D  Q  S  A  C

1261 ACCACCGCCCGGGTGAGAAGTAAAAGCTTTTTGCAGGTCTGCTGCTGTGTGGGGTCCTCG 1320
     T  T  A  R  V  R  S  K  S  F  L  Q  V  C  C  C  V  G  S  S

1321 ACCCCCAGCCTTGAAGAAAATCACCAGGTTCCAACCATTAAGATCCACACCATCTCCCTT 1380
     T  P  S  L  E  E  N  H  Q  V  P  T  I  K  I  H  T  I  S  L

1381 GGCGAAAACGGGGAGGAAGTCTAG                                    1404
     G  E  N  G  E  E  V  *
```

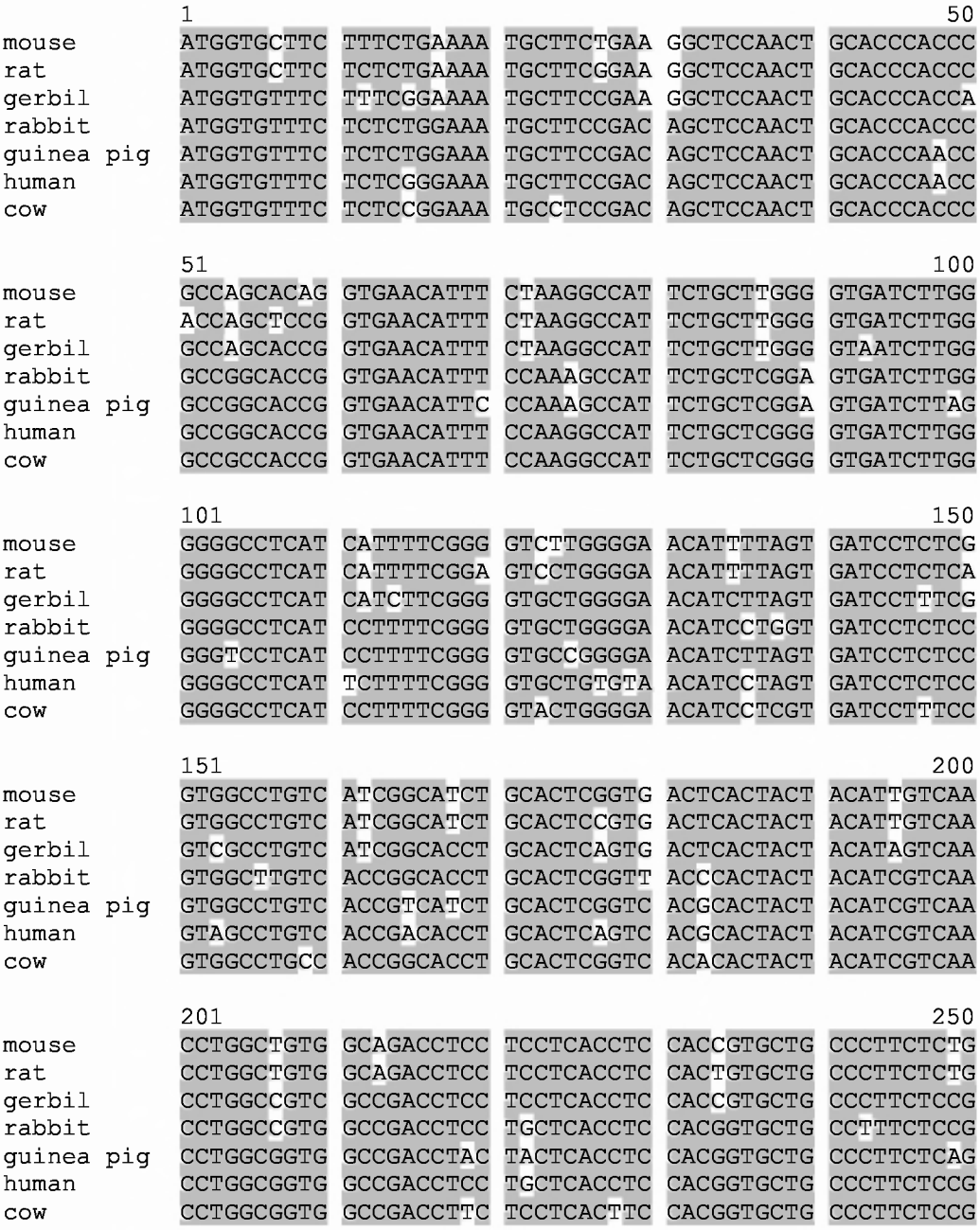

Figure 35. Comparison of nucleotide sequences of mouse, rat, gerbil, rabbit, guinea pig, human and cow α_{1a}-adrenergic receptors. Conserved nucleotides are shaded.

```
            251                                                     300
mouse       CCATCTTTGA GATCCTGGGA TACTGGGCCT TTGGCAGGGT GTTCTGCAAC
rat         CCATCTTTGA GATCCTGGGC TACTGGGCCT TTGGCAGGGT GTTCTGCAAT
gerbil      CCATCTTTGA GATCCTGGGC TACTGGGCCT TTGGCAGGGT CTTCTGCAAC
rabbit      CCATCTTCGA GATCCTGGGC TACTGGGCCT TCGGCAGAGT GTTCTGCAAT
guinea pig  CCATCTTTGA GATCCTGGGC TACTGGGCCT TCGGCAGGGT CTTCTGCAAC
human       CCATCTTCGA GGTCCTAGGC TACTGGGCCT TCGGCAGGGT CTTCTGCAAC
cow         CTATCTTCGA GATCTTGGGC TACTGGGCCT TCGGCAGGGT CTTCTGCAAT

            301                                                     350
mouse       ATCTGGGCGG CGGTGGACGT CTTATGCTGC ACAGCGTCCA TCATGGGCCT
rat         ATCTGGGCGG CCGTGGACGT CTTATGCTGC ACAGCGTCCA TCATGGGCCT
gerbil      ATCTGGGCTG CGGTGGACGT CCTGTGCTGC ACGGCGTCCA TCATGGGCCT
rabbit      ATCTGGGCGG CGGTGGACGT CCTGTGCTGC ACCGCGTCCA TCATAAGCCT
guinea pig  ATCTGGGCGG CGGTGGACGT CCTGTGCTGC ACCGCGTCCA TCATGAGCCT
human       ATCTGGGCGG CAGTGGATGT GCTGTGCTGC ACCGCGTCCA TCATGGGCCT
cow         GTCTGGGCGG CGGTGGACGT CCTGTGCTGC ACGGCTTCCA TCATGGGACT

            351                                                     400
mouse       CTGCATCATC TCCATCGACC GATACATTGG TGTGAGCTAC CCGCTGCGCT
rat         CTGCATCATC TCCATCGACC GATACATTGG TGTGAGCTAC CCGCTGCGCT
gerbil      CTGCATCATC TCCATCGACA GATACATTGG CGTGAGCTAC CCGCTGCGCT
rabbit      CTGCGTGATC TCCATCGACC GCTACATCGG CGTGAGCTAC CCGCTGCGCT
guinea pig  CTGCATCATC TCCATCGACC GCTACATCGG CGTGAGCTAC CCGCTACGCT
human       CTGCATCATC TCCATCGACC GCTACATCGG CGTGACGTAC CCGCTGCGCT
cow         CTGCATCATC TCCATCGACC GCTACATCGG CGTGAGCTAT CCTCTGCGCT

            401                                                     450
mouse       ACCCCACCAT TGTCACCCAG AGGAGGGGCG TCAGGGCTCT GCTCTGCGTC
rat         ATCCCACCAT TGTCACCCAG AGGAGGGGCG TCAGGGCTCT GCTCTGCGTC
gerbil      ACCCTGCCAT TGTCACCCAG AGGAGGGGCG TCAGGGCTCT GCTCTGCGTC
rabbit      ACCCCACCAT CGTCACCCAG CGCAGAGGCC TCCGGGCTCT GCTCTGCGTC
guinea pig  ACCCCACCAT CGTCACCCAG AGGCGGGGGC TCCGGGCTCT GCTCTGCCTC
human       ACCCAACCAT CGTCACCCAG AGGAGGGGTC TCATGGCTCT GCTCTGCGTC
cow         ACCCCACCAT CGTCACCCAG AAGAGGGGCC TCATGGCCCT GCTCTGCGTC

            451                                                     500
mouse       TGGGCGCTTT CCTTGGTCAT CTCCATCGGA CCCCTGTTCG GCTGGAGGCA
rat         TGGGTGCTTT CTTTGGTCAT CTCCATCGGA CCCCTGTTCG GCTGGAGGCA
gerbil      TGGGCGCTTT CCCTGGTCAT CTCCATCGGA CCGTTGTTCG GCTGGAGGCA
rabbit      TGGGCCTTCT CCCTGGTCAT CTCCGTCGGG CCCCTGTTCG GCTGGAGGCA
guinea pig  TGGGCGCTGT CCCTGGTCAT CTCCATCGGG CCGCTGTTTG GCTGGAGGCA
human       TGGGCACTCT CCCTGGTCAT ATCCATTGGA CCCCTGTTCG GCTGGAGGCA
cow         TGGGCGCTCT CTTTGGTCAT CTCCATCGGG CCCCTCTTCG GCTGGAGGCA

            501                                                     550
mouse       GCAGGCTCCG GAGGATGAGA CCATCTGCCA AATCAATGAG GAGCCAGGAT
rat         GCCGGCTCCA GAGGATGAGA CCATCTGCCA GATCAATGAG GAGCCGGGCT
gerbil      GCCGGCTCCT GAGGATGAGA CAATCTGCCA GATCAATGAG GAGCCTGGCT
rabbit      GCCGGCCCCG GACGACGAGA CCATCTGCCA GATCAACGAG GAGCCGGGCT
guinea pig  GCCGGCCCCC CAGGACGAGA CCATCTGCCA GATCAACGAG GATCCCAGCT
human       GCCGGCCCCC GAGGACGAGA CCATCTGCCA GATCAACGAG GAGCCGGGCT
cow         GCCGGCCCCG GAGGACGAGA CCATCTGCCA GATCAACGAG GAGCCGGGCT
```

```
            551                                                       600
mouse       ACGTGCTGTT CTCAGCGCTG GGCTCTTTCT ACGTGCCACT GACCATCATC
rat         ACGTGCTGTT CTCAGCGCTG GGCTCTTTCT ACGTGCCACT GGCCATCATT
gerbil      ACGTGCTGTT CTCCGCGCTG GGCTCTTTCT ACGTGCCCCT GGCCATCATC
rabbit      ACGTGCTCTT CTCGGCCCTG GGCTCCTTCT ACGTGCCTCT GACCATCATC
guinea pig  ACGTGCTCTT CTCCGCGCTG GGATCCTTCT ACGTGCCGCT GGCCATCATC
human       ACGTGCTCTT CTCAGCGCTG GGCTCCTTCT ACCTGCCTCT GGCCATCATC
cow         ACGTGCTCTT CTCGGCTCTG GGCTCCTTCT ACGTGCCGCT GACCATCATC

            601                                                       650
mouse       CTGGTTATGT ACTGTCGAGT CTACGTGGTA GCCAAGAGAG AAAGCCGAGG
rat         CTGGTTATGT ACTGTCGAGT CTACGTAGTA GCCAAGAGAG AAAGCCGGGG
gerbil      CTGGTTATGT ACTGTCGGGT CTACGTGGTA GCCAAGAGGG AAAGCCGGGG
rabbit      TTGGCCATGT ACTGCCGGGT CTACGTGGTG GCCAAGAGGG AGAGCCGGGG
guinea pig  CTGGTCATGT ACTGCCGGGT CTACGTGGTG GCCAAAAGGG AGAGCCGGGG
human       CTGGTCATGT ACTGCCGCGT CTACGTGGTG GCCAAGAGGG AGAGCCGGGG
cow         CTGGTCATGT ACTGCCGGGT CTACGTCGTG GCCAAGAGGG AGAGCCGGGG

            651                                                       700
mouse       CCTCAAGTCC GGCCTCAAGA CCGACAAGTC AGACTCAGAG CAAGTGACGC
rat         CCTCAAGTCC GGCCTCAAGA CGGACAAGTC AGACTCAGAG CAAGTGACGC
gerbil      CCTCAAGTCC GGCCTCAAGA CCGACAAGTC GGACTCAGAG CAAGTGACGC
rabbit      CCTCAAGTCC GGCCTCAAGA CCGACAAATC CGACTCGGAG CAAGTGACGC
guinea pig  CCTCACATCC GGCCTCAAGA CCGACAAGTC GGATTCAGAG CAAGTCACGC
human       CCTCAAGTCT GGCCTCAAGA CCGACAAGTC GGACTCGGAG CAAGTGACGC
cow         CCTCAAGTCG GGCCTTAAGA CCGACAAGTC AGACTCGGAG CAGGTGACGC

            701                                                       750
mouse       TCCGTATCCA CCGTAAAAAT GTCCCTGCAG AAGGCAGCGG AG...TAAGC
rat         TCCGCATCCA CCGTAAAAAT GTCCCTGCAG AAGGCGGCGG AG...TCAGC
gerbil      TCCGTATCCA CCGGAAAAAT GTCCCCGCAG AAGGCGGCGG AGGGCTGAGC
rabbit      TCCGCATCCA CCGGAAAAAT GCTCCCGCCG GAGGCAGCGG GG...TGGCC
guinea pig  TGCGCATCCA CCGGAAAAAT GCCCCGCTAG GAGGCAGTGG GG...TGGCC
human       TCCGCATCCA TCGGAAAAAC GCCCCGGCAG GAGGCAGCGG GA...TGGCC
cow         TCCGCATCCA TCGCAAAAAC GCCCAGGTAG GAGGCAGCGG GG...TGACC

            751                                                       800
mouse       AGTGCCAAGA ATAAGACTCA CTTCTCCGTG AGGCTGCTCA AGTTTTCCCG
rat         AGTGCCAAGA ATAAGACTCA CTTCTCAGTG AGGCTGCTCA AGTTTTCTCG
gerbil      AGTGCCAAGA ATAAGACTCA CTTCTCCGTG CGGCTGCTCA AGTTTTCCCG
rabbit      AGCGCCAAAA ACAAGACGCA CTTCTCCGTG AGGCTCCTCA AGTTTTCCCG
guinea pig  AGCTCCAAGA ACAAGACGCA CTTCTCTGTG CGGCTCCTCA AGTTTTCCCG
human       AGCGCCAAGA CCAAGACGCA CTTCTCAGTG AGGCTCCTCA AGTTCTCCCG
cow         AGCGCCAAGA ACAAGACGCA CTTCTCCGTG AGACTGCTCA AATTTTCCCG

            801                                                       850
mouse       AGAGAAGAAA GCCGCCAAGA CGCTGGGCAT TGTGGTGGGA TGCTTCGTCC
rat         AGAGAAGAAA GCTGCCAAGA CGCTGGGCAT CGTGGTGGGT TGCTTCGTCC
gerbil      GGAGAAAAAA GCGGCCAAGA CGCTGGGCAT CGTGGTGGGT TGCTTTGTCC
rabbit      GGAGAAGAAA GCGGCCAAAA CGCTGGGCAT CGTGGTCGGC TGCTTCGTCC
guinea pig  GGAGAAGAAA GCGGCCAAAA CGCTGGGCAT CGTGGTCGGC TGCTTCGTCC
human       GGAGAAGAAA GCGGCCAAAA CGCTGGGCAT CGTGGTCGGC TGCTTCGTCC
cow         CGAGAAGAAA GCGGCCAAAA CGCTGGGCAT CGTGGTCGGC TGCTTCGTCC
```

```
            851                                                       900
mouse       TCTGCTGGCT GCCGTTCTTC CTCGTGATGC CCATTGGGTC CTTCTTCCCG
rat         TCTGCTGGCT GCCGTTCTTC CTAGTGATGC CCATTGGGTC TTTCTTCCCG
gerbil      TCTGCTGGCT GCCCTTCTTC CTAGTGATGC CCATTGGGTC CTTCTTCCCG
rabbit      TCTGCTGGCT GCCCTTCTTC TTGGTGATGC CCATCGGGTC TTTCTTCCCT
guinea pig  TCTGCTGGCT GCCCTTCTTC TTAGTGATGC CCATTGGGTC TTTCTTCCCT
human       TCTGCTGGCT GCCTTTTTTC TTAGTCATGC CCATTGGGTC TTTCTTCCCT
cow         TCTGCTGGCT GCCTTTTTTC TTAGTGATGC CCATTGGGTC TTTCTTTCCT

            901                                                       950
mouse       AATTTCAAGC CACCGGAAAC AGTTTTCAAA ATAGTATTTT GGCTTGGGTA
rat         GATTTCAAGC CTTCGGAAAC CGTTTTTAAA ATAGTATTTT GGCTCGGGTA
gerbil      GATTTCAAGC CTCCGGAAAC CGTTTTCAAA ATAGTGTTTT GGCTCGGGTA
rabbit      GATTTCAAGC CCCCGGAAAC TGTTTTTAAA ATAGTGTTTT GGCTCGGATA
guinea pig  GATTTCAAGC CCTCGGAAAC AGTTTTTAAA ATAGTATTTT GGCTCGGATA
human       GATTTCAAGC CCTCTGAAAC AGTTTTTAAA ATAGTATTTT GGCTCGGATA
cow         GATTTCAGGC CCTCAGAAAC CGTTTTTAAA ATAGCATTTT GGCTCGGTTA

            951                                                      1000
mouse       CCTAAATAGT TGCATCAACC CTATCATATA CCCATGCTCC AGCCAGGAGT
rat         TCTAAATAGT TGCATCAACC CTATCATATA CCCATGCTCC AGCCAGGAGT
gerbil      CCTCAACAGC TGCATCAACC CCATCATATA CCCATGCTCC AGCCAAGAGT
rabbit      CCTAAACAGC TGCATCAATC CCATCATATA CCCATGCTCC AGTCAAGAGT
guinea pig  CCTAAACAGC TGCATCAACC CCATCATATA CCCATGCTCC AGTCAAGAGT
human       TCTAAACAGC TGCATCAACC CCATCATATA CCCATGCTCC AGCCAAGAGT
cow         CCTAAACAGC TGCATCAACC CCATTATATA CCCATGCTCC AGTCAAGAGT

            1001                                                     1050
mouse       TCAAGAAAGC CTTTCAGAAT GTGCTGCGAA TCCAGTGTCT TCGCAGAAGG
rat         TCAAGAAAGC CTTTCAGAAT GTCCTGCGAA TCCAGTGTCT TCGCAGAAGG
gerbil      TCAAGAAAGC CTTTCAGAAT GTCCTGAGAA TCCAGTGTCT CCGCAGAAGG
rabbit      TCAAAAAGGC CTTTCAGAAT GTCTTGAAAA TCCAGTGTCT TCGCAGAAAG
guinea pig  TCAAAAAGGC CTTTCAGAAT GTCTTGAAAA TCCAGTGTCT TCGCAGAAAG
human       TCAAAAAGGC CTTTCAGAAT GTCTTGAGAA TCCAGTGTCT CTGCAGAAAG
cow         TTAAAAAGGC CTTTCAGAAT GTCTTGAGAA TCCAGTGTCT GCGACGAAAG

            1051                                                     1100
mouse       CAGTCTTCCA AGCATGCCCT GGGCTACACT CTGCACCCAC CCAGCCAGGC
rat         CAGTCTTCCA AGCATGCCCT GGGCTATACC CTGCACCCGC CCAGCCAGGC
gerbil      CCGTCTTCCA AGCATGCCCT GGGCTACACC CTGCACCCGC CCAGCCAGGC
rabbit      CAGTCTTCCA AGCATGCCCT GGGCTATACT CTGCATGCCC CCAGCCAGGC
guinea pig  CAGTCTTCCA AACATGCCCT GGGCTACACT CTGCACCCGC CCAGCCAGGC
human       CAGTCTTCCA AACATGCCCT GGGCTACCCC CTGCACCCGC CCAGCCAGGC
cow         CAGTCCTCCA AACACACCCT GGGCTACACG CTGCACGCAC CCAGCCACGT

            1101                                                     1150
mouse       TGTAGAGGAA CAGCACAGAG GCATGGTGCG TATCCCGGTG GGCTCAGGAG
rat         TCTAGAGGGA CAGCACAGAG ACATGGTGCG TATCCCGGTG GGCTCGGGAG
gerbil      TGTAGAAGGA CAGCACAGAG GCATGGTGCG TATCCCGGTG GGCTCGGGAG
rabbit      CCTGGAAGGG CAGCATAAGG ACATGGTGCG CATCCCAGTG GGATCTGGAG
guinea pig  CGTGGAAGGG CAGCACAAGG ACATGGTGCG CATCCCAGTG GGATCTAGAG
human       CGTGGAAGGG CAACACAAGG ACATGGTGCG CATCCCCGTG GGATCAAGAG
cow         CCTGGAGGGA CAGCACAAGG ACCTGGTTCG CATTCCGGTG GGATCTGCAG
```

```
            1151                                                1200
mouse       AGACTTTCTA TAAGATCTCC AAGACAGATG GAGTCTGTGA ATGGAAGTTT
rat         AGACTTTCTA TAAGATCTCC AAGACAGATG GAGTCTGTGA ATGGAAGTTT
gerbil      AGACTTTCTA TAAGATCTCC AAAGCGGACG GAGTCTGTGA ATGGAAGCTT
rabbit      AGACCTTCTA TAAGATCTCC AAGACGGATG GGGTTTGTGA ATGGAAGTTT
guinea pig  AGACCTTCTA TAAGATCTCC AAGACGGATG GCGTTTGTGA ATGGAAGTTT
human       AGACCTTCTA CAGGATCTCC AAGACGGATG GCGTTTGTGA ATGGAAATTT
cow         AGACCTTCTA TAAGATCTCC AAGACGGATG GGGTCTGTGA ATGGAAAATT

            1201                                                1250
mouse       TTCTCTTCCA TGCCCCAGGG ATCGGCCAGG ATTACCATGC CGAAGGACCA
rat         TTCTCTTCCA TGCCCCAGGG ATCGGCCAGG ATTACAGTGC CAAAGGACCA
gerbil      CTCTCTTCCA TGCCCCAGGG GTCAGCCAGG ATTACAGTGC CGAAGGACCA
rabbit      TTCTCTTCCA TGCCCCGTGG ATCTGCCAGG ATCACTGTGC CCAAAGACCA
guinea pig  TTCTCTTCCA TGCCCCGTGG ATCTGCCAGG ATTACAGTGC CCAAAGACCA
human       TTCTCTTCCA TGCCCCGTGG ATCTGCCAGG ATTACAGTGT CCAAAGACCA
cow         TTCTCTTCCC TACCCCGCGG ATCTGCCAGG ATGGCGGTGG CCAGAGACCC

            1251                                                1300
mouse       ATCCGCCTGT ACCACAGCCC GGGTGAGAAG TAAAAGCTTT TTGCAGGTCT
rat         ATCTGCCTGT ACCACAGCCC GGGTGAGAAG TAAAAGCTTT TTGCAGGTCT
gerbil      ATCTGCCTGC ACCACCGCCC GGGTGAGAAG TAAAAGCTTT TTGCAGGTCT
rabbit      ATCAGCCTGC ACTACAGCCC GGGTGAGAAG TAAAAGCTTT TTGCAGGTCT
guinea pig  ATCAGCCTGC ACCACAGCCC GGGTGAGAAG TAAAAGCTTT TTGCAGGTCT
human       ATCCTCCTGT ACCACAGCCC GGGTGAGAAG TAAAAGCTTT TTGCAGGTCT
cow         ATCAGCCTGC ACCACTGCCC GGGTGAGAAG TAAAAGCTTT TTGCAAGTGT

            1301                                                1350
mouse       GCTGCTGTGT GGGGTCGTCG ACCCCACGCC CTGAAGAAAA TCACCAAGTT
rat         GCTGCTGTGT GGGGTCCTCG GCCCCGCGCC CTGAAGAAAA TCACCAAGTT
gerbil      GCTGCTGTGT GGGGTCCTCG ACCCCCAGCC TTGAAGAAAA TCACCAGGTT
rabbit      GCTGCTGTGT AGGGCCCTCA ACCCCCAACC CCGGAGAGAA CCATCAAGTT
guinea pig  GCTGCTGTGT AGGGCCCTCA ACCCCCAACC CCGGAGAGAA CCATCAAGTT
human       GCTGCTGTGT AGGGCCCTCA ACCCCCTGCC TTGACAAGAA CCATCAAGTT
cow         GCTGTTGCCT GGGGCCCTCG ACCCCCAGTC ATGGAGAGAA TCATCAGATT

            1351                                                1400
mouse       CCAACCATTA AGATCCACAC CATCTCCCTC GGTGAAAACG GGGAGGAAGT
rat         CCAACCATTA AGATCCACAC CATCTCCCTC GGTGAAAACG GGGAGGAAGT
gerbil      CCAACCATTA AGATCCACAC CATCTCCCTT GGCGAAAACG GGGAGGAAGT
rabbit      CCAACTATTA AGATCCACAC CATCTCCCTC AGTGAAAATG GGGAGGAAGT
guinea pig  CCAACCATTA AGATCCACAC CATCTCCCTC AGTGAAAATG GGGAGGAAGT
human       CCAACCATTA AGGTCCACAC CATCTCCCTC AGTGAGAACG GGGAGGAAGT
cow         CCGACCATTA AGATCCACAC CATCTCCCTC AGTGAAAATG GGGAGGAAGT

            1401
mouse       CTAG
rat         CTAG
gerbil      CTAG
rabbit      CTAG
guinea pig  CTAG
human       CTAG
cow         CTAA
```

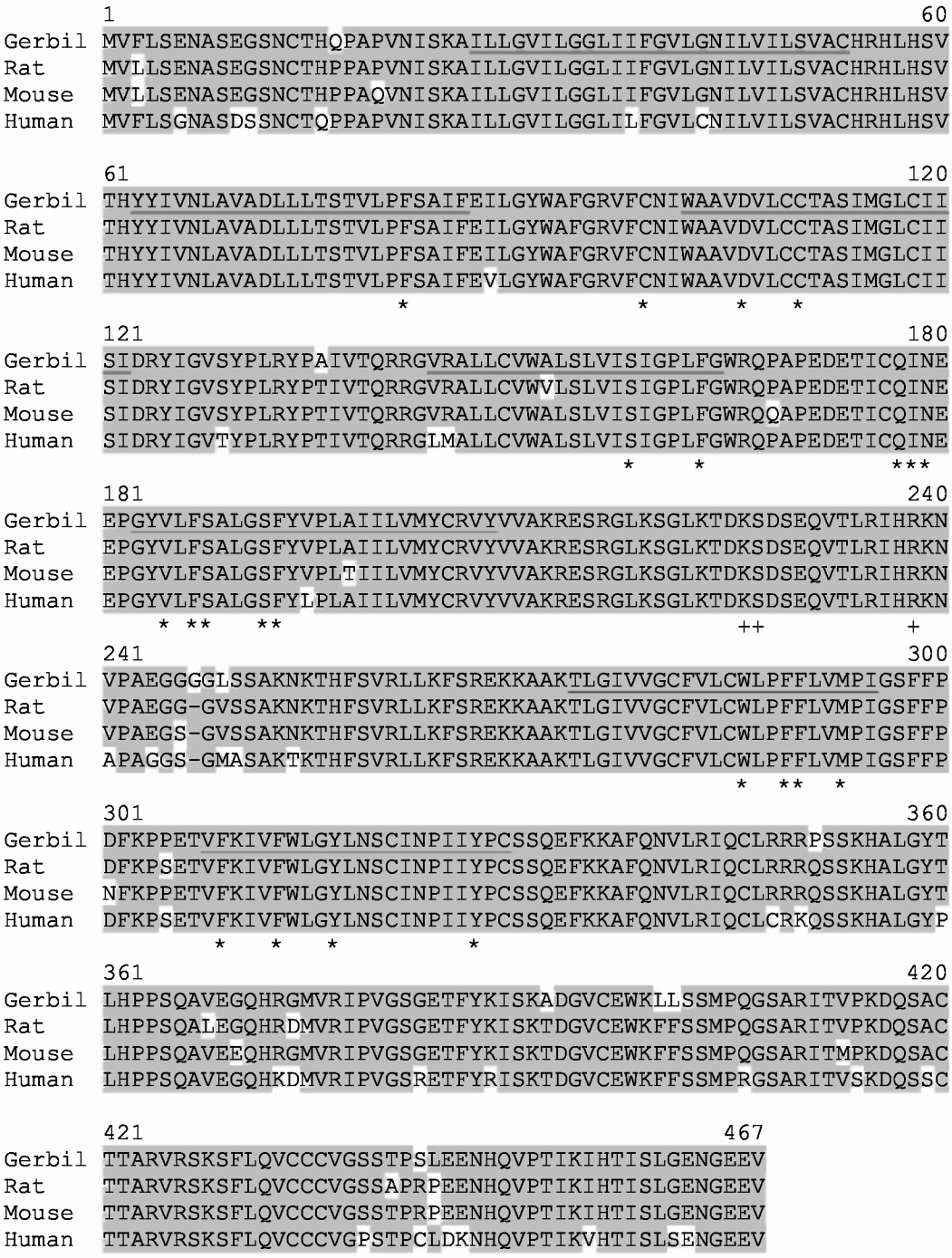

Figure 36. Comparison of putative amino acid sequences of gerbil (GenBank accession number HM754402), rat (U071126), mouse (AF031431), and human (U02569) α_{1a}-adrenergic receptors. Proposed membrane spanning domains are underlined. Conserved amino acids are shaded. Asterisks indicate important amino acids for agonist and/ or antagonist binding. Plus signs indicate amino acids important for RGS2 interaction (Hague et al., 2005).

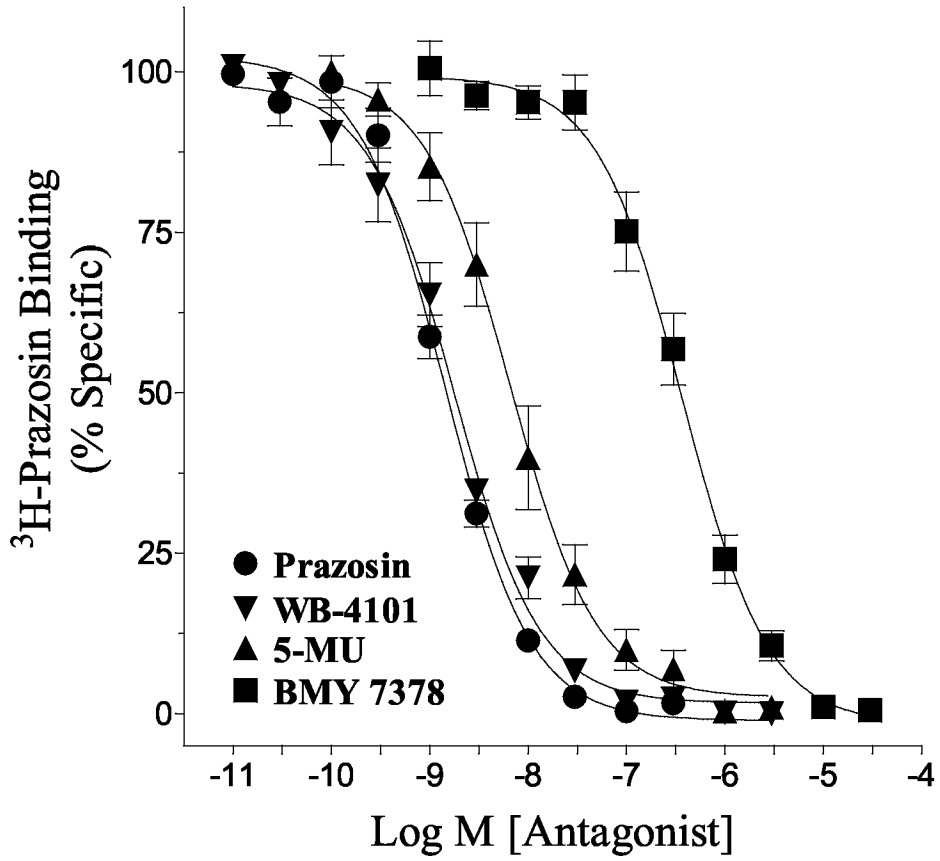

Figure 37. Mean competition binding curves showing α_1-adrenergic receptor antagonist inhibition of [7-methoxy-^{3}H]prazosin (^{3}H-prazosin) binding in COS-1 cells transiently transfected with the gerbil α_{1a}-adrenergic receptor. For each concentration of antagonists, [^{3}H]prazosin binding is expressed as a percentage of the specific binding in the absence of any drug. One- and two-site binding models were fit to individual and mean competition binding curves by using a nonlinear least-squares curve-fitting program to obtain K_i values. Competition binding curves for all of the antagonists fit to a one-site binding model.

for α_1-AR antagonists in COS-1 cells transfected with the cloned gerbil α_{1a}-AR. Figure 37 shows the competition curves for [^{3}H]prazosin inhibition of the α_1-AR nonselective antagonist prazosin, the α_{1D}-AR subtype-selective antagonist BMY 7378, and the α_{1A}-AR subtype-selective antagonists 5-MU and WB-4101 (Morrow and Creese, 1986; Gross et al., 1988; Goetz et al., 1995). The affinity values for 5-MU (4.9±1 nM) and WB-4101 (1.0±0.1 nM) confirm the existence of a typical α_{1a}-AR. The K_i value for BMY 7378was 260±60 nM, which is consistent with the pharmacology for an α_{1a}-AR. The presence of an α_1-AR is also indicated by the prazosin affinity value (0.89±0.09). These K_i values for the gerbil α_{1a}-AR were compared with published K_i values for the rat, mouse, and human α_{1a}-ARs (Table 8) and demonstrate that there are no discernable differences in the affinity values between the recombinant gerbil α_{1a}-AR and those of other recombinant α_{1a}-AR or endogenous α_{1A}-AR from the rat, mouse and human.

Discussion

The cloning and sequencing of the gerbil α_{1a}-AR have established that the cloned receptor is representative of an α_{1a}-AR and contains 1404 nucleotides and 467 putative amino acid residues. Translation of the gerbil α_{1a}-AR nucleotide sequence and comparison of the putative sequence to α_{1a}-AR of other species revealed an extra glycine residue, which contain the amino acids responsible for interaction with RGS2 (Hague et al., 2005). In addition, the amino acid percent identities between the gerbil α_{1a}-AR and rat, mouse, and human α_{1a}-AR sequences were 96.8, 96.4 and 91.6%, respectively. Alignment of the amino acid residues of the various species did not reveal any

Table 8. Affinity values for α_1-adrenergic receptor antagonists.

Drug	Gerbil	Human	Mouse	Rat
Prazosin	0.89±0.09	0.13 - 0.21	0.042 - 0.48	0.26 - 0.69
WB-4101	1.0±0.1	0.23 - 1.3	0.72 - 1.4	0.063 - 2.1
5-MU	4.9±1	3.2 - 30	0.24 - 2.8	0.16 - 1.5
BMY 7378	260±60	250	95 - 720	160 - 260

The values are expressed in nanomolar values. Affinities of the antagonist are from a collection of radioligand binding studies (Morrow and Creese, 1986; Lomasney et al., 1991; Porter et al., 1992; Hirasawa et al., 1993; Weinberg et al., 1994; Goetz et al., 1995; Schwinn et al., 1995; Xiao et al., 1998; Yang et al., 1998; Patel et al., 2001; Waugh et al., 2001). The gerbil α_{1a}-adrenergic receptor was transiently transfected in COS-1 cells. These membranes incubated with [^{3}H]prazosin in the absence or presence of increasing concentrations of the antagonists for 30 minutes. Each point represents the mean of at least three individual experiments done in duplicate. K_i values were generated using GraphPad Prism (GraphPad Software, San Diego, USA).

differences in amino acid sequence that would necessarily affect any known agonist or antagonist binding sites.

Many of the amino acid residues that have been determined to be important for α_{1a}-AR ligand binding have been revealed by mutagenesis experiments. Catecholamines form interactions with Ser^{188} and Ser^{192} in transmembrane 5 (TM5) (Hwa and Perez, 1996) and with the aspartic acid residue (Asp^{106}) on TM3 (Porter et al., 1996). Phe^{163} in TM4 and Phe^{187} in TM5 form the agonist binding pocket (Waugh et al., 2000). Asp^{106} is also important for antagonists WB-4101, tamsulosin, and compound 1 (Pedretti et al., 2004; Kinsella et al., 2005). Phentolamine and WB-4101 interact with Gln^{177}, Ile^{178}, and Asn^{179} of the second extracellular loop (Zhao et al., 1996). Phe^{308} and Phe^{312} on TM7 interact with many α_{1a}-AR antagonist including prazosin, WB-4101, BMY 7378, (+) niguldipine, and 5-MU and imidazoline-type agonists such as oxymetazoline but not phenethylamine-type agonists such as epinephrine, methoxamine, or phenylephrine (Waugh et al., 2001).

Chimeric studies by Zhao et al. show that α_{1b}-AR mutated with the α_{1a}-AR amino acid residues G196Q, V197I, T198N (or Gln^{177}, Ile^{178}, Asn^{179}) on the extracellular loop of TM5 can determine the AR subtype selectivity with the antagonists phentolamine, WB-4101, and partially 5-MU (Zhao et al., 1996). Hamaguchi et al. has shown that Phe^{86} confer α_{1a}-AR versus α_{1d}-AR selectivity for niguldipine, an α_{1a}-AR subtype selective dihydropyridine antagonist (Hamaguchi et al., 1996). Agonist subtype selectivity for the α_{1a}-AR requires Val^{185} in TM5 and Met^{293} in TM6 (Hwa et al., 1995).

Bovine rhodopsin, which has a low sequence homology of 11.9% with α_{1a}-AR, has been the only three-dimensional structure available (Palczewski et al., 2000; Kinsella

et al., 2005). Pedretti et al., using homology modeling to the crystal structure of bovine rhodopsin and BioDock program, has identified many amino acid residues involved in agonist and antagonist binding sites (Pedretti et al., 2004). Their model suggests that Asp^{106}, Ser^{158}, Ser^{188}, Ser^{192}, Gln^{177}, and Trp^{285} significantly interact in the α_{1a}-AR-norepinephrine complex (Pedretti et al., 2004). The α_{1a}-AR-WB-4101 complex involves the amino acid residues Asp^{106}, Cys^{110}, Gln^{177}, Phe^{193}, Phe^{312}, and Tyr^{316} (Pedretti et al., 2004). Very recently, improvements have been made to crystallization techniques such that the crystals are more stable and can be formed in the active and inactive states (Salom et al., 2006). This new method may help identify more key amino acid residues in ligand binding. However, none of the amino acids unique to the gerbil α_{1a}–AR corresponded to the above important amino acids.

In view of no known amino acid differences that are critical for ligand binding, we further assessed the pharmacological characteristics of the cloned receptor with [^{3}H]prazosin competition binding experiments of membranes from transiently transfected COS-1 cells. The K_i values for the α_{1A}-AR selective antagonists 5-MU and WB-4101 were 4.9 ± 1 nM and 1.0 ± 0.1 nM, respectively indicating high affinity binding for these antagonists and the presence of α_{1a}-ARs. BMY 7378 bound with low affinity (260 ± 60 nM), where the low affinity of this antagonist for the α_1-AR suggests the absence of α_{1d}-ARs. Unlabeled prazosin, a nonselective α_1-adrenergic receptor antagonist, bound with a high affinity, K_i of 0.89 ± 0.09 nM, a value which is representative of the affinity of the recombinant α_1-AR subtype expressed in cell culture (Table 4). Therefore, the cloned gerbil α_{1a}-AR expressed in COS-1 cells showed similar pharmacology to that of other cloned α_{1a}-ARs from other species.

We further characterized the recombinant gerbil α_{1a}-AR with radioligand binding experiments and showed that the antagonist 5-MU bound to the expressed receptor with an affinity constant of K_i=4.9 ± 1 nM. This value is representative of the K_i determined from radioligand binding assays of the cloned and expressed α_{1a}-ARs from other species. However, the affinity exhibited by 5-MU from these assays is significantly different from the K_{DB} values for 5-MU in the functional norepinephrine induced vasoconstriction experiments on the gerbil SMA, K_{DB} of 0.27 ± 0.07 nM (Gruber et al., 1998). Higher affinity values for 5-MU have also been noted in non-functional radioligand binding studies of the parotid gland by Porter et al. and Abel et al. (Porter et al., 1992; Abel et al., 1995) where affinity values were as low as K_{iH}=0.16 ± 0.03 nM. In addition, these investigators also showed that α_{1B}-AR sites were present in the rat parotid gland (Porter et al., 1992).

When prazosin was used as a competitive antagonist at 10 nM the K_{DB} value in gerbil SMA was 0.06 ± 0.03 nM (n=7) which represents a higher affinity than would be expected of α_{1A}–AR (Gruber et al., 1998). Other investigators have also noticed differences in K_i values between systems. However, the affinities are lower than those derived from α_{1a}-AR expressed in cell cultures and these discoveries have led to proposals of the putative low affinity α_{1L}-AR, (Flavahan and Vanhoutte, 1986; Abel et al., 1995). In the investigations by Abel et al., prazosin and 5-MU affinities were derived from either radioligand binding of rat parotid gland (prazosin, 1.0 ± 0.4 nM; 5-MU, 75 ± 18 nM) or vasoconstriction of guinea-pig ileum (prazosin, 1 ± 0.9 nM; 5-MU, 72 ± 12 nM) and illustrated the presence of the putative low affinity α_{1L}-AR. It is has been postulated by Ford et al. that these discrepancies between radioligand binding assays of

recombinant gene expression systems in cell cultures and radioligand binding or functional assays of natural tissues are not due to differences of expressed genes but are a result of the differences in the assay conditions used to determine the affinity constants. These conditions include whether or not the assay is measuring functional responses such as stimulation of contraction of tissues and/or performing radioligand binding on tissues rather than gene expression systems (Ford et al., 1997). Ford et al. has further postulated that these different pharmacological phenotypes are a result of the conformational state of the receptor, where the homogenate radioligand binding assays may provide a different environment for receptor binding than is present in whole cells or intact tissues.

Analogous to our results, Mackenzie et al. have shown an increase in antagonist affinity, where they have shown that their prazosin analog has a higher affinity in human prostate cells than in cell cultures expressing recombinant α_{1a}-AR (Mackenzie et al., 2000). They also suggest that these variant affinities can be potentially explained by tissue-specific affinity states rather than a difference in an endogenous α_{1A}-AR transcript. Similarly we suggest that the higher affinities for 5-MU and prazosin may be a result of the difference between conformational states of the receptor during functional studies and radioligand binding on cellular membranes of recombinant clones rather than due to a variant α_{1a}-AR gene.

In summary we have cloned and pharmacologically characterized the recombinant gerbil α_{1a}-AR in COS-1 cells. Our results show that the pharmacological and sequence data of the putative gerbil α_{1a}-AR from the SMA clearly indicates that it is an α_{1a}-AR subtype of the adrenergic receptors. These results may be particularly useful when determining the contribution of α_{1A} -AR in gerbil tissues which are used as hearing

models. Finally, the difference in affinity data between functional and cloned expression systems is evidence for affinity states that are tissue specific and this might be an important consideration when determining the effectiveness of α_{1A}-AR antagonists in specific tissues.

REFERENCES

Abel PW, Zeng W, Porter JE, Scofield MA, Liu F, Gonzalez-Cabrera I, Dowd FJ and Jeffries WB (1995) The atypical α_1-adrenoceptor. *Pharmacology Communications* **6**:29-38.

Albrandt K, Brady EM, Moore CX, Mull E, Sierzega ME and Beaumont K (1995) Molecular cloning and functional expression of a third isoform of the human calcitonin receptor and partial characterization of the calcitonin receptor gene. *Endocrinology* **136**:5377-5384.

Allaker RP, Zihni C and Kapas S (1999) An investigation into the antimicrobial effects of adrenomedullin on members of the skin, oral, respiratory tract and gut microflora. *FEMS Immunol Med Microbiol* **23**:289-293.

Amara SG, Jonas V, Rosenfeld MG, Ong ES and Evans RM (1982) Alternative RNA processing in calcitonin gene expression generates mRNAs encoding different polypeptide products. *Nature* **298**:240-244.

Beaudreuil J, Balasubramanian S, Chenais J, Taboulet J, Frenkian M, Orcel P, Jullienne A, Horne WC, de Vernejoul MC and Cressent M (2004) Molecular characterization of two novel isoforms of the human calcitonin receptor. *Gene* **343**:143-151.

Bendtsen JD, Nielsen H, von Heijne G and Brunak S (2004) Improved prediction of signal peptides: SignalP 3.0. *J Mol Biol* **340**:783-795.

Benitez-Paez A (2006) Sequence analysis of the Receptor Activity-Modifying Proteins family, new putative peptides and structural conformation inference. *In Silico Biol* **6**:467-483.

Bevilacqua PC and Blose JM (2008) Structures, kinetics, thermodynamics, and biological functions of RNA hairpins. *Annu Rev Phys Chem* **59**:79-103.

Black DL (2003) Mechanisms of alternative pre-messenger RNA splicing. *Annu Rev Biochem* **72**:291-336.

Blobel G and Dobberstein B (1975) Transfer of proteins across membranes. I. Presence of proteolytically processed and unprocessed nascent immunoglobulin light chains on membrane-bound ribosomes of murine myeloma. *J Cell Biol* **67**:835-851.

Bockman CS, Bruchas MR, Zeng W, O'Connell KA, Abel PW, Scofield MA and Dowd FJ (2004) Submandibular gland acinar cells express multiple α_1-adrenoceptor subtypes. *J Pharmacol Exp Ther* **311**:364-372.

Bomberger JM, Parameswaran N, Hall CS, Aiyar N and Spielman WS (2005a) Novel function for receptor activity-modifying proteins (RAMPs) in post-endocytic receptor trafficking. *J Biol Chem* **280**:9297-9307.

Bomberger JM, Spielman WS, Hall CS, Weinman EJ and Parameswaran N (2005b) Receptor activity-modifying protein (RAMP) isoform-specific regulation of adrenomedullin receptor trafficking by NHERF-1. *J Biol Chem* **280**:23926-23935.

Bouschet T, Martin S and Henley JM (2005) Receptor-activity-modifying proteins are required for forward trafficking of the calcium-sensing receptor to the plasma membrane. *J Cell Sci* **118**:4709-4720.

Bradford MM (1976) A rapid and sensitive method for the quantitation of microgram quantities of protein utilizing the principle of protein-dye binding. *Anal Biochem* **72**:248-254.

Brain SD and Grant AD (2004) Vascular actions of calcitonin gene-related peptide and adrenomedullin. *Physiol Rev* **84**:903-934.

Brendel C, Rehbein M, Kreienkamp HJ, Buck F, Richter D and Kindler S (2004) Characterization of Staufen 1 ribonucleoprotein complexes. *Biochem J* **384**:239-246.

Brunstein J, Soderlund-Venermo M and Hedman K (2000) Identification of a novel RNA splicing pattern as a basis of restricted cell tropism of erythrovirus B19. *Virology* **274**:284-291.

Buhlmann N, Leuthauser K, Muff R, Fischer JA and Born W (1999) A receptor activity modifying protein (RAMP)2-dependent adrenomedullin receptor is a calcitonin gene-related peptide receptor when coexpressed with human RAMP1. *Endocrinology* **140**:2883-2890.

Carlisle L, Aberdeen J, Forge A and Burnstock G (1990) Neural basis for regulation of cochlear blood flow: peptidergic and adrenergic innervation of the spiral modiolar artery of the guinea pig. *Hear Res* **43**:107-113.

Carothers AM, Urlaub G, Grunberger D and Chasin LA (1993) Splicing mutants and their second-site suppressors at the dihydrofolate reductase locus in Chinese hamster ovary cells. *Mol Cell Biol* **13**:5085-5098.

Cheng Y and Prusoff WH (1973) Relationship between the inhibition constant (K_I) and the concentration of inhibitor which causes 50 per cent inhibition (IC_{50}) of an enzymatic reaction. *Biochem Pharmacol* **22**:3099-3108.

Christopoulos A, Christopoulos G, Morfis M, Udawela M, Laburthe M, Couvineau A, Kuwasako K, Tilakaratne N and Sexton PM (2003) Novel receptor partners and function of receptor activity-modifying proteins. *J Biol Chem* **278**:3293-3297.

Christopoulos G, Perry KJ, Morfis M, Tilakaratne N, Gao Y, Fraser NJ, Main MJ, Foord SM and Sexton PM (1999) Multiple amylin receptors arise from receptor activity-modifying protein interaction with the calcitonin receptor gene product. *Mol Pharmacol* **56**:235-242.

Colley NJ, Baker EK, Stamnes MA and Zuker CS (1991) The cyclophilin homolog ninaA is required in the secretory pathway. *Cell* **67**:255-263.

Davis NG and Hsu MC (1986) The fusion-related hydrophobic domain of Sendai F protein can be moved through the cytoplasmic membrane of Escherichia coli. *Proc Natl Acad Sci U S A* **83**:5091-5095.

Davis NG and Model P (1985) An artificial anchor domain: hydrophobicity suffices to stop transfer. *Cell* **41**:607-614.

Derst C, Engel H, Grzeschik K and Daut J (2000) Genomic structure and chromosome mapping of human and mouse RAMP genes. *Cytogenet Cell Genet* **90**:115-118.

Dong YL, Green KE, Vegiragu S, Hankins GD, Martin E, Chauhan M, Thota C and Yallampalli C (2005) Evidence for decreased calcitonin gene-related peptide (CGRP) receptors and compromised responsiveness to CGRP of fetoplacental vessels in preeclamptic pregnancies. *J Clin Endocrinol Metab* **90**:2336-2343.

Dong YL, Vegiraju S, Chauhan M and Yallampalli C (2003) Expression of calcitonin gene-related peptide receptor components, calcitonin receptor-like receptor and

receptor activity modifying protein 1, in the rat placenta during pregnancy and their cellular localization. *Mol Hum Reprod* **9**:481-490.

Doods H, Hallermayer G, Wu D, Entzeroth M, Rudolf K, Engel W and Eberlein W (2000) Pharmacological profile of BIBN4096BS, the first selective small molecule CGRP antagonist. *Br J Pharmacol* **129**:420-423.

Duchaine TF, Hemraj I, Furic L, Deitinghoff A, Kiebler MA and DesGroseillers L (2002) Staufen2 isoforms localize to the somatodendritic domain of neurons and interact with different organelles. *J Cell Sci* **115**:3285-3295.

Eden E and Brunak S (2004) Analysis and recognition of 5' UTR intron splice sites in human pre-mRNA. *Nucleic Acids Res* **32**:1131-1142.

Evans BN, Rosenblatt MI, Mnayer LO, Oliver KR and Dickerson IM (2000) CGRP-RCP, a novel protein required for signal transduction at calcitonin gene-related peptide and adrenomedullin receptors. *J Biol Chem* **275**:31438-31443.

Fernandez-Sauze S, Delfino C, Mabrouk K, Dussert C, Chinot O, Martin PM, Grisoli F, Ouafik L and Boudouresque F (2004) Effects of adrenomedullin on endothelial cells in the multistep process of angiogenesis: involvement of CRLR/RAMP2 and CRLR/RAMP3 receptors. *Int J Cancer* **108**:797-804.

Ferreira PA, Nakayama TA, Pak WL and Travis GH (1996) Cyclophilin-related protein RanBP2 acts as chaperone for red/green opsin. *Nature* **383**:637-640.

Flahaut M, Rossier BC and Firsov D (2002) Respective roles of calcitonin receptor-like receptor (CRLR) and receptor activity-modifying proteins (RAMP) in cell surface expression of CRLR/RAMP heterodimeric receptors. *J Biol Chem* **277**:14731-14737.

Flavahan NA and Vanhoutte PM (1986) α_1-Adrenoceptor subclassification in vascular smooth muscle. *Trends in Pharmacological Sciences* **7**:347-349.

Foglio MH and Duester G (1996) Characterization of the functional gene encoding mouse class III alcohol dehydrogenase (glutathione-dependent formaldehyde dehydrogenase) and an unexpressed processed pseudogene with an intact open reading frame. *Eur J Biochem* **237**:496-504.

Ford AP, Daniels DV, Chang DJ, Gever JR, Jasper JR, Lesnick JD and Clarke DE (1997) Pharmacological pleiotropism of the human recombinant α_{1A}-adrenoceptor: implications for α_1-adrenoceptor classification. *Br J Pharmacol* **121**:1127-1135.

Fraser NJ, Wise A, Brown J, McLatchie LM, Main MJ and Foord SM (1999) The amino terminus of receptor activity modifying proteins is a critical determinant of glycosylation state and ligand binding of calcitonin receptor-like receptor. *Mol Pharmacol* **55**:1054-1059.

Fukai N, Yoshimoto T, Sugiyama T, Ozawa N, Sato R, Shichiri M and Hirata Y (2005) Concomitant expression of adrenomedullin and its receptor components in rat adipose tissues. *Am J Physiol Endocrinol Metab* **288**:E56-62.

Galgano A, Forrer M, Jaskiewicz L, Kanitz A, Zavolan M and Gerber AP (2008) Comparative analysis of mRNA targets for human PUF-family proteins suggests extensive interaction with the miRNA regulatory system. *PLoS One* **3**:e3164.

Gangula PR, Thota C, Wimalawansa SJ, Bukoski RD and Yallampalli C (2003) Mechanisms involved in calcitonin gene-related Peptide-induced relaxation in pregnant rat uterine artery. *Biol Reprod* **69**:1635-1641.

Goetz AS, King HK, Ward SD, True TA, Rimele TJ and Saussy DL, Jr. (1995) BMY 7378 is a selective antagonist of the D subtype of α_1-adrenoceptors. *Eur J Pharmacol* **272**:R5-6.

Gollnick P, Babitzke P, Antson A and Yanofsky C (2005) Complexity in regulation of tryptophan biosynthesis in Bacillus subtilis. *Annu Rev Genet* **39**:47-68.

Gorn AH, Rudolph SM, Flannery MR, Morton CC, Weremowicz S, Wang TZ, Krane SM and Goldring SR (1995) Expression of two human skeletal calcitonin receptor isoforms cloned from a giant cell tumor of bone. The first intracellular domain modulates ligand binding and signal transduction. *J Clin Invest* **95**:2680-2691.

Grallath S, Schwarz JP, Bottcher UM, Bracher A, Hartl FU and Siegers K (2006) L25 functions as a conserved ribosomal docking site shared by nascent chain-associated complex and signal-recognition particle. *EMBO Rep* **7**:78-84.

Gross G, Hanft G and Rugevics C (1988) 5-Methyl-urapidil discriminates between subtypes of the α_1-adrenoceptor. *Eur J Pharmacol* **151**:333-335.

Gruber DD, Dang H, Shimozono M, Scofield MA and Wangemann P (1998) α_{1A}-adrenergic receptors mediate vasoconstriction of the isolated spiral modiolar artery in vitro. *Hear Res* **119**:113-124.

Hague C, Bernstein LS, Ramineni S, Chen Z, Minneman KP and Hepler JR (2005) Selective inhibition of α_{1A}-adrenergic receptor signaling by RGS2 association with the receptor third intracellular loop. *J Biol Chem* **280**:27289-27295.

Hague C, Uberti MA, Chen Z, Hall RA and Minneman KP (2004) Cell surface expression of α_{1D}-adrenergic receptors is controlled by heterodimerization with α_{1B}-adrenergic receptors. *J Biol Chem* **279**:15541-15549.

Hamaguchi N, True TA, Saussy DL, Jr. and Jeffs PW (1996) Phenylalanine in the second membrane-spanning domain of α_{1A}-adrenergic receptor determines subtype selectivity of dihydropyridine antagonists. *Biochemistry* **35**:14312-14317.

Hann BC and Walter P (1991) The signal recognition particle in S. cerevisiae. *Cell* **67**:131-144.

Harikumar KG, Simms J, Christopoulos G, Sexton PM and Miller LJ (2009) The Molecular Basis of Association of Receptor Activity-Modifying Protein 3 with the Family B G Protein-Coupled Secretin Receptor. *Biochemistry*.

Hata T, Miyazaki K and Matsui K (1997) Decreased circulating adrenomedullin in pre-eclampsia. *Lancet* **350**:1600.

Hay DL, Howitt SG, Conner AC, Schindler M, Smith DM and Poyner DR (2003) CL/RAMP2 and CL/RAMP3 produce pharmacologically distinct adrenomedullin receptors: a comparison of effects of adrenomedullin22-52, CGRP8-37 and BIBN4096BS. *Br J Pharmacol* **140**:477-486.

Hay DL, Poyner DR and Sexton PM (2006) GPCR modulation by RAMPs. *Pharmacol Ther* **109**:173-197.

Hegde RS and Bernstein HD (2006) The surprising complexity of signal sequences. *Trends Biochem Sci* **31**:563-571.

Heroux M, Hogue M, Lemieux S and Bouvier M (2007) Functional calcitonin gene-related peptide receptors are formed by the asymmetric assembly of a calcitonin receptor-like receptor homo-oligomer and a monomer of receptor activity-modifying protein-1. *J Biol Chem* **282**:31610-31620.

Hieble JP, Bylund DB, Clarke DE, Eikenburg DC, Langer SZ, Lefkowitz RJ, Minneman KP and Ruffolo RR, Jr. (1995) International Union of Pharmacology. X. Recommendation for nomenclature of α_1-adrenoceptors: consensus update. *Pharmacol Rev* **47**:267-270.

Higuchi (1989) *PCR Technology: Principles and Applications for DNA Amplification* Stockton Press

Hilairet S, Belanger C, Bertrand J, Laperriere A, Foord SM and Bouvier M (2001a) Agonist-promoted internalization of a ternary complex between calcitonin receptor-like receptor, receptor activity-modifying protein 1 (RAMP1), and beta-arrestin. *J Biol Chem* **276**:42182-42190.

Hilairet S, Foord SM, Marshall FH and Bouvier M (2001b) Protein-protein interaction and not glycosylation determines the binding selectivity of heterodimers between the calcitonin receptor-like receptor and the receptor activity-modifying proteins. *J Biol Chem* **276**:29575-29581.

Hiragushi K, Wada J, Eguchi J, Matsuoka T, Yasuhara A, Hashimoto I, Yamashita T, Hida K, Nakamura Y, Shikata K, Minamino N, Kangawa K and Makino H (2004) The role of adrenomedullin and receptors in glomerular hyperfiltration in streptozotocin-induced diabetic rats. *Kidney Int* **65**:540-550.

Hirasawa A, Horie K, Tanaka T, Takagaki K, Murai M, Yano J and Tsujimoto G (1993) Cloning, functional expression and tissue distribution of human cDNA for the α_{1C}-adrenergic receptor. *Biochem Biophys Res Commun* **195**:902-909.

Holgate ST, Davies DE, Murphy G, Powell RM and Holloway JW (2003) ADAM 33: just another asthma gene or a breakthrough in understanding the origins of bronchial hyperresponsiveness? *Thorax* **58**:466-469.

Hui J, Hung LH, Heiner M, Schreiner S, Neumuller N, Reither G, Haas SA and Bindereif A (2005) Intronic CA-repeat and CA-rich elements: a new class of regulators of mammalian alternative splicing. *Embo J* **24**:1988-1998.

Husmann K, Sexton PM, Fischer JA and Born W (2000) Mouse receptor-activity-modifying proteins 1, -2 and -3: amino acid sequence, expression and function. *Mol Cell Endocrinol* **162**:35-43.

Hwa J, Graham RM and Perez DM (1995) Identification of critical determinants of α_1-adrenergic receptor subtype selective agonist binding. *J Biol Chem* **270**:23189-23195.

Hwa J and Perez DM (1996) The unique nature of the serine interactions for α_1-adrenergic receptor agonist binding and activation. *J Biol Chem* **271**:6322-6327.

Isumi Y, Minamino N, Kubo A, Nishimoto N, Yoshizaki K, Yoshioka M, Kangawa K and Matsuo H (1998) Adrenomedullin stimulates interleukin-6 production in Swiss 3T3 cells. *Biochem Biophys Res Commun* **244**:325-331.

Jacob A, Kandpal G, Patanjali SR and Kandpal RP (1995) Molecular cloning and expression pattern of genes from a 470 Kb region near BRCA1 locus on chromosome 17q21. *Oncogene* **11**:981-986.

Jaillon O, Aury JM, Brunet F, Petit JL, Stange-Thomann N, Mauceli E, Bouneau L, Fischer C, Ozouf-Costaz C, Bernot A, Nicaud S, Jaffe D, Fisher S, Lutfalla G, Dossat C, Segurens B, Dasilva C, Salanoubat M, Levy M, Boudet N, Castellano

S, Anthouard V, Jubin C, Castelli V, Katinka M, Vacherie B, Biemont C, Skalli Z, Cattolico L, Poulain J, De Berardinis V, Cruaud C, Duprat S, Brottier P, Coutanceau JP, Gouzy J, Parra G, Lardier G, Chapple C, McKernan KJ, McEwan P, Bosak S, Kellis M, Volff JN, Guigo R, Zody MC, Mesirov J, Lindblad-Toh K, Birren B, Nusbaum C, Kahn D, Robinson-Rechavi M, Laudet V, Schachter V, Quetier F, Saurin W, Scarpelli C, Wincker P, Lander ES, Weissenbach J and Roest Crollius H (2004) Genome duplication in the teleost fish Tetraodon nigroviridis reveals the early vertebrate proto-karyotype. *Nature* **431**:946-957.

Joun H, Lanske B, Karperien M, Qian F, Defize L and Abou-Samra A (1997) Tissue-specific transcription start sites and alternative splicing of the parathyroid hormone (PTH)/PTH-related peptide (PTHrP) receptor gene: a new PTH/PTHrP receptor splice variant that lacks the signal peptide. *Endocrinology* **138**:1742-1749.

Kaiser CA, Preuss D, Grisafi P and Botstein D (1987) Many random sequences functionally replace the secretion signal sequence of yeast invertase. *Science* **235**:312-317.

Kato A, Doi H, Nakada T, Sakai H and Hirose S (2005) Takifugu obscurus is a euryhaline fugu species very close to Takifugu rubripes and suitable for studying osmoregulation. *BMC Physiol* **5**:18.

Kiebler MA, Hemraj I, Verkade P, Kohrmann M, Fortes P, Marion RM, Ortin J and Dotti CG (1999) The mammalian staufen protein localizes to the somatodendritic domain of cultured hippocampal neurons: implications for its involvement in mRNA transport. *J Neurosci* **19**:288-297.

Kikumoto K, Katafuchi T and Minamino N (2003) Specificity of porcine calcitonin receptor and calcitonin receptor-like receptor in the presence of receptor-activity-modifying proteins. *Hypertens Res* **26 Suppl**:S15-23.

Kinsella GK, Rozas I and Watson GW (2005) Comparative molecular dynamics simulations of uncomplexed, 'agonist-bound' and 'antagonist-bound' α_{1A} adrenoceptor models. *Biochem Biophys Res Commun* **333**:737-741.

Kitamura K, Kangawa K, Kawamoto M, Ichiki Y, Nakamura S, Matsuo H and Eto T (1993) Adrenomedullin: a novel hypotensive peptide isolated from human pheochromocytoma. *Biochem Biophys Res Commun* **192**:553-560.

Knerr I, Dachert C, Beinder E, Metzler M, Dotsch J, Repp R and Rascher W (2002) Adrenomedullin, calcitonin gene-related peptide and their receptors: evidence for a decreased placental mRNA content in preeclampsia and HELLP syndrome. *Eur J Obstet Gynecol Reprod Biol* **101**:47-53.

Kozak M (1987) An analysis of 5'-noncoding sequences from 699 vertebrate messenger RNAs. *Nucleic Acids Res* **15**:8125-8148.

Kraut-Cohen J and Gerst JE (2010) Addressing mRNAs to the ER: cis sequences act up! *Trends Biochem Sci.*

Kusano S, Kukimoto-Niino M, Akasaka R, Toyama M, Terada T, Shirouzu M, Shindo T and Yokoyama S (2008) Crystal structure of the human receptor activity-modifying protein 1 extracellular domain. *Protein Sci* **17**:1907-1914.

Kuwasako K, Kitamura K, Ito K, Uemura T, Yanagita Y, Kato J, Sakata T and Eto T (2001) The seven amino acids of human RAMP2 (86) and RAMP3 (59) are

critical for agonist binding to human adrenomedullin receptors. *J Biol Chem* **276**:49459-49465.

Kuwasako K, Kitamura K, Nagata S and Kato J (2008) Functions of the extracellular histidine residues of receptor activity-modifying proteins vary within adrenomedullin receptors. *Biochem Biophys Res Commun* **377**:109-113.

Kuwasako K, Kitamura K, Nagata S and Kato J (2009) Flow cytometric analysis of the calcitonin receptor-like receptor domains responsible for cell-surface translocation of receptor activity-modifying proteins. *Biochem Biophys Res Commun* **384**:249-254.

Kuwasako K, Kitamura K, Nagoshi Y, Cao YN and Eto T (2003) Identification of the human receptor activity-modifying protein 1 domains responsible for agonist binding specificity. *J Biol Chem* **278**:22623-22630.

Kuwasako K, Kitamura K, Onitsuka H, Uemura T, Nagoshi Y, Kato J and Eto T (2002) Rat RAMP domains involved in adrenomedullin binding specificity. *FEBS Lett* **519**:113-116.

Kuwasako K, Kitamura, K., Uemura, T., Nagoshi, Y., Kato, J., & Eto, T. (2003) The function of extracellular cysteines in the human AM receptor. *Hypertens Res* **26(Suppl)**:S25– S31.

Kuwasako K, Shimekake Y, Masuda M, Nakahara K, Yoshida T, Kitaura M, Kitamura K, Eto T and Sakata T (2000) Visualization of the calcitonin receptor-like receptor and its receptor activity-modifying proteins during internalization and recycling. *J Biol Chem* **275**:29602-29609.

Kyte J and Doolittle RF (1982) A simple method for displaying the hydropathic character of a protein. *J Mol Biol* **157**:105-132.

Lee HC and Bernstein HD (2001) The targeting pathway of Escherichia coli presecretory and integral membrane proteins is specified by the hydrophobicity of the targeting signal. *Proc Natl Acad Sci U S A* **98**:3471-3476.

Lee J, Gomez-Ramirez J, Johnston TH, Visanji N and Brotchie JM (2008) Receptor-activity modifying protein 1 expression is increased in the striatum following repeated L-DOPA administration in a 6-hydroxydopamine lesioned rat model of Parkinson's disease. *Synapse* **62**:310-313.

Liu Z, Qiu J, Cheng F, Chu Y, Yoto Y, O'Sullivan MG, Brown KE and Pintel DJ (2004) Comparison of the transcription profile of simian parvovirus with that of the human erythrovirus B19 reveals a number of unique features. *J Virol* **78**:12929-12939.

Lomasney JW, Cotecchia S, Lorenz W, Leung WY, Schwinn DA, Yang-Feng TL, Brownstein M, Lefkowitz RJ and Caron MG (1991) Molecular cloning and expression of the cDNA for the α_{1A}-adrenergic receptor. The gene for which is located on human chromosome 5. *J Biol Chem* **266**:6365-6369.

Luebke AE, Dahl GP, Roos BA and Dickerson IM (1996) Identification of a protein that confers calcitonin gene-related peptide responsiveness to oocytes by using a cystic fibrosis transmembrane conductance regulator assay. *Proc Natl Acad Sci U S A* **93**:3455-3460.

Mackenzie JF, Daly CJ, Pediani JD and McGrath JC (2000) Quantitative imaging in live human cells reveals intracellular α_1-adrenoceptor ligand-binding sites. *J Pharmacol Exp Ther* **294**:434-443.

Makino Y, Shibata K, Makino I, Kangawa K and Kawarabayashi T (2001) Alteration of the adrenomedullin receptor components gene expression associated with the blood pressure in pregnancy-induced hypertension. *J Clin Endocrinol Metab* **86**:5079-5082.

Mallee JJ, Salvatore CA, LeBourdelles B, Oliver KR, Longmore J, Koblan KS and Kane SA (2002) Receptor activity-modifying protein 1 determines the species selectivity of non-peptide CGRP receptor antagonists. *J Biol Chem* **277**:14294-14298.

Martoglio B, Graf R and Dobberstein B (1997) Signal peptide fragments of preprolactin and HIV-1 p-gp160 interact with calmodulin. *The EMBO Journal* **16**:6636–6645.

McLatchie LM, Fraser NJ, Main MJ, Wise A, Brown J, Thompson N, Solari R, Lee MG and Foord SM (1998) RAMPs regulate the transport and ligand specificity of the calcitonin-receptor-like receptor. *Nature* **393**:333-339.

Miller PS, Barwell J, Poyner DR, Wigglesworth MJ, Garland SL and Donnelly D (2010) Non-peptidic antagonists of the CGRP receptor, BIBN4096BS and MK-0974, interact with the calcitonin receptor-like receptor via methionine-42 and RAMP1 via tryptophan-74. *Biochem Biophys Res Commun* **391**:437-442.

Mitchell PJ, Urlaub G and Chasin L (1986) Spontaneous splicing mutations at the dihydrofolate reductase locus in Chinese hamster ovary cells. *Mol Cell Biol* **6**:1926-1935.

Mom T, Avan P, Bonfils P and Gilain L (1999) A model of cochlear function assessment during reversible ischemia in the Mongolian gerbil. *Brain Res Brain Res Protoc* **4**:249-257.

Moore EE, Kuestner RE, Stroop SD, Grant FJ, Matthewes SL, Brady CL, Sexton PM and Findlay DM (1995) Functionally different isoforms of the human calcitonin receptor result from alternative splicing of the gene transcript. *Mol Endocrinol* **9**:959-968.

Morrow AL and Creese I (1986) Characterization of α_1-adrenergic receptor subtypes in rat brain: a reevaluation of [^{3}H]WB4104 and [^{3}H]prazosin binding. *Mol Pharmacol* **29**:321-330.

Muff R, Born W and Fischer JA (2001) Adrenomedullin and related peptides: receptors and accessory proteins. *Peptides* **22**:1765-1772.

Nag K, Kato A, Nakada T, Hoshijima K, Mistry AC, Takei Y and Hirose S (2006) Molecular and functional characterization of adrenomedullin receptors in pufferfish. *Am J Physiol Regul Integr Comp Physiol* **290**:R467-478.

Nagae T, Mukoyama M, Sugawara A, Mori K, Yahata K, Kasahara M, Suganami T, Makino H, Fujinaga Y, Yoshioka T, Tanaka I and Nakao K (2000) Rat receptor-activity-modifying proteins (RAMPs) for adrenomedullin/CGRP receptor: cloning and upregulation in obstructive nephropathy. *Biochem Biophys Res Commun* **270**:89-93.

Nam DK, Lee S, Zhou G, Cao X, Wang C, Clark T, Chen J, Rowley JD and Wang SM (2002) Oligo(dT) primer generates a high frequency of truncated cDNAs through

internal poly(A) priming during reverse transcription. *Proc Natl Acad Sci U S A* **99**:6152-6156.

Ng DT, Brown JD and Walter P (1996) Signal sequences specify the targeting route to the endoplasmic reticulum membrane. *J Cell Biol* **134**:269-278.

Nielsen H, Engelbrecht J, Brunak S and von Heijne G (1997) Identification of prokaryotic and eukaryotic signal peptides and prediction of their cleavage sites. *Protein Eng* **10**:1-6.

Nielsen H and Krogh A (1998) Prediction of signal peptides and signal anchors by a hidden Markov model. *Proc Int Conf Intell Syst Mol Biol* **6**:122-130.

Nishikimi T, Wang X, Akimoto K, Tadokoro K, Mori Y, Ishikawa Y, Ishimura K, Yoshihara F, Minamino N, Kangawa K and Matsuoka H (2005) Alteration of renal adrenomedullin and its receptor system in the severely hypertensive rat: effect of diuretic. *Regul Pept* **124**:89-98.

Nishikimi T, Yoshihara F, Kanazawa A, Okano I, Horio T, Nagaya N, Yutani C, Matsuo H, Matsuoka H and Kangawa K (2001) Role of increased circulating and renal adrenomedullin in rats with malignant hypertension. *Am J Physiol Regul Integr Comp Physiol* **281**:R2079-2087.

Nishikimi T, Yoshihara F, Mori Y, Kangawa K and Matsuoka H (2003) Cardioprotective effect of adrenomedullin in heart failure. *Hypertens Res* **26 Suppl**:S121-127.

Nixon JE, Wang A, Morrison HG, McArthur AG, Sogin ML, Loftus BJ and Samuelson J (2002) A spliceosomal intron in Giardia lamblia. *Proc Natl Acad Sci U S A* **99**:3701-3705.

Ohlsen KA, Baldwin DL, Nuttall AL and Miller JM (1991) Influence of topically applied adrenergic agents on cochlear blood flow. *Circ Res* **69**:509-518.

Oie E, Vinge LE, Andersen GO, Yndestad A, Krobert KA, Sandberg C, Ahmed MS, Haug T, Levy FO, Skomedal T and Attramadal H (2005) RAMP2 and RAMP3 mRNA levels are increased in failing rat cardiomyocytes and associated with increased responsiveness to adrenomedullin. *J Mol Cell Cardiol* **38**:145-151.

Oie E, Vinge LE, Yndestad A, Sandberg C, Grogaard HK and Attramadal H (2000) Induction of a myocardial adrenomedullin signaling system during ischemic heart failure in rats. *Circulation* **101**:415-422.

Ono Y, Okano I, Kojima M, Okada K and Kangawa K (2000) Decreased gene expression of adrenomedullin receptor in mouse lungs during sepsis. *Biochem Biophys Res Commun* **271**:197-202.

Palczewski K, Kumasaka T, Hori T, Behnke CA, Motoshima H, Fox BA, Le Trong I, Teller DC, Okada T, Stenkamp RE, Yamamoto M and Miyano M (2000) Crystal structure of rhodopsin: A G protein-coupled receptor. *Science* **289**:739-745.

Parameswaran N, Aiyar N, Wu H, Brooks DP, Nambi P and Spielman WS (2000) Desensitization and resensitization of adrenomedullin-sensitive receptor in rat mesangial cells. *Eur J Pharmacol* **407**:205-210.

Patel S, Fernandez-Garcia E and Hutson PH (2001) An in vivo binding assay to determine central α_1-adrenoceptor occupancy using [^{3}H]prazosin. *Brain Res Brain Res Protoc* **8**:191-198.

Pedretti A, Elena Silva M, Villa L and Vistoli G (2004) Binding site analysis of full-length α_1 adrenergic receptor using homology modeling and molecular docking. *Biochem Biophys Res Commun* **319**:493-500.

Piascik MT and Perez DM (2001) α_1-adrenergic receptors: new insights and directions. *J Pharmacol Exp Ther* **298**:403-410.

Porter JE, Dowd FJ and Abel PW (1992) Atypical *alpha*-1 adrenergic receptors on the rat parotid gland acinar cell. *J Pharmacol Exp Ther* **263**:1062-1067.

Porter JE, Hwa J and Perez DM (1996) Activation of the α_{1b}-adrenergic receptor is initiated by disruption of an interhelical salt bridge constraint. *J Biol Chem* **271**:28318-28323.

Poyner DR, Sexton PM, Marshall I, Smith DM, Quirion R, Born W, Muff R, Fischer JA and Foord SM (2002) International Union of Pharmacology. XXXII. The mammalian calcitonin gene-related peptides, adrenomedullin, amylin, and calcitonin receptors. *Pharmacol Rev* **54**:233-246.

Prado MA, Evans-Bain B, Oliver KR and Dickerson IM (2001) The role of the CGRP-receptor component protein (RCP) in adrenomedullin receptor signal transduction. *Peptides* **22**:1773-1781.

Qi T, Christopoulos G, Bailey RJ, Christopoulos A, Sexton PM and Hay DL (2008) Identification of N-terminal receptor activity-modifying protein residues important for calcitonin gene-related peptide, adrenomedullin, and amylin receptor function. *Mol Pharmacol* **74**:1059-1071.

Qi YF, Shi YR, Bu DF, Pang YZ and Tang CS (2003) Changes of adrenomedullin and receptor activity modifying protein 2 (RAMP2) in myocardium and aorta in rats with isoproterenol-induced myocardial ischemia. *Peptides* **24**:463-468.

Rival-Gervier S, Thepot D, Jolivet G and Houdebine LM (2003) Pig whey acidic protein gene is surrounded by two ubiquitously expressed genes. *Biochim Biophys Acta* **1627**:7-14.

Rodriguez-Boulan E and Gonzalez A (1999) Glycans in post-Golgi apical targeting: sorting signals or structural props? *Trends Cell Biol* **9**:291-294.

Rorabaugh BR (2002) A Pharmacological Study of Calcitonin Gene-Related Peptide Receptor Subtypes, in *Pharmacology Department* p 132, Creighton University, Omaha.

Rorabaugh BR, Scofield MA, Smith DD, Jeffries WB and Abel PW (2001) Functional calcitonin gene-related peptide subtype 2 receptors in porcine coronary arteries are identified as calcitonin gene-related peptide subtype 1 receptors by radioligand binding and reverse transcription-polymerase chain reaction. *J Pharmacol Exp Ther* **299**:1086-1094.

Salom D, Le Trong I, Pohl E, Ballesteros JA, Stenkamp RE, Palczewski K and Lodowski DT (2006) Improvements in G protein-coupled receptor purification yield light stable rhodopsin crystals. *J Struct Biol.*

Schlenstedt G, Gudmundsson GH, Boman HG and Zimmermann R (1990) A large presecretory protein translocates both cotranslationally, using signal recognition particle and ribosome, and post-translationally, without these ribonucleoparticles,

when synthesized in the presence of mammalian microsomes. *J Biol Chem* **265**:13960-13968.

Schwinn DA, Johnston GI, Page SO, Mosley MJ, Wilson KH, Worman NP, Campbell S, Fidock MD, Furness LM, Parry-Smith DJ and et al. (1995) Cloning and pharmacological characterization of human *Alpha*-1 adrenergic receptors: sequence corrections and direct comparison with other species homologues. *J Pharmacol Exp Ther* **272**:134-142.

Scofield MA, Liu F, Abel PW and Jeffries WB (1995) Quantification of steady state expression of mRNA for *alpha*-1 adrenergic receptor subtypes using reverse transcription and a competitive polymerase chain reaction. *J Pharmacol Exp Ther* **275**:1035-1042.

Sexton PM, Albiston A, Morfis M and Tilakaratne N (2001) Receptor activity modifying proteins. *Cell Signal* **13**:73-83.

Sexton PM, Morfis M, Tilakaratne N, Hay DL, Udawela M, Christopoulos G and Christopoulos A (2006) Complexing Receptor Pharmacology: Modulation of Family B G Protein-Coupled Receptor Function by RAMPs. *Ann N Y Acad Sci* **1070**:90-104.

Sharma S and Black DL (2006) Maps, codes, and sequence elements: can we predict the protein output from an alternatively spliced locus? *Neuron* **52**:574-576.

Simms J, Hay DL, Bailey RJ, Konycheva G, Bailey G, Wheatley M and Poyner DR (2009) Structure-function analysis of RAMP1 by alanine mutagenesis. *Biochemistry* **48**:198-205.

Steiner S, Born W, Fischer JA and Muff R (2003) The function of conserved cysteine residues in the extracellular domain of human receptor-activity-modifying protein. *FEBS Lett* **555**:285-290.

Strausberg RL, Feingold EA, Grouse LH, Derge JG, Klausner RD, Collins FS, Wagner L, Shenmen CM, Schuler GD, Altschul SF, Zeeberg B, Buetow KH, Schaefer CF, Bhat NK, Hopkins RF, Jordan H, Moore T, Max SI, Wang J, Hsieh F, Diatchenko L, Marusina K, Farmer AA, Rubin GM, Hong L, Stapleton M, Soares MB, Bonaldo MF, Casavant TL, Scheetz TE, Brownstein MJ, Usdin TB, Toshiyuki S, Carninci P, Prange C, Raha SS, Loquellano NA, Peters GJ, Abramson RD, Mullahy SJ, Bosak SA, McEwan PJ, McKernan KJ, Malek JA, Gunaratne PH, Richards S, Worley KC, Hale S, Garcia AM, Gay LJ, Hulyk SW, Villalon DK, Muzny DM, Sodergren EJ, Lu X, Gibbs RA, Fahey J, Helton E, Ketteman M, Madan A, Rodrigues S, Sanchez A, Whiting M, Madan A, Young AC, Shevchenko Y, Bouffard GG, Blakesley RW, Touchman JW, Green ED, Dickson MC, Rodriguez AC, Grimwood J, Schmutz J, Myers RM, Butterfield YS, Krzywinski MI, Skalska U, Smailus DE, Schnerch A, Schein JE, Jones SJ and Marra MA (2002) Generation and initial analysis of more than 15,000 full-length human and mouse cDNA sequences. *Proc Natl Acad Sci U S A* **99**:16899-16903.

Takhshid MA, Poyner DR, Chabot JG, Fournier A, Ma W, Zheng WH, Owji AA and Quirion R (2006) Characterization and effects on cAMP accumulation of adrenomedullin and calcitonin gene-related peptide (CGRP) receptors in dissociated rat spinal cord cell culture. *Br J Pharmacol* **148**:459-468.

Taylor CK, Smith DD, Hulce M and Abel PW (2006) Pharmacological characterization of novel α-Calcitonin Gene-Related Peptide (CGRP) receptor peptide antagonists that are selective for human CGRP receptors. *J Pharmacol Exp Ther* **319**:749-757.

Thota C, Gangula PR, Dong YL and Yallampalli C (2003) Changes in the expression of calcitonin receptor-like receptor, receptor activity-modifying protein (RAMP) 1, RAMP2, and RAMP3 in rat uterus during pregnancy, labor, and by steroid hormone treatments. *Biol Reprod* **69**:1432-1437.

Thota C and Yallampalli C (2005) Progesterone upregulates calcitonin gene-related peptide and adrenomedullin receptor components and cyclic adenosine 3'5'-monophosphate generation in Eker rat uterine smooth muscle cell line. *Biol Reprod* **72**:416-422.

Tilakaratne N, Christopoulos G, Zumpe ET, Foord SM and Sexton PM (2000) Amylin receptor phenotypes derived from human calcitonin receptor/RAMP coexpression exhibit pharmacological differences dependent on receptor isoform and host cell environment. *J Pharmacol Exp Ther* **294**:61-72.

Tilakaratne N, Smyth K, Popp B, Summers R and Sexton PM (2002) Beta-adrenergic receptor properties in SK-N-MC cells are altered by receptor activity modifying proteins (RAMPs). *Proc. Australian Health and Medical Research Congress*:Abstract 2145.

Totsune K, Takahashi K, Mackenzie HS, Murakami O, Arihara Z, Sone M, Mouri T, Brenner BM and Ito S (2000) Increased gene expression of adrenomedullin and adrenomedullin-receptor complexes, receptor-activity modifying protein

(RAMP)2 and calcitonin-receptor-like receptor (CRLR) in the hearts of rats with congestive heart failure. *Clin Sci (Lond)* **99**:541-546.

Uzan B, de Vernejoul MC and Cressent M (2004) RAMPs and CRLR expressions in osteoblastic cells after dexamethasone treatment. *Biochem Biophys Res Commun* **321**:802-808.

Uzan B, Ea HK, Launay JM, Garel JM, Champy R, Cressent M and Liote F (2006) A critical role for adrenomedullin-calcitonin receptor-like receptor in regulating rheumatoid fibroblast-like synoviocyte apoptosis. *J Immunol* **176**:5548-5558.

Vashisht K, Faaberg KS, Aber AL, Brown KE and O'Sullivan MG (2004) Splice junction map of simian parvovirus transcripts. *J Virol* **78**:10911-10919.

von Heijne G (1985) Signal sequences. The limits of variation. *J Mol Biol* **184**:99-105.

von Heijne G (1998) Protein transport: Life and death of a signal peptide. *Nature* **396**:111-113.

Wallin E and von Heijne G (1995) Properties of N-terminal tails in G-protein coupled receptors: a statistical study. *Protein Eng* **8**:693-698.

Walsh T, Martinez A, Peter J, Unsworth E and Cuttitta F (1996) Antimicrobial activity of adrenomedullin and its gene-related peptides. *Clin Infect Dis* **23**:96.

Walter P and Blobel G (1980) Purification of a membrane-associated protein complex required for protein translocation across the endoplasmic reticulum. *Proc Natl Acad Sci U S A* **77**:7112-7116.

Wang X, Nishikimi T, Akimoto K, Tadokoro K, Mori Y and Minamino N (2003) Upregulation of ligand, receptor system, and amidating activity of adrenomedullin in left ventricular hypertrophy of severely hypertensive rats: effects of

angiotensin-converting enzyme inhibitors and diuretic. *J Hypertens* **21**:1171-1181.

Wang Y, Wang Z, Li J, Wang Y and Leung FC (2007) Database for chicken full-length cDNAs. *Physiol Genomics* **28**:141-145.

Wangemann P and Wonneberger K (2005) Neurogenic regulation of cochlear blood flow occurs along the basilar artery, the anterior inferior cerebellar artery and at branch points of the spiral modiolar artery. *Hear Res* **209**:91-96.

Waugh DJ, Gaivin RJ, Zuscik MJ, Gonzalez-Cabrera P, Ross SA, Yun J and Perez DM (2001) Phe-308 and Phe-312 in transmembrane domain 7 are major sites of α_1-adrenergic receptor antagonist binding. Imidazoline agonists bind like antagonists. *J Biol Chem* **276**:25366-25371.

Waugh DJ, Zhao MM, Zuscik MJ and Perez DM (2000) Novel aromatic residues in transmembrane domains IV and V involved in agonist binding at α_{1A}-adrenergic receptors. *J Biol Chem* **275**:11698-11705.

Weinberg DH, Trivedi P, Tan CP, Mitra S, Perkins-Barrow A, Borkowski D, Strader CD and Bayne M (1994) Cloning, expression and characterization of human α adrenergic receptors α_{1a}, α_{1b} and α_{1c}. *Biochem Biophys Res Commun* **201**:1296-1304.

Xiao L, Scofield MA and Jeffries WB (1998) Molecular cloning, expression and characterization of cDNA encoding a mouse α_{1a}-adrenoceptor. *Br J Pharmacol* **124**:213-221.

Yang M, Reese J, Cotecchia S and Michel MC (1998) Murine *Alpha*1-adrenoceptor subtypes. I. Radioligand binding studies. *J Pharmacol Exp Ther* **286**:841-847.

Yoshihara F, Nishikimi T, Okano I, Hino J, Horio T, Tokudome T, Suga S, Matsuoka H, Kangawa K and Kawano Y (2005) Upregulation of intracardiac adrenomedullin and its receptor system in rats with volume overload-induced cardiac hypertrophy. *Regul Pept* **127**:239-244.

Yoshimoto T, Fukai N, Sato R, Sugiyama T, Ozawa N, Shichiri M and Hirata Y (2004) Antioxidant effect of adrenomedullin on angiotensin II-induced reactive oxygen species generation in vascular smooth muscle cells. *Endocrinology* **145**:3331-3337.

Zhang JJ, Yoshida H, Chao L and Chao J (2000) Human adrenomedullin gene delivery protects against cardiac hypertrophy, fibrosis, and renal damage in hypertensive dahl salt-sensitive rats. *Hum Gene Ther* **11**:1817-1827.

Zhao MM, Hwa J and Perez DM (1996) Identification of critical extracellular loop residues involved in α_1-adrenergic receptor subtype-selective antagonist binding. *Mol Pharmacol* **50**:1118-1126.

Zhao Y, Bell D, Smith LR, Zhao L, Devine AB, McHenry EM, Nicholls DP and McDermott BJ (2006) Differential expression of components of the cardiomyocyte adrenomedullin/intermedin receptor system following blood pressure reduction in nitric oxide-deficient hypertension. *J Pharmacol Exp Ther* **316**:1269-1281.

Zuker M (2003) Mfold web server for nucleic acid folding and hybridization prediction. *Nucleic Acids Res* **31**:3406-3415.